SHRP-H-673

An Improved Displacement Snowplow

Kynric M. Pell
The Department of Mechanical Engineering
University of Wyoming

Strategic Highway Research Program
National Research Council
Washington, DC 1994

SHRP-H-673
Contract H-206
Product Nos.: 3026, 3027

Program Manager: *Don M. Harriott*
Project Manager: *L. David Minsk*
Production Editor: *Marsha Barrett*
Program Area Secretary: *Carina Hreib*

May 1994

key words:
snow plow cutting blade
snow plow moldboard
snow plow safety
snow and ice control
snow plow

Strategic Highway Research Program
National Academy of Sciences
2101 Constitution Avenue N.W.
Washington, DC 20418

(202) 334-3774

425/NAP/594

Acknowledgments

The research described herein was supported by the Strategic Highway Research Program (SHRP). SHRP is a unit of the National Research Council that was authorized by section 128 of the Surface Transportation and Uniform Relocation Assistance Act of 1987.

Project H-206 was administered for the Strategic Highway Research Program (SHRP) by David Minsk within the Highway Operations portion of the program which was coordinated by Don Harriott.

Faculty at the University of Wyoming involved in various portions of the analytical modelling and laboratory scale experimentation included: Dr. John George, Professor and Head, Department of Mathematics; Dr. Richard Schmidt, Assistant Professor of Civil Engineering; Dr. William Lindberg, Dr. John Nydahl, and Dr. Donald Smith, Professors of Mechanical Engineering as well as Associate Professors, Dr. David Walrath, and Dr. Andrew Hansen, Department of Mechanical Engineering, all of whom made substantial contributions to the analytical models as well as laboratory and full-scale testing. Professor Emeritus, Robert Sutherland assisted with program coordination.

All of these activities were supported by a technical support staff drawn from a research group within the Department of Mechanical Engineering (Center for Information Technology (CIT)): Jerome Popp, Manager, Technical Programs, CIT; Julie McGinnis, Accountant, CIT; Wade Steiger, Mechanical Engineer, CIT; John Benko, Programming Engineer, CIT; George Chakmakian, Programming Engineer, CIT; Simon Lacey, Programming Engineer, CIT; Todd Peake, Electrical Engineer, CIT; Mike Klecha, Mechanical Engineer, CIT; Lisa Johnston, Receptionist, CIT; Stephen Ownbey, Computer Engineer, CIT; George Twitchell, Electrical Engineer, Department of Mechanical Engineering; Robert Adame, Master Machinist, Department of Mechanical Engineering; and Clarence Porter, Master Machinist, Department of Mechanical Engineering.

More than twenty students including graduate students and undergraduate students worked on the project. Some of these completed Masters' thesis and Doctoral dissertations in related areas. The students' names are listed along with the title of their thesis or dissertation.

Robert Crane, M.S., Mechanical Engineering, 1993
"Analysis of the Large Deformation and Flow Characteristics of Developable Surface Snowplow Moldboards"
Dennis Horning, Ph.D, Mechanical Engineering, 1994
"Concurrent Scheduling of Multiprocessors for Efficient Eigenproblem Solution"
Paul Bruss, M.S., Mechanical Engineering, 1992
"Stress Wave Interaction at the Ice/Road Interface"
Mike Damson, M.S., Mechanical Engineering, 1990
"Numerical Investigation of Flow on a Snowplow"
Robert Yraceburu, M.S., Mechanical Engineering, 1992
"Dynamic High Density Snow Compaction for Polar Runways"
Bo Ruan, M.S., Mechanical Engineering, 1992 "Heavy Vehicle Stability"
Harold Adkins, B.S., Mechanical Engineering
Will Bieg, B.S., Mechanical Engineering
Wayne Foslien, B.S., Mechanical Engineering
Leonard Frank, B.S., Mechanical Engineering
Marilyn Higgins, B.S., Micro Biology
John Leach
Gi-Fei Li, B.S., M.S., Mechanical Engineering
Roland Miller, B.S., Mechanical Engineering
Norman Rhines, B.S., Mechanical Engineering
Troy Willoughby, B.S., Mechanical Engineering
Karen Wolcott, B.S., Mechanical Engineering
Shannyn Adkins, B.S., Accounting, 1995
Jennifer Bruss, B.A., Liberal Arts
Melanie Burkhardt, Mechanical Engineering
Robert Crouch, B.S., Mechanical Engineering
Kynric Pell, Jr., B.S., Geography, 1995
Stephen Sartori, B.S., Mechanical Engineering, 1994

A portion of the funding for the students listed came through the SHRP program. Each area of research presented in dissertations and theses represents a significant contribution to our understanding of the mechanics of snow and ice which influence their removal from roadways. Every engineering student that participated in the program is a better engineer, with an understanding of the role of basic science and the experimental method in development of innovative technology, because of his/her participation in the project. This new knowledge represented in the theses, the professional growth of the faculty as well as the group of graduate engineers generated are major contributions of the SHRP program to our nation's intellectual capital.

Early in the project a Russian language book written by D.A. Shalman entitled "Snowplows" was found in the literature search. It was apparent that this was a key reference which needed to be translated to English. Language student Matthew Feeney and Dr. John Nydahl collaborated in this effort and produced a draft which was subsequently edited by Dr. Nydahl and Dr. Dmitry Laptev.

Major contributions to the success of this project were provided by the Expert Task Group formed by SHRP which reviewed technical progress and refined the goals at strategic times in the project. The Wyoming Department of Transportation provided a Ford LT9000 for use as a research platform throughout the project. Don Diller, Director of the Wyoming Department of Transportation and his staff, Richard Stapp, State Maintenance Engineer; Curt Helzer, State Equipment Engineer; Joseph Yovich, District Engineer; Tim McGary, District Maintenance Engineer; and Jim Murdock, District Foreman have been not only enthusiastic supporters of the research, but active participants in its planning and conduct. The entire University research team is deeply indebted to this group and all the Laramie District snowplow foremen and operators for their patience in educating us to the reality of snowplow operation in a severe environment.

Frink America Inc. served as a subcontractor on this project. The insightful suggestions of Chief Engineer, Jan Verseef, were extremely helpful to those of us at the University of Wyoming. President Gerry Reitz was supportive throughout the project and provided historical records of Frink's corporate research.

Within SHRP project H-206 there was a portion of the research which addressed blowing snow control and road design. This portion of the research was subcontracted to R.D. Tabler and Associates and the work was conducted by Dr. Ron Tabler. The results of this project have been reported separately and are summarized in "Designing for Blowing Snow Control."

I will close this section by expressing my deep gratitude to all of those named above, and the many people not listed, who have contributed to the project and my education.

Kynric M. Pell
Principal Investigator

Contents

Introduction

Project H-206, "Improved Displacement Plow and Blowing Snow Research" was awarded to the University of Wyoming in October 1988. The research required covered two distinct areas. One focused on developing an improved snowplow and the second addressed snow control for highways. The project extended over a four and one-half year period. The research team largely consisting of University personnel investigated snowplows whereas the University subcontracted with R.D. Tabler and Associates for the technical effort related to snow control. This report describes the research on improving the design of snowplows, as well as design, fabrication and test of plows incorporating improvements. The project included a variety of features which were intended to promote technology transfer. These efforts are also documented. Finally, a recommended design for an improved reversible plow is presented.

The primary goal of the research was to decrease the energy consumption during plowing by twenty percent. Secondary goals included increasing the cast performance, improving visibility for the operator and the motoring public, and improving the safety of the plow especially on impact with hazards found on and along roadways.

Research Plan

The research plan incorporated a literature survey, user survey, development of mathematical models of snow flow, as well as design, fabrication and testing of experimental snowplows.

Literature and patent survey

The literature and patent survey showed that considerable research has been conducted on the mechanics of snow; however, very little new work focused on plowing was found in the English language literature subsequent to that summarized by Minsk (1). A Russian language book by Shalman (2) was found to contain a model for snow flow on the moldboard of snowplows which considered the effects of both gravity and friction. This work has been translated and is available from the Department of Mechanical Engineering at the University of Wyoming.

User surveys

The University of Wyoming mailed survey questionnaires regarding snowplows and snowplow operation to 33 states considered in the snow belt. The purpose of the survey was to gain information on the type of equipment in current use, the buying trends of this equipment, and the procurement process used to acquire snowplow equipment. Also sought was insight on the operational aspects of the equipment in the various state inventories. Twenty states* responded to the survey with either completed questionnaires or related information in an alternative format. The total number of plows in inventory for these

* AK, CA, CO, IA, ID, IL, IN, MD, NH, NJ, NM, NY, OR, SD, TX, UT, VA, VT, WV, WY.

states was 18,732. The most common type of plow is the reversible type, comprising seventy-three percent of the inventory of reporting states. Nineteen percent of the plows are one-way and eight percent are Vee-type. Five states (AK, NH, OR, VT, WV) reported that their inventories contained a majority of one-way plows. Iowa, New Hampshire and New York reported that a majority of their plows are equipped with wing plows. Eight of the twenty reporting states indicated that they have wing plows of some type. Only the states of Utah and Idaho manufacture significant percentages of their plows, however CA has fabricated virtually all of its reversible plows. Of the plows that were purchased in the 20 states, approximately one-half were purchased through a distributor and the other half were purchased directly from a manufacturer. These states reported total snowplow purchases of approximately 1100 units annually over the past four years and ninety percent of these purchases were of reversible plows.

A linear regression analysis was used to estimate the total number of plows in inventory in state DOTs. The result was approximately 34,000 plows of all types. It was also concluded that the vast majority of plows operated by state DOTs are of the reversible type. Analysis of recent purchases indicates that the percentage of reversible plows is increasing.

The surveys were filled out by state equipment managers who were solicited for problems with their current equipment. Four problems were mentioned. Several individuals indicated the weight of the plows is excessive. At the same time the decrease in durability of the equipment was mentioned. Snow blowing over the top of the moldboards creates a visibility problem for the operators and the snow entrained in the wake of the snowplow creates a visibility problem for motorists.

Analytical Studies

During the first year of the project Hansen and his students developed a model for the compression of snow immediately in front of the cutting blade which was subsequently used in the design of shallow angle blades for snow removal. This work is summarized in the section on design of the cutting blade. In spite of the fact that intensive effort was committed to modelling the flow on the moldboard a comprehensive model was not successfully developed until the last year of the project. As a result, the three experimental plows designed and fabricated in the course of the project were built without benefit of simulated flow on the moldboard. The flow model which was developed was verified by simulating the geometry and flow conditions encountered during two test runs of the second experimental plow and this work is presented in the section entitled Moldboard Flow Analysis.

Laboratory Experiments

Plume Studies

In situations where snow is moving in sheet like motion over the moldboard it exits the moldboard with a speed and direction that depends on the exit location. Prediction of the fate of a small parcel of snow leaving the moldboard with a particular velocity has been based on a ballistic model which is empirically corrected to provide an estimate of cast distance. The basic physical model has some validity for wet snow which tends to be aggregated in relatively large clumps. For low density snow which tends to leave the plow in the form of small discrete particles the ballistic model lacks the essential physical features of the flow. A small portion of the snow flow exiting the throat may be conceptualized as a negatively buoyant jet in a cross flow. Some experimental work on vertical jets of this type is reported in the literature; however for more general geometric situations there is no data. William Lindberg and his students have conducted a comprehensive study of inclined negatively buoyant jets in a cross flow for this project and reported the results(3).

Water Table Flow Experiments

The analytical models of flow on the moldboard were not developed in time to aid with the design of the experimental plows. Water table flow experiments were used to provide qualitative information on the nature of flow on the moldboards. A thin sheet of water was formed by directing numerous water jets from a manifold along a flat surface. The sheet of water was directed at various model plows and the flow on the moldboard was video taped. Models constructed for test included the experimental plows fabricated for this project as well as several one-way and reversible plows typical of those currently used by the state of Wyoming. An edited video of the tests is available from the University of Wyoming, Department of Mechanical Engineering. These tests led to the design of the third experimental plow: However; the results are not documented in narrative form.

Wind Tunnel Simulations

Flow visualization studies over a model plow/truck combination were conducted in a wind tunnel using both smoke and yarn tufts for flow visualization. The results were recorded photographically. Separated flow with recirculation was observed between the plow and

the truck, in front of the windshield of the truck, over the bed of the truck and in the vehicle wake. Recirculating flow regions can entrain snow in the flow field and can impact visibility for both the operator and motorists. It was shown that the ratio of the distance between the plow and the truck and the height of the hood has an impact on the flow over the plow/truck combination. For the limited range of Reynolds number tested the use of a bug deflector was actually found to be detrimental. It was shown that airfoil devices on the plow can decrease the size of the recirculation regions and may be useful for improving visibility. These tests were terminated in the preliminary phases.

Numerical Studies

Dynamic Simulations of Vehicle Performance

There were two major objectives for the dynamic simulation of snowplow performance. One objective was to provide an analysis of the kinematics of motion and the forces transmitted to the plow drive frame and the truck during both normal plowing and tripping of either a tripping edge or a full tripping moldboard. The second major objective of the simulations was to analyze the effect of the snow plow and typical sand load on the stability and control of the vehicle. The commercial software ADAMS™ (Automated Dynamic Analysis of Mechanical Systems) from Mechanical Dynamics, Inc. was used to model a Ford LT9000 as the prime mover. The model had to be simplified since many of the parameters required were unavailable. In any event, tripping edge dynamics were investigated for a generic tripping edge geometry and an air spring return actuator. Lane change maneuvers with and without plows with varying amounts of sand in the sander on bare pavement and ice were investigated. The results are reported in a thesis by Ruan (4).

Aerodynamic Modelling of the Snowplow

Numerical modeling of the flow in the neighborhood of the plow truck combination was attempted using the commercial software PHEONICS™ from CHAM Inc. Two dimensional models indicated flow separation with recirculating flow in the same regions found in the wind tunnel studies. These two dimensional studies indicated that the exact nature of the separated flow was sensitive to the Reynolds number. For example, the separated region in front of the windshield of the truck was sensitive to Reynolds number and the direction of flow over the windshield could be reversed by addition of a bug deflector in some Reynolds number regimes. The aerodynamic flow in front of the moldboard is highly three

dimensional and aerodynamic interaction with light snow in this region probably has an impact on the visibility problem. Unfortunately, the three dimensional modeling of the plow/truck combination was not successful. This research is described in more detail by Damson (5).

Field Tests

Aerodynamic Flow

Two rectangular steel frames approximately 2.5 x 2 meters (8 x 5 feet) were fabricated and equipped with horizontal wires on 0.3 meter (1 foot) spacings. A support system to maintain these frames in a vertical position over the plow, truck and intervening gap was also fabricated. A series of tests was conducted where yarn tufts were tied to the wires on approximately 0.3 meter spacings. The frames were moved in two foot increments from an axial station above the plow to the rear tail gate of the truck. During an experimental run the test vehicle was video taped from a second vehicle travelling alongside and the yarn tufts provided a two dimensional indication of the direction of the local flow velocity vector. Separated flow regimes with recirculation similar to those observed in the wind tunnel experiments were observed. These tests also confirmed the general flow features observed in the two dimensional numerical simulations.

1st Experimental Plow

The first experimental plow incorporated a 3.5 x 2 meter (12 x 5 foot) ultra high molecular weight polyethylene moldboard fixed to a steel lower plow frame which also supported the tripping edge. The upper support was adjustable using three turnbuckles on compound arms on each end of the plow. This provided continuous independent adjustment of the moldboard shape at each end of the plow. The plow incorporated a rigidly mounted snow scoop and a tripping edge wherein the restoring force was provided by airsprings adapted from hydraulic cylinders.

2nd Experimental Plow

Based on testing of the first experimental plow and the water table tests of various plow shapes a second experimental plow was designed. This plow incorporated a planar lower moldboard with a surface composed of 2.5 millimeter thick thermoplastic composite called

AZLOY™. This surface retained the low coefficient of friction typical of polymers. The flat lower moldboard was approximately 1 meter (4 feet) tall. One cylindrical and one conical upper moldboard were fabricated and these could be mounted horizontally or at angles of 6 and 12 degrees relative to horizontal. The cylindrical moldboard was slightly less than 1 meter (32 inches) in diameter as was the throat of the conical section. Both of these units were surfaced with AZLOY™. This plow also incorporated a tripping edge powered by an airspring however the spring was a rubber airbag typically used on truck suspension systems. A new snow scoop incorporating a hinged mount and 25 millimeter thick ultra high molecular weight polyethylene scoop surface and larger area snow exhaust was also fabricated for this plow.

3rd Experimental Plow

Fabrication of the third experimental plow was actually funded by the Science, Technology and Energy Authority of the State of Wyoming, however, its design was based on the research conducted under the SHRP program. The shape of the third experimental plow was essentially the same as the second experimental plow with a symmetric upper moldboard incorporating a cylindrical upper section inclined at 5 degrees. This plow also incorporated a tripping edge with restoration force provided by a rubber airspring. WOTCO Inc. of Casper Wyoming provided a snowscoop for this plow which they redesigned for manufacturability. The significant feature of this plow was that the moldboard was fabricated as a laminated composite structure utilizing a pine core surfaced with AZLOY™. There are no ribs or other supporting structure. The AZLOY™ was bonded to the wood.

Design of the Cutting Blade and Trip Mechanism

The Cutting Blade

Hansen (6) conjectured that a plastic wave forms in the snow ahead of the cutting blade during snowplowing at higher speeds. This wave would compress the snow prior to flow up the moldboard thereby dissipating energy provided by the prime mover. Using an approximate analytical technique he showed that the energy dissipated in compression is a function of speed, density of the snow, and the angle of the cutting blade. This is illustrated in Figure 1 and 2 where it was assumed that the plow was 3.33 meters (11 ft.) in

width, with an attack angle of 33 degrees and that it was plowing 15 cm (6 in.) of snow. It may be seen that at speeds greater than 10 m/s (22 mph) the power dissipated in compression increases rapidly for steep blade angles. It should also be noted that the higher the initial density of the snow the larger the dissipated power for a particular speed.

Experimental verification of Hansen's analytical work took two forms. An experiment was designed to observe dilatation of the snow ahead of the blade of a full scale test plow. Coal dust and spray paint were used to place lines on the surface of the snow transverse to the direction of plowing. A video camera was mounted above the compression region and aimed vertically downward to document any change in spacing between the lines ahead of the cutting edge. These experiments were unsuccessful. Few frames were obtained with clear views of the lines and it was not possible to measure the change in line spacing accurately enough to quantify compression in these frames.

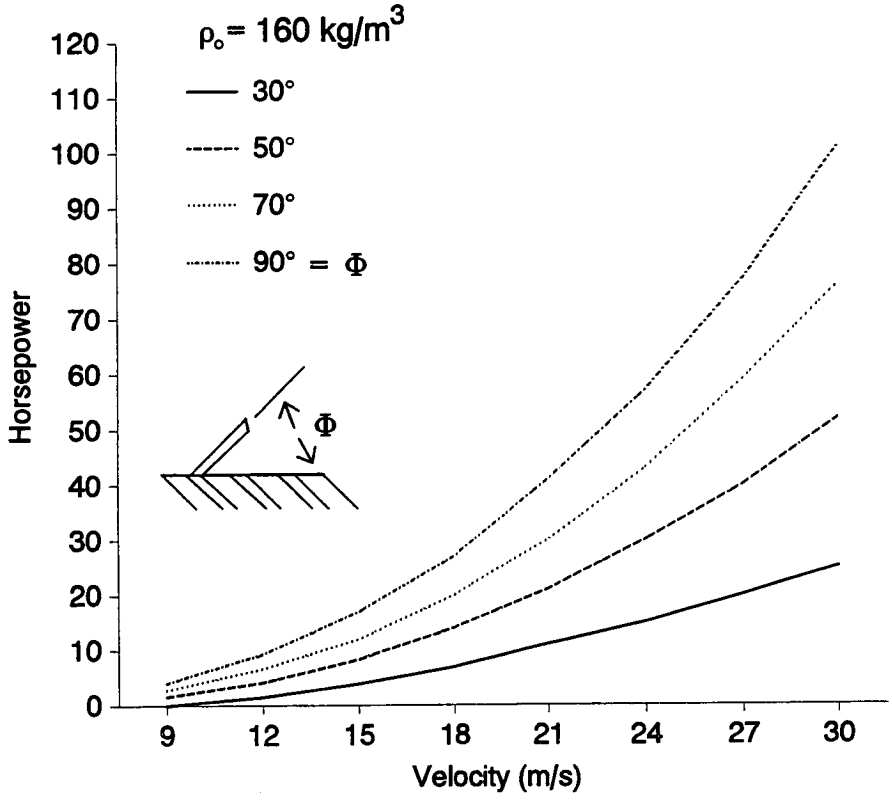

Figure 1. Horsepower dissipated in compressing snow as a function of velocity. The parameter is blade angle to the road surface.

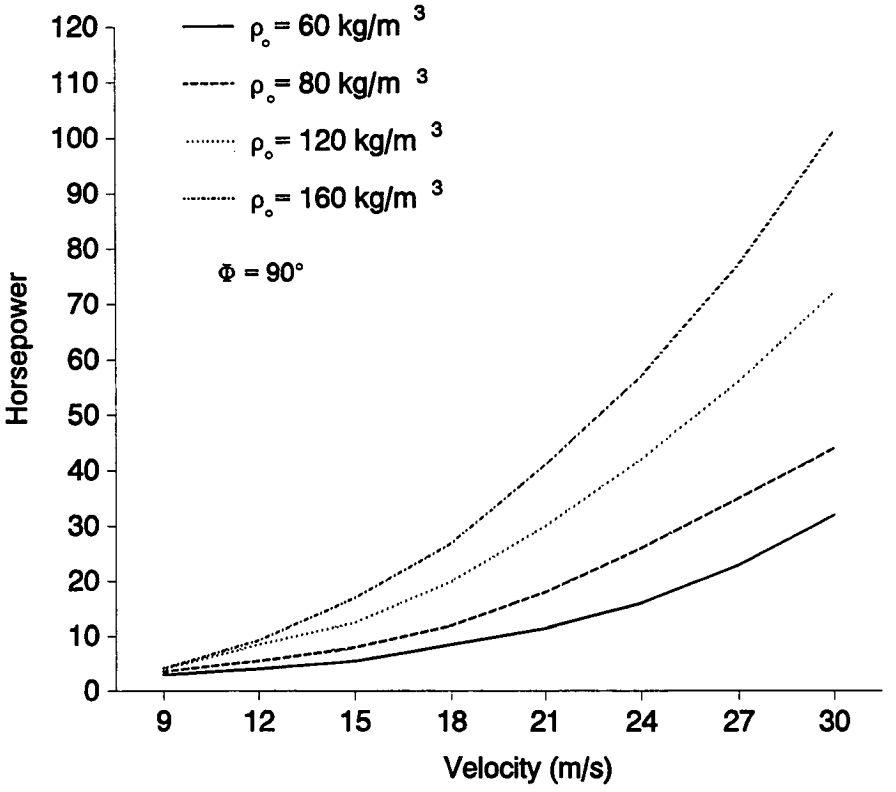

Figure 2. Horsepower dissipated in compressing snow as a function of velocity. Initial snow density as the parameter.

The second approach used to verify the effect of blade angle on compressive dissipation was a direct measurement of the forces associated with plowing. The first experimental plow, shown in Figure 3, was instrumented with strain gauge load cells to measure the force perpendicular to the blade, on the tripping edge referenced to the point of contact with the road. It was also instrumented to measure the axial and transverse loads at the truck/hitch interface. A series of tests was conducted at 17 m/s (37 mph) in 7 cm (2.75 in.) of snow with a density of 140 kg/m^3 (.272 slugs/ft^3). Runs were made with a blade angle of 85 degrees and with a shallow angle attachment mounted ahead of the blade (snowscoops) at an angle of 45 degrees. Use of the snowscoops provided a 34 percent reduction in the axial force measured at the tripping edge which corresponds to a decrease from 94 to 62 horsepower. Extrapolating the data presented in Figure 1, Hansen predicted a decrease of approximately 15 horsepower. It is not reasonable to make quantitative

inferences on the validity of Hansen's approximate solution based on the paucity of data obtained. It should be noted that the axial and transverse forces measured at the truck/hitch interface during these tests showed decreases in both axial and side forces of approximately fifty percent. Without attempting to rationalize the differences between the various measurements it is clear that the shallow angle snowscoops decrease the plowing forces relative to steeper cutting blades.

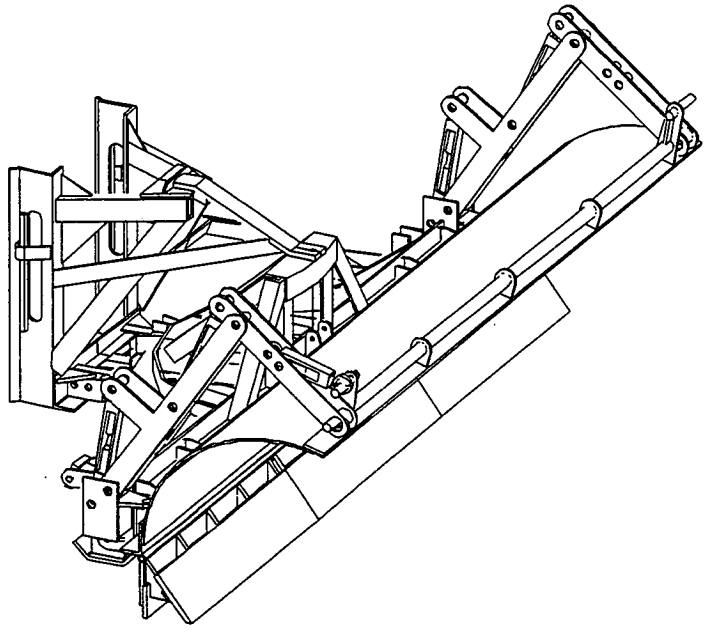

Figure 3. The first experimental snowplow.

Snowscoops

For the tests of shallow angle blades described above it was convenient simply to attach a plastic blade at an angle of 45 degrees relative to the road surface to the near normal cutting blade of the experimental plow. Review of the various state specifications and manufacturer's catalogs showed that many states utilize very steep cutting blade angles especially for reversible plows. In discussions with plow operators it was found that they generally prefer the cutting blade to be oriented approximately 80 degrees to the road surface. This is a compromise from the 90 degrees they have found removes compacted snow and ice most effectively, which reduces a phenomena they characterize as chatter. Random inspection of reversible plows in many western and midwestern states showed that

most reversible plows are operated with the cutting blade oriented approximately 80 degrees to the road surface. In order to retain this feature of the reversible plows and provide the energy efficiency associated with a shallow angle blade, a retrofittable snowscoop was developed as shown in Figure 4. Scoops of this design were mounted on a second experimental plow developed by the University and on a modified Frink Revers-a-cast plow. In addition, North Dakota, New Hampshire, Iowa and California DOT's, as well as the Port Authority of New York and New Jersey, were provided snowscoops for installation and test on their reversible plows.

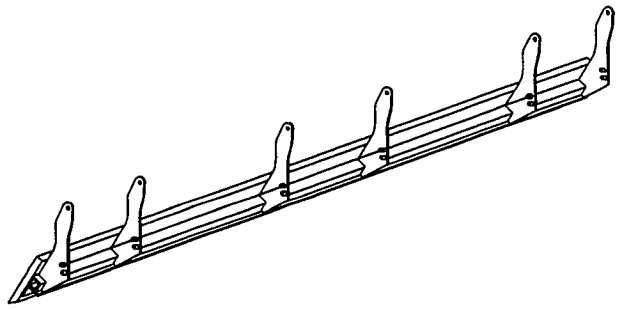

Figure 4. Retrofit Snowscoop Design.

Videotaped tests of the snowscoops on the experimental plow made by the University in Montana and Wyoming indicated good flow characteristics on the scoops and up the moldboard as shown in Figure 5. This could be contrasted with the situation when no scoops were employed as shown in Figure 6. Operators commented on the stability of the plow/truck combination when the scoops were mounted on the plow. The video tapes also documented marked improvement in the visibility for both the operator and motorists when snowscoops were utilized. No tests of the modified Frink Revers-a-cast plow have been completed.

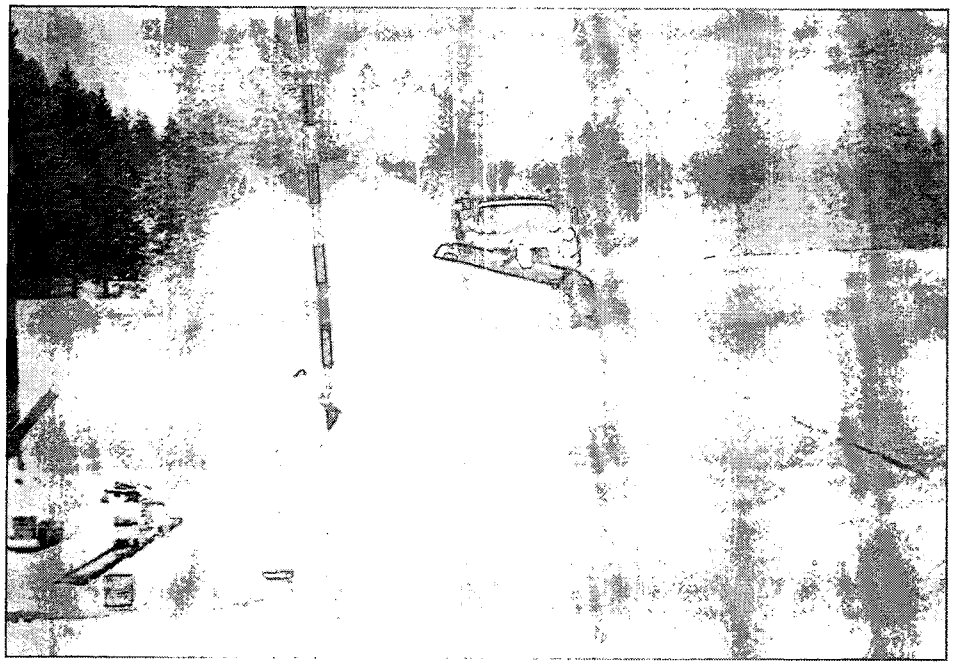

Figure 5. Snowscoops providing smooth flow.

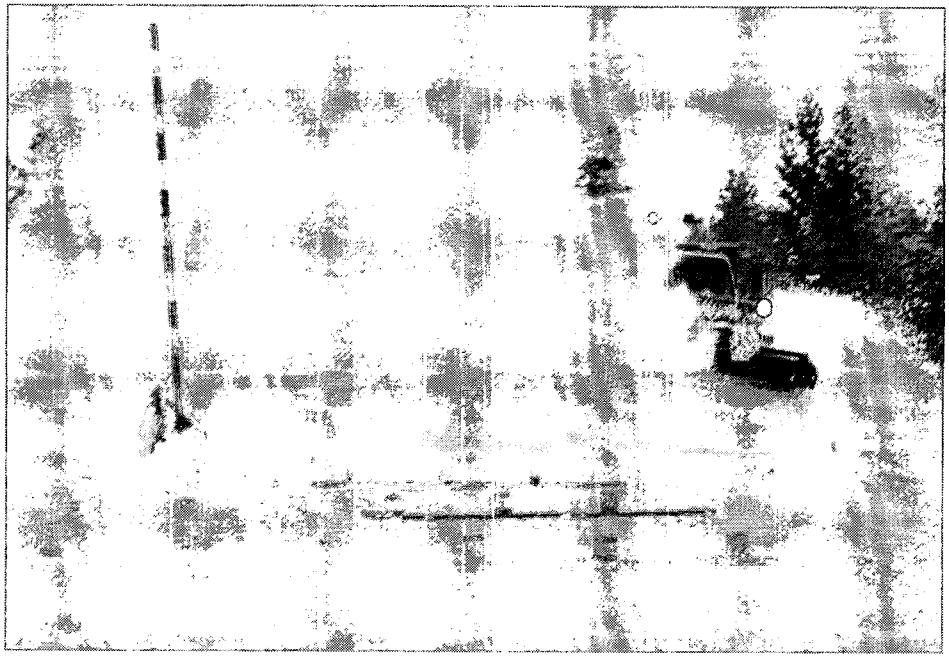

Figure 6. Flow caused by near normal cutting edge without snowscoops.

Three states have provided reports on testing of the snowscoops. The reports indicated problems with blockage in wet snow and the fact that a lack of snow provided little opportunity for testing. WOTCO, Inc. of Casper, Wyoming has redesigned the snowscoops to simplify manufacture and improve strength, and is marketing them.

In spite of the fact that the limited testing by users to date has not substantiated the improved performance observed by the research team it is recommended that shallow angle blades be incorporated in the design of new reversible plows and that retrofit of snowscoops for the existing fleet be studied in a more comprehensive manner.

Tripping Mechanisms

Tripping mechanisms incorporated on snowplows are intended to change the geometry of the plow when the cutting blade encounters an obstruction of a sufficiently high force. The geometry change allows the plow to move over the obstruction without mechanical damage to the plow or truck. Tripping mechanisms generally are of two distinct types: those designs in which the entire moldboard assembly trips and those in which only the cutting blade, or a section, is allowed to trip. Any tripping mechanism increases the capital cost of a plow and increases maintenance cost simply due to the increased mechanical complexity. Operators tend to dislike tripping mechanisms because in the event of a trip there are rapid changes in the forces imposed on the plow/truck combination which may cause control problems. In spite of this, virtually all state agencies utilize plows incorporating a tripping mechanism.

Full tripping moldboards have a number of problems:

1. The hinge point is above and behind the cutting blade so that when the cutting blade hits an obstruction the plow must move upward as the cutting blade rotates about the hinge. Due to the fact that the moldboard assembly is relatively massive, this imposes large inertial forces on the truck. It can also damage the road surface due to gouging by the cutting edge.

2. If the truck is operating with some of the weight of the plow transferred to the truck, the weight on the truck can fluctuate rapidly during the tripping event altering the steering effectiveness.

3. Tripping moldboard designs can incorporate springs to reset the plow in the event of a trip, or they may require the operator to manually reset the plow and replace

the mechanical fuse. Operators generally do not like to manually reset the plows. Mechanical springs can present safety problems in the event of failure of the spring or the attachment.

Tripping blades present many of the same problems as full tripping moldboards; however, in some cases the magnitude of the problem is reduced:

1. Figure 7 shows a typical tripping edge geometry at various positions during a tripping event. Just as in the case of tripping moldboards the hinge is above and behind the cutting edge contact with the road causing vertical movement of the plow and possibly gouging the road. These effects are decreased in the design shown in Figure 8 where the hinge is moved forward.

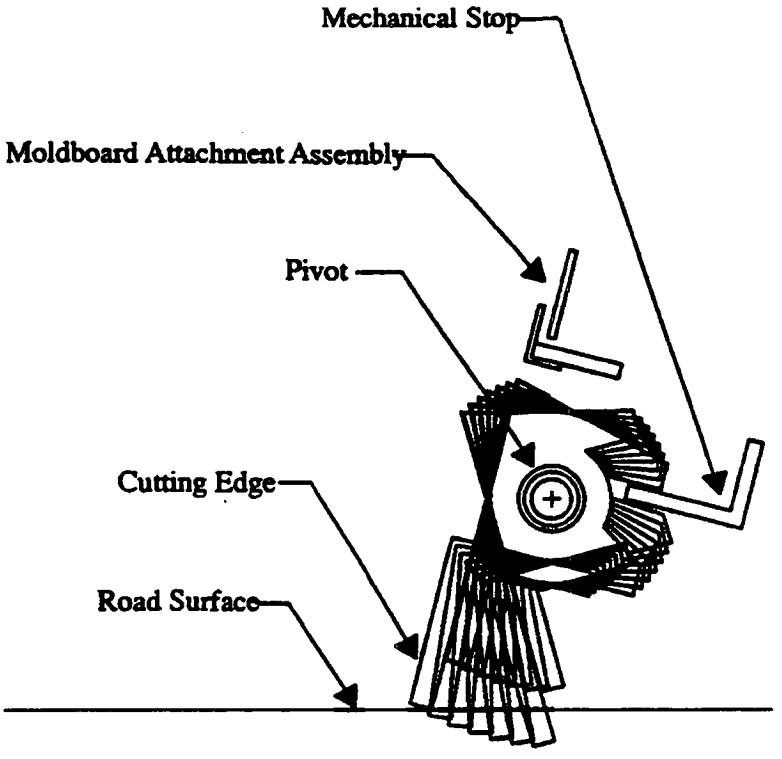

Figure 7. A typical tripping edge design.

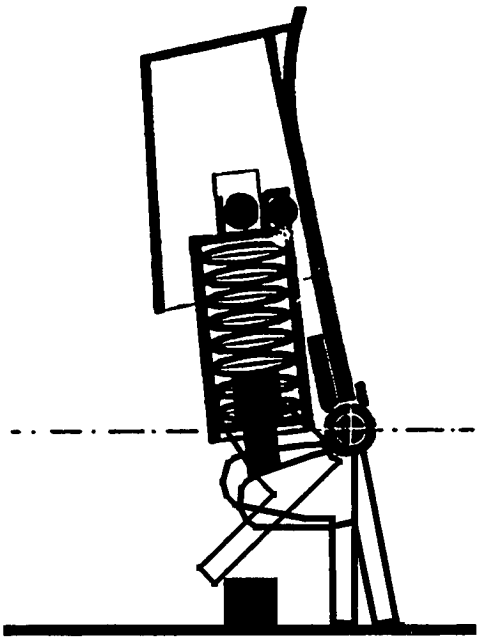

Figure 8. An alternative tripping edge design.

2. The large surface area of a tripped moldboard can cause the plow to ride up on snow under the moldboard. This may be contrasted with a relatively small horizontal projected surface of a tripping blade which will have less of a tendency to ride up.

3. Tripping blade plows always incorporate springs to automatically reset the plow in the event of a trip. Several manufacturers have employed torsion springs contained by the tripping blade hinge pin to provide the restoring force. This generally precludes pieces of a failed spring from flying off or dropping to the road surface.

Based on the discussion above a tripping blade design is recommended rather than tripping moldboard. The hinge should be located as close to a vertical line from the cutting edge contact with the road surface as possible. The rotation of the tripped section should be enough to allow clearance of an obstacle without lifting the plow.

Two different types of air spring have been used to provide the restoring force for tripping blades on the experimental plows. The reasons for using air springs were to provide for adjustable tripping blade force and to improve safety. Hydraulic cylinders were modified for use with compressed air and used as compression springs in the first experimental plow. These units were costly and required very high pressure to obtain an appropriate restoring force due to their small diameter. The second experimental plow utilized air bag type springs commonly employed on commercial trucks. These large diameter units were operated at pressures compatible with the compressors used on trucks to power air brakes and were in fact run off the truck air. Air springs of this type are competitively priced with mechanical springs.

Moldboard Flow Analysis*

Background

Traditional attempts at determining flow characteristics on a moldboard surface have used various "sheet" models (Minsk (1) and Shalman (2)). These models assume that snow flows as a sheet over a developable moldboard surface so that no tearing or stretching of the sheet occurs. These theories use conservation of mass to yield velocities at the outlet that are identical to the inlet velocity. Some experimentally derived velocity coefficient can be introduced to account for the decrease in velocity observed from the inlet to the outlet (Mellor (7)).

To achieve better approximations of the discharge of snow from a snowplow, Shalman (2) took into account the effects of friction between a snow particle and the moldboard surface, and the increase in the potential energy as the particle is lifted up the moldboard. His derivation was limited to a one-dimensional analysis of motion of a snow particle up a cylindrical surface. Nydahl (8) included these effects in deriving the relationships for two-dimensional flow over an inclined plane. He also independently derived the same relationship for the cylinder as Shalman.

Most of the above investigations were limited to the geometries of the cone, cylinder, and flat plate. All of these analyses, except that done by Nydahl, were done prior to the availability of computers and used fairly complicated geometrical relations specific to the cases being studied in order to reach closed form solutions. The only analyses found that take into account gravitational or frictional effects are those by Shalman and Nydahl.

---

*Substantial portions of this section are reproduced with permission of the author from "Analysis of the Large Deformation and Flow Characteristics of Developable Surface Snowplow Moldboards," a thesis by R. L. Crane (10).

Experimental results indicate that changing the moldboard surface to a material having a low coefficient of sliding friction significantly reduces the power required to remove the snow (Shalman (2) and Verseef (9)). Nydahl (8) points out that velocity changes due to the change in potential energy of the snow particle can be significant. A more general analysis which includes both of the above effects was first introduced by Nydahl (8). He derives a kinematical approach that can be used to calculate the trajectory of a particle over a general developable surface.

Starting with the initial analysis done by Nydahl, Crane (10) developed formulas for the position, velocity, and acceleration of a particle on a developable surface (moldboard) by using the position vector formula for a developable surface. Crane further developed the kinematical theory and implemented this theory into two fairly general computer programs. The first computer program can be useful for modelling existing snowplow moldboard shapes but it relies on a large deformation solution of a plate in order to obtain the geometrical information needed. The second computer program generates the geometrical information in a more efficient manner and is more useful in designing moldboard shapes. This theory was checked against earlier theoretical models and qualitatively against experimental data.

Theoretical Development

Most of the snowplows in use today have surfaces that are developable surfaces or some combination of developable surfaces. Various methods can be used to characterize a developable surface. Simmonds and Libai (11) used a curve (designated as ß) to characterize the developable surface. This curve is an involute of the edge of regression so it is orthogonal to the generators of the developed midplane of the plate and passes through the middle of the loaded rigid edge as shown in Figure 9 (11).

One reason for choosing this curve, rather than the edge of regression, is that this curve exists even for the degenerate cases of the cone and cylinder. The undeformed (x,y) Cartesian coordinate system with origin O at the middle of the loaded edge is shown in Figure 9. The orthogonal coordinate directions ξ and η for the deformed midplane are also shown in this figure. The ξ-coordinate follows the curve ß from the origin O, while the η-coordinate measures distance from the curve ß along a generator of the surface. The curves C_+ and C_- are given as arbitrary curves defined by some function $f_\pm$ defining the free edges in Figure 9. A developable surface can be defined when the curvature $\kappa(\xi)$ and torsion $\tau(\xi)$ are given for any space curve, such as ß (12). Simmonds and Libai use the geodesic (or tangential) curvature, **g**, and the normal curvature, **k**, of the involute ß which are given in terms of the curvature and torsion of ß (11). The problem of determining the deformation of a thin plate can be reduced to the determination of the geodesic and normal curvature of the curve ß once

the geometry of the plate and the loading applied at the origin O are defined. The angle α is defined as the angle between a generator of the developed midplane (η-direction) and the x-axis as is shown in Figure 9. The change in the angle α gives the geodesic curvature, $\mathbf{g}$, of the plate. Figure 10 (11) shows the unit vectors $\underline{\mathbf{t}}$, $\underline{\mathbf{u}}$, and $\underline{\mathbf{m}}$ associated with the (ξ,η) system and the unit vectors $\underline{\mathbf{i}}$, $\underline{\mathbf{j}}$, and $\underline{\mathbf{k}}$ associated with the (x,y) system. The $\underline{\mathbf{t}}$, $\underline{\mathbf{u}}$, and $\underline{\mathbf{m}}$ system of orthogonal unit vectors changes orientation as it moves along the curve ß in the deformed plate. Simmonds and Libai use the Serret-Frenet differential equations (9) for solving the vector equation, $\underline{\mathbf{X}}$, for ß (11). A tangential developable surface can be described (11) by the equation:

$$\underline{\mathbf{Y}}(\xi,\eta) = \underline{\mathbf{X}}(\xi) + \eta\,\underline{\mathbf{u}}(\xi) \; . \tag{1}$$

The derivatives of the base vectors $\underline{\mathbf{t}}$, $\underline{\mathbf{u}}$, and $\underline{\mathbf{m}}$ with respect to ξ are given (11) by:

$$\underline{\mathbf{t}}' = g\underline{\mathbf{u}} + k\underline{\mathbf{m}} \quad , \quad \underline{\mathbf{u}}' = -g\underline{\mathbf{t}} \quad , \quad \underline{\mathbf{m}}' = -k\underline{\mathbf{t}} \; . \tag{2}$$

The equation describing the developable surface (Eq. 1) is a position vector for a point on the surface. The covariant base vectors can be calculated by taking the derivative of this position vector (13) using the following:

$$g_s = \frac{\partial \underline{\mathbf{Y}}}{\partial x^s} \; . \tag{3}$$

Applying the above formula to the position vector (Eq. 1), noting that $x^1 = \xi$ and $x^2 = \eta$, yields the covariant (or natural) basis for the (ξ,η) system:

$$g_1 = (1 - \eta\, g)\underline{\mathbf{t}} \quad , \quad g_2 = \underline{\mathbf{u}} \quad , \quad g_3 = \underline{\mathbf{t}} \times \underline{\mathbf{u}} = \underline{\mathbf{m}} \; . \tag{4}$$

In the above, the third covariant base vector was arbitrarily taken as the cross product of $\underline{\mathbf{t}}$ and $\underline{\mathbf{u}}$ which results in an orthogonal basis.

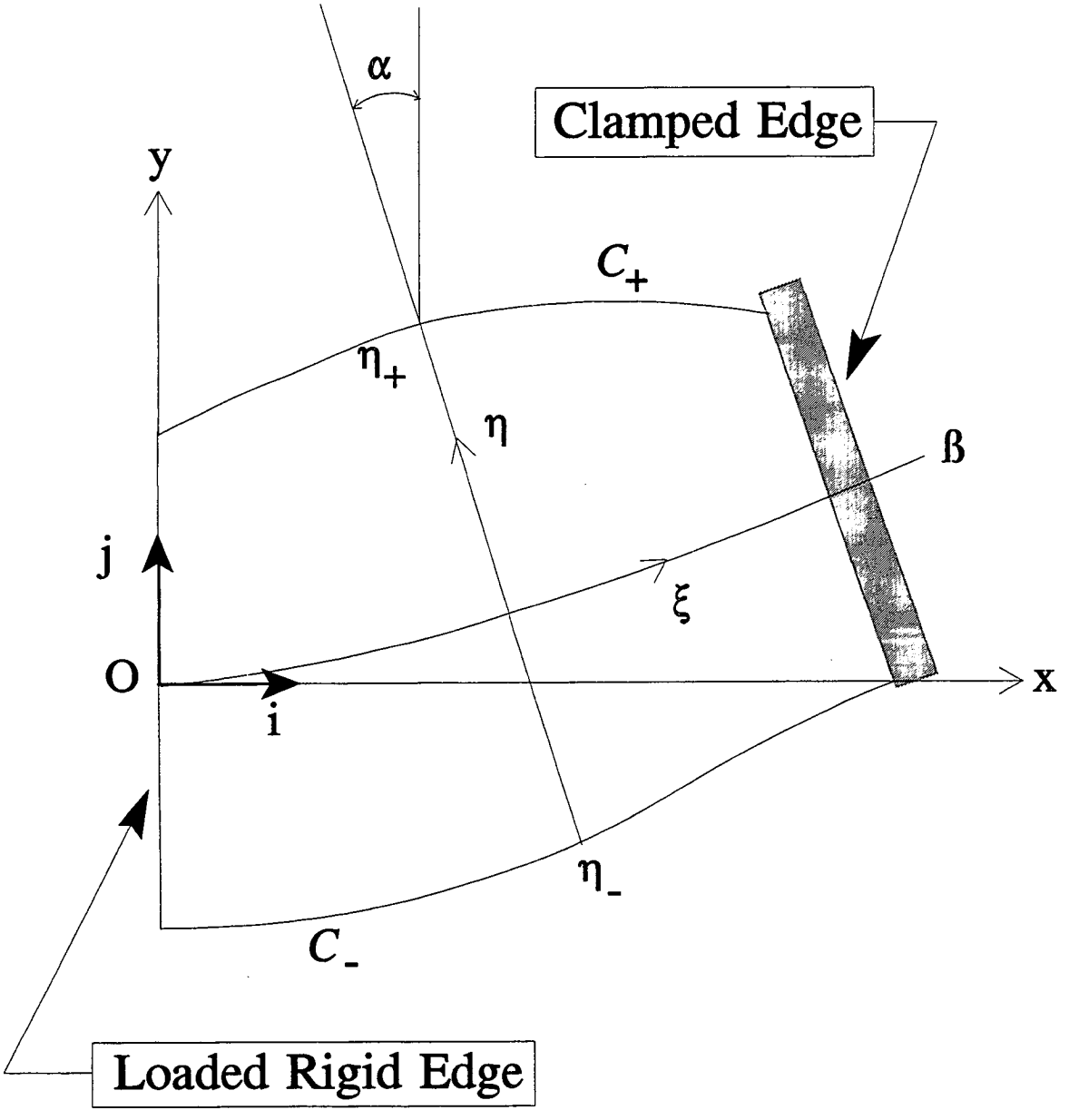

Figure 9. Definition of coordinate directions and curve ß on the developed midplane of an arbitrary plate.

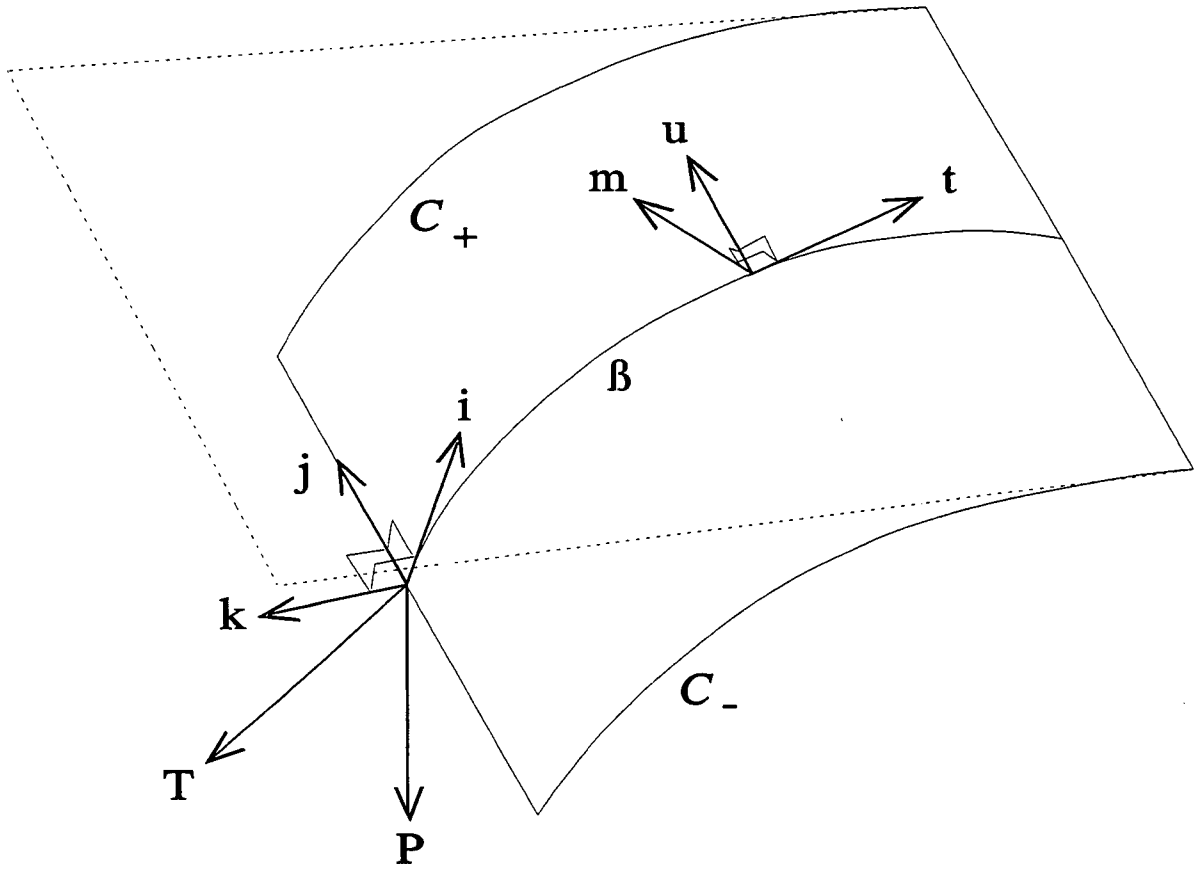

Figure 10. Geometry of an arbitrary plate showing definitions of coordinate systems and loading.

The velocity at any point on the surface is given by the time derivative of the position vector (13). Here, both ξ and η are time dependent, $\xi(t)$ and $\eta(t)$, so we get the following, where the dots represent differentiation with time:

$$\vec{v}_t = (1 - \eta g)\dot{\xi}\, \underline{t} \quad , \quad \vec{v}_u = \dot{\eta}\, \underline{u} \quad , \quad \vec{v}_m = 0\, \underline{m} \, . \tag{5}$$

Note that the velocity given for $\vec{v}_t$ differs from the velocity v^1 by a factor of $(1 - \eta g)$, although $\vec{v}_u = v^2$ and $\vec{v}_m = v^3$, since the second and third base vectors are identical, ie., $g_2 = \underline{\mathbf{u}}$ and $g_3 = \underline{\mathbf{m}}$.

The total derivative of the velocity will yield the acceleration of the particle. This is given (13) by the following formula :

$$a^q = \frac{dv^q}{dt} + \left\{ \begin{matrix} q \\ r \quad s \end{matrix} \right\} v^r \frac{dx^s}{dt} \, . \tag{6}$$

The symbol $\left\{ \begin{matrix} q \\ r \quad s \end{matrix} \right\}$ is a Christoffel symbol of the second kind (often represented by the symbol Γ^q_{rs}). This Christoffel symbol is a three-index quantity that relates the derivatives of the covariant base vectors as follows (13):

$$\frac{\partial g_r}{\partial x^s} = \left\{ \begin{matrix} q \\ r \quad s \end{matrix} \right\} g_q \, . \tag{7}$$

The curvilinear base vectors are orthogonal since the metric tensor has only diagonal components as shown in the following (13):

$$[g_{mn}] = [g_m \cdot g_n] = \begin{bmatrix} (1 - \eta g)^2 & 0 & 0 \\ 0 & 1 & 0 \\ 0 & 0 & 1 \end{bmatrix} . \tag{8}$$

The only non-zero Christoffel symbols of the second kind for an orthogonal curvilinear coordinate system are those in which two indices are equal (13). These were derived using Eq. 7 given above and are listed here:

$$\left\{ \begin{matrix} 1 \\ 1 \quad 1 \end{matrix} \right\} = - \frac{\eta g'}{1 - \eta g} \quad , \quad \left\{ \begin{matrix} 2 \\ 1 \quad 1 \end{matrix} \right\} = (1 - \eta g) g$$

$$\left\{ \begin{matrix} 3 \\ 1 \quad 1 \end{matrix} \right\} = (1 - \eta g) k \quad , \quad \left\{ \begin{matrix} 1 \\ 1 \quad 2 \end{matrix} \right\} = \left\{ \begin{matrix} 1 \\ 2 \quad 1 \end{matrix} \right\} = -g$$

$$\left\{ \begin{matrix} 1 \\ 1 \quad 3 \end{matrix} \right\} = \left\{ \begin{matrix} 1 \\ 3 \quad 1 \end{matrix} \right\} = -k \, .$$

The components of the acceleration can be calculated using the above Christoffel symbols and the velocities in terms of the natural basis by using Eq. 6 shown above. As with the velocities, the acceleration in terms of the first covariant basis vector will differ from the acceleration in the $\underline{t}$-direction by a factor of $(1 - \eta g)$. These accelerations were derived and appear as follows:

$$a^1 = \ddot{\xi} - 2g\dot{\xi}\dot{\eta} - \frac{\eta g'}{1 - \eta g}(\dot{\xi})^2$$

$$a^2 = \ddot{\eta} + (1 - \eta g) g (\dot{\xi})^2 \qquad \textbf{(10)}$$

$$a^3 = (1 - \eta g) k (\dot{\xi})^2 \, .$$

The corresponding accelerations in the **t**, **u**, **m**, basis are then:

$$\begin{aligned} a_t &= (1-\eta g)\ddot{\xi} - 2(1-\eta g)g\dot{\xi}\dot{\eta} - \eta g'(\dot{\xi})^2 \\ a_u &= \ddot{\eta} + (1-\eta g)g(\dot{\xi})^2 \\ a_m &= (1-\eta g)k(\dot{\xi})^2 \ . \end{aligned} \tag{11}$$

Following the work done by Nydahl (8), we can take an infinitesimal mass element on the surface subject to frictional and gravitational forces. Summing these forces in the **t**, **u**, and **m** directions we obtain the following balance equations:

$$\begin{aligned} \Sigma F_t &= mG_t - \mu N\frac{v_t}{|\vec{v}|} = ma_t \\ \Sigma F_u &= mG_u - \mu N\frac{v_u}{|\vec{v}|} = ma_u \\ \Sigma F_m &= mG_m + N = ma_m \ . \end{aligned} \tag{12}$$

In the above, μ is the coefficient of kinetic friction between the particle and the surface (not to be confused with the Euler parameter in the last chapter), the G_i's are the components of the acceleration of gravity acting on the particle, N is the normal force, and $|\vec{v}|$ is the magnitude of the velocity.

We can solve for the normal force by using the third equation above and the acceleration in the **m**-direction from equation (14) to get:

$$N = \left[(1-\eta g)k(\dot{\xi})^2 - G_m \right] m \ . \tag{13}$$

Dividing the balance equations (Eq. 12) in the $\underline{t}$ and $\underline{u}$ directions by the mass, substituting the above normal force, and recalling the form of the velocities given by Eq. 5 results in the following forms for a_t and a_u:

$$\sum \frac{F_t}{m} = G_t - \mu \frac{\left[(1-\eta g)k(\dot{\xi})^2 - G_m\right](1-\eta g)\dot{\xi}}{\left[(1-\eta g)^2(\dot{\xi})^2 + (\dot{\eta})^2\right]^{1/2}} = a_t$$

$$\sum \frac{F_u}{m} = G_u - \mu \frac{\left[(1-\eta g)k(\dot{\xi})^2 - G_m\right]\dot{\eta}}{\left[(1-\eta g)^2(\dot{\xi})^2 + (\dot{\eta})^2\right]^{1/2}} = a_u \quad . \tag{14}$$

Now, by substituting in the values for a_t and a_u from Eq. 11 we can solve for $\ddot{\xi}$ and $\ddot{\eta}$:

$$\ddot{\xi} = \frac{G_t + \eta g'(\dot{\xi})^2}{(1-\eta g)} + 2\dot{\xi}\dot{\eta} g - \mu \frac{\left[(1-\eta g)k(\dot{\xi})^2 - G_m\right]\dot{\xi}}{\left[(1-\eta g)^2(\dot{\xi})^2 + (\dot{\eta})^2\right]^{1/2}}$$

$$\ddot{\eta} = G_u - (1-\eta g)g(\dot{\xi})^2 - \mu \frac{\left[(1-\eta g)k(\dot{\xi})^2 - G_m\right]\dot{\eta}}{\left[(1-\eta g)^2(\dot{\xi})^2 + (\dot{\eta})^2\right]^{1/2}} \quad .$$

Numerical Approach

The relations governing the acceleration of the snow particle in the ξ and η directions is in the following form:

$$\ddot{\xi} = f\left[\xi, \eta, \dot{\xi}, \dot{\eta}\right]$$

$$\ddot{\eta} = f\left[\xi, \eta, \dot{\xi}, \dot{\eta}\right] \tag{16}$$

These second-order equations can be arranged as an equivalent system of first order ordinary differential equations as follows:

$$y_1 = \frac{d\xi}{dt} = \dot{\xi}\ , \qquad y_2 = \frac{dy_1}{dt} = \ddot{\xi}$$
$$y_3 = \frac{d\eta}{dt} = \dot{\eta}\ , \qquad y_4 = \frac{dy_3}{dt} = \ddot{\eta} \tag{17}$$

The initial conditions for this system are the initial values of ξ, $\dot{\xi}$, η, and $\dot{\eta}$. Single blade displacement snowplows are generally set with an "attack" angle with relation to the direction the snowplow truck travels as shown in Figure 11. The initial velocities in the ξ,η-coordinate system are calculated from the snowplow truck velocity, V_{plow}, using the "attack" angle, ϕ, as follows:

$$\dot{\xi} = -\frac{V_{plow}\cos\phi}{1 - \eta g}$$
$$\dot{\eta} = -V_{plow}\sin\phi \tag{18}$$

A program for determining large deformation of cantilevered plates was used to obtain the developable surface shape of a snowplow moldboard (or multiple sections of a moldboard). This program was similar to a program written by Darmon (14). Darmon refers to the program as the "Simmonds-Libai-Darmon" program, or "SLD" for short, since Simmonds and Libai developed the initial theory (11). The negative signs in the above definitions for the velocities arise from the coordinate definitions used in the SLD program. Movement from the bottom to the top edge of the moldboard is in the negative ξ-direction since the plate solution uses the loaded edge as the origin of the plate. This means that the initial ξ-value for the program is actually ξ_{max} given by the SLD program. The initial η-value can be given as any value between η_+ and η_- at the clamped edge of the plate. The program uses eleven equally spaced η-values across the clamped edge which ordinarily will result in ten separate flow lines (this would give eleven only if $\phi = 0$).

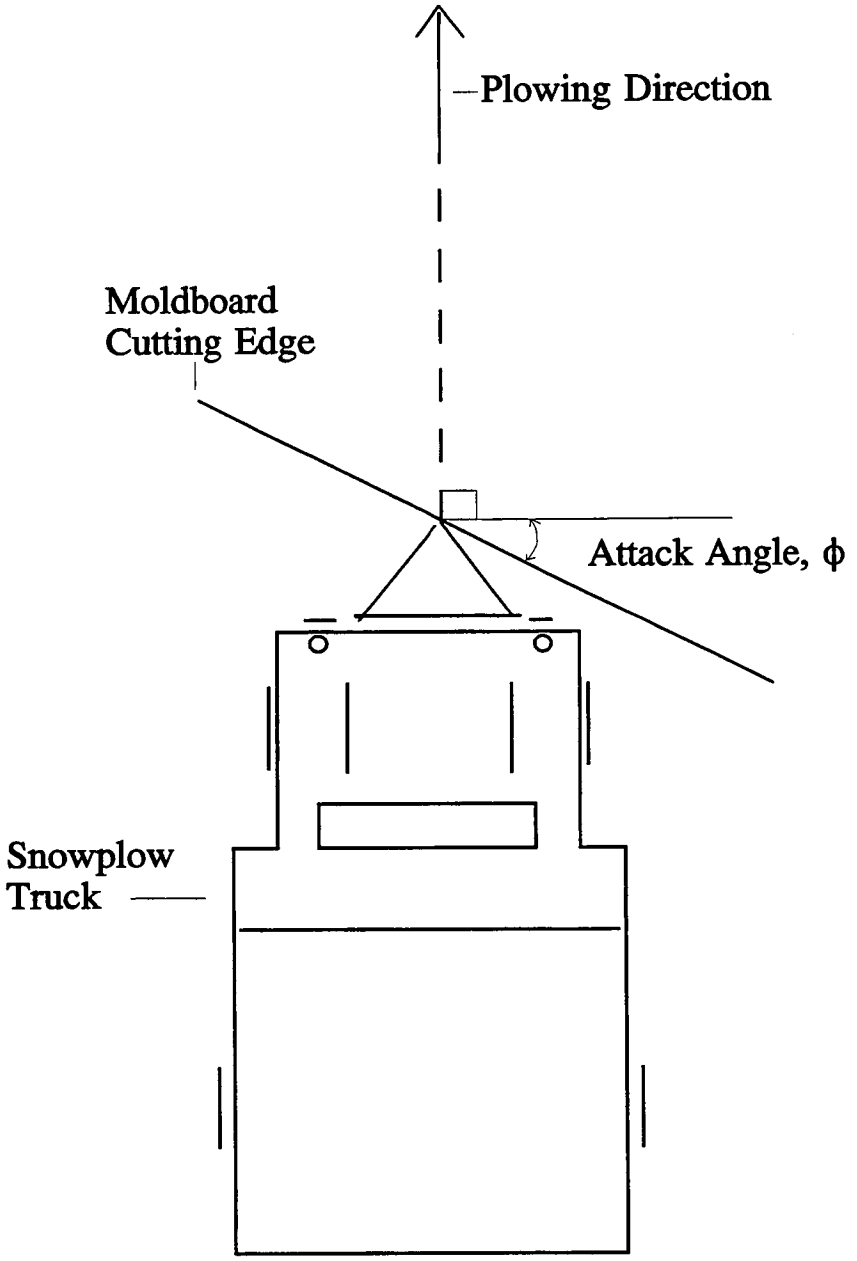

Figure 11. Definition of the Attack Angle, ϕ.

The other input variables that must be given in order to solve this problem are the coefficient of kinetic friction, μ; the acceleration of gravity, G; the clamp angle used in the SLD program; and the width of the plow. The plow width is needed since the SLD program data is given in a non-dimensional form.

A simplified flow chart is given in Figure 12 showing how these equations are solved. Here, the bold lines show the main route of the program and the boxes represent input and output files. The file "curv.out" from a run by the SLD program is input into the program. This file contains the geometric information, such as the normal and geodesic curvatures, given at discrete values of ξ. This information is dimensionalized by the plow width. Then tables are formed using spline interpolation routines "spline" and "splint" (15). The subroutine "rhside" retrieves values from these tables and uses this information evaluating the differential equations given above. A relatively simple fourth order Runge-Kutta method was used to solve these equations (15). The solution is stopped when either the particle leaves the boundaries of the moldboard or the particle loses contact with the plate.

The position, velocity, and acceleration of the particle in the ξ,η-coordinate system are written to the file "snow.out". The frequency of this output is controlled by the input parameter "nprint" given in the file "flow.dat". The velocity components and magnitude just prior to the particle leaving the moldboard surface in terms of a coordinate system attached to the cutting edge of the moldboard are written to the file "snow.sum". The coordinates of the particle at each solution point in terms of the cutting edge coordinate system are written to the file "snow.gra". This file can be used in conjunction with the SLD file "graf.out" to construct a three-dimensional model of the moldboard and the flow lines for a given problem.

The details of the program execution along with a listing of the input file, program, and sample output are given in Appendix B of (10). A brief explanation of how to get the desired input from the SLD program (file "curv.out") for different moldboard geometries is also given in this Appendix.

Numerical Results

The "flow" program was checked by comparing its results to the existing solutions for a cylinder and a flat plate.

The cylinder solution (2) is used for the first comparison. This solution is limited to flow in the ξ-direction (η is constant) but does include the effects of friction and gravity. The closed

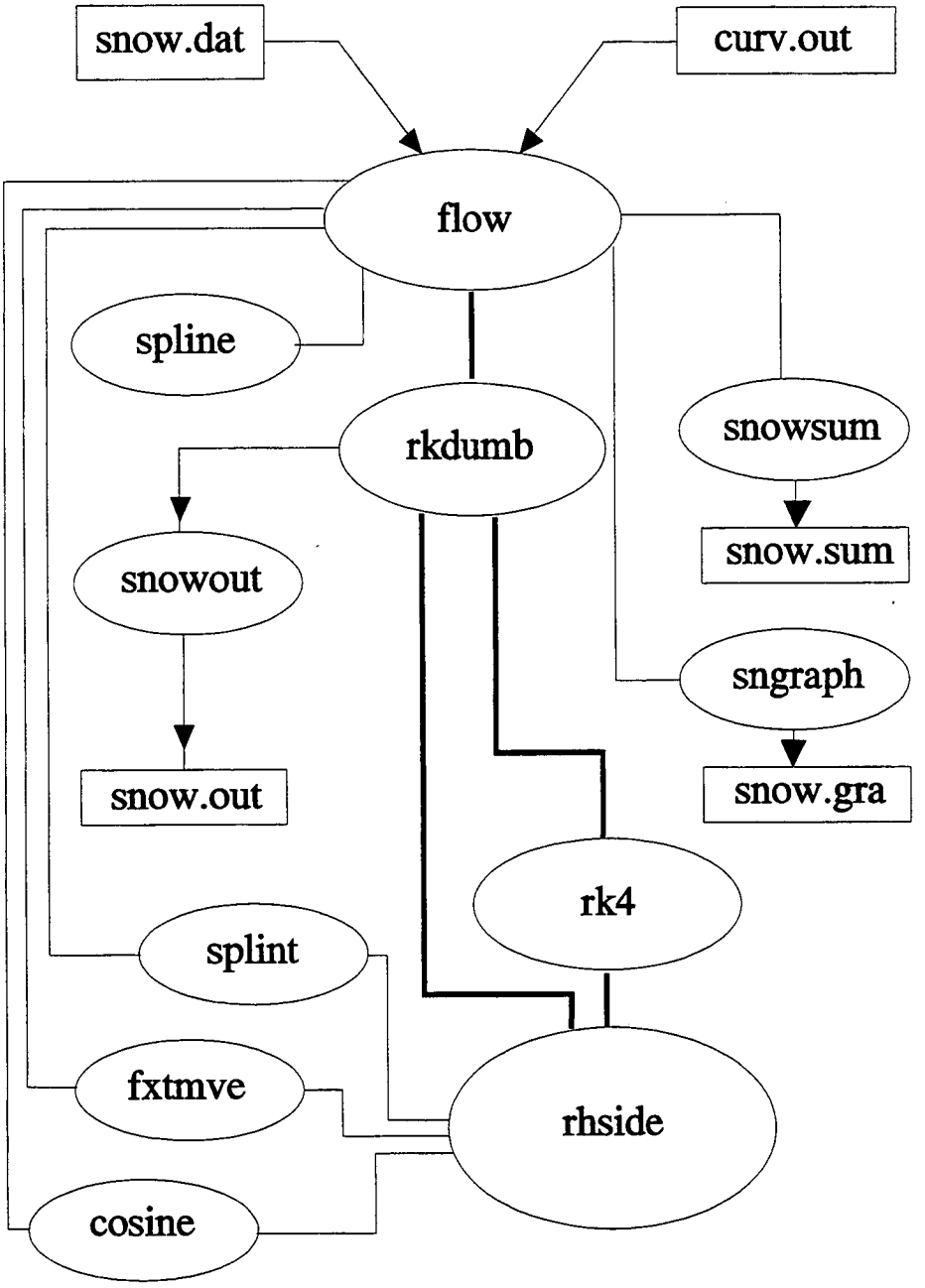

Figure 12. Layout of the Flow Program.

form solution for a cylindrical moldboard with an attack angle equal to zero ($\phi = 0$) is given by Shalman (2) as:

$$V = \sqrt{\frac{v_o^2 + 2Rg}{\exp(2C_f\tau)} - \frac{2Rg[2C_f\sin(\tau + \mu_0 + \phi) - \cos(\tau + \mu_0 + \phi)]}{(1 + 4C_f^2)\cos\phi}} \qquad (19)$$

In the above, the coefficient of friction is denoted by C_f, $\phi = \tan^{-1} C_f$, the angles μ_0 (the angle between the blade edge and the road) and τ (the angle locating the particle relative to the leading edge of the moldboard) are given in Figure 13 (2) and gravitational acceleration is given by the symbol g. The equations for the accelerations in the ξ and η directions using the present theory simplify to the following for a cylinder with a attack angle of zero:

$$\ddot{\xi} = G_t - \mu(k(\dot{\xi})^2 - G_m)$$
$$\ddot{\eta} = 0 \qquad (20)$$

The Shalman equation and the "flow" program results are shown in Figure 14. The results are identical which shows that the "flow" program correctly collapses to the simple case solved by the Shalman equations. The two cases shown are for a cylinder with μ_0 of 30 degrees, a radius of curvature of 1.0 m (normal curvature, $k = 1.0\ m^{-1}$), initial velocity of 10 m/s, and coefficient of friction (C_f or μ) of 0.3 both with and without the effects of gravity ($g = -9.81\ m/s^2$). The importance of including the effect of gravity in this problem is shown by the drop in the exit velocity ratio of approximately twenty percent as compared to the case without gravity.

The second comparison is with the equations for flow over a flat plate developed by Nydahl (8). Figure 15 shows the symbols used for this case. Here, μ is the angle the flat plate is inclined with respect to the horizontal road surface (in the "flow" parameters, $\mu = 90^0 + \Omega$), the angle θ_0 is identical to the attack angle, ϕ, and again the gravitational acceleration is g. Nydahl used complex variables to solve for the velocity and Cartesian coordinates of a particle

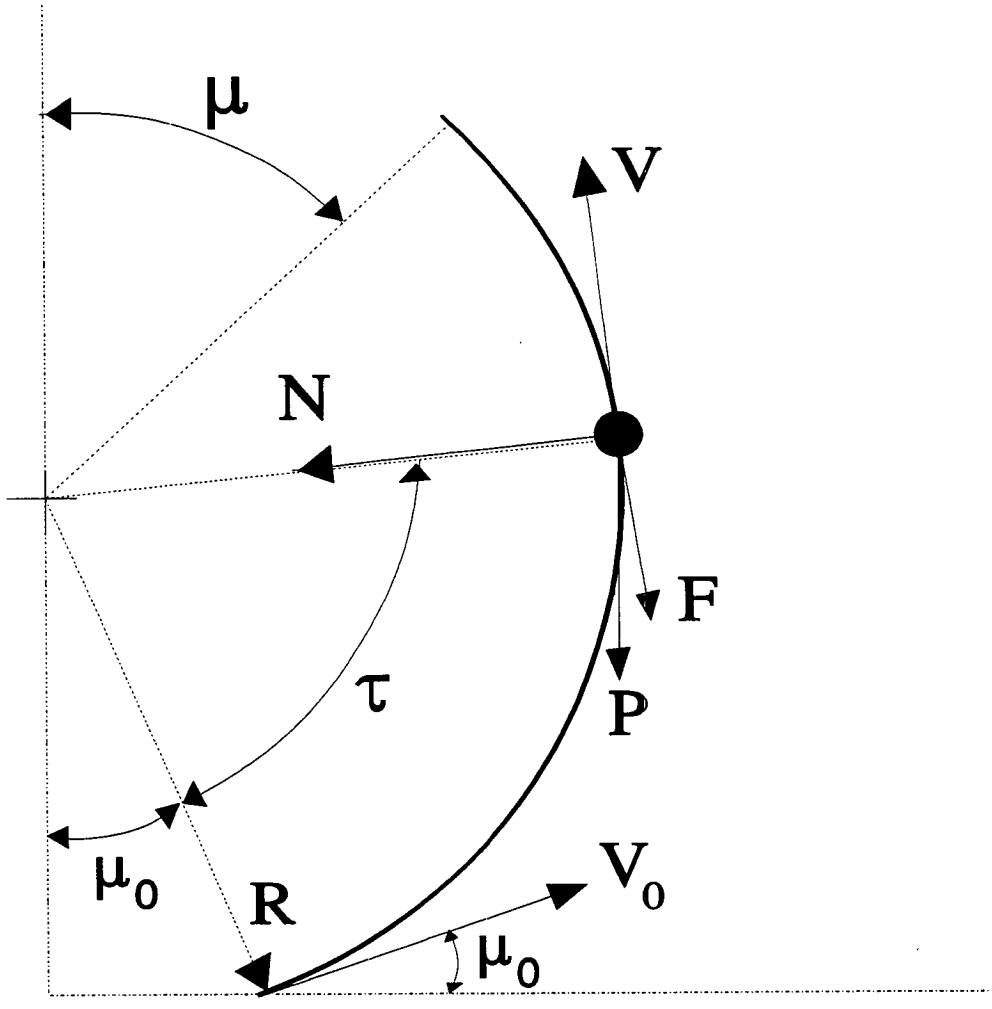

Figure 13. Description of the Parameters Used in Shalman's Cylindrical Analysis.

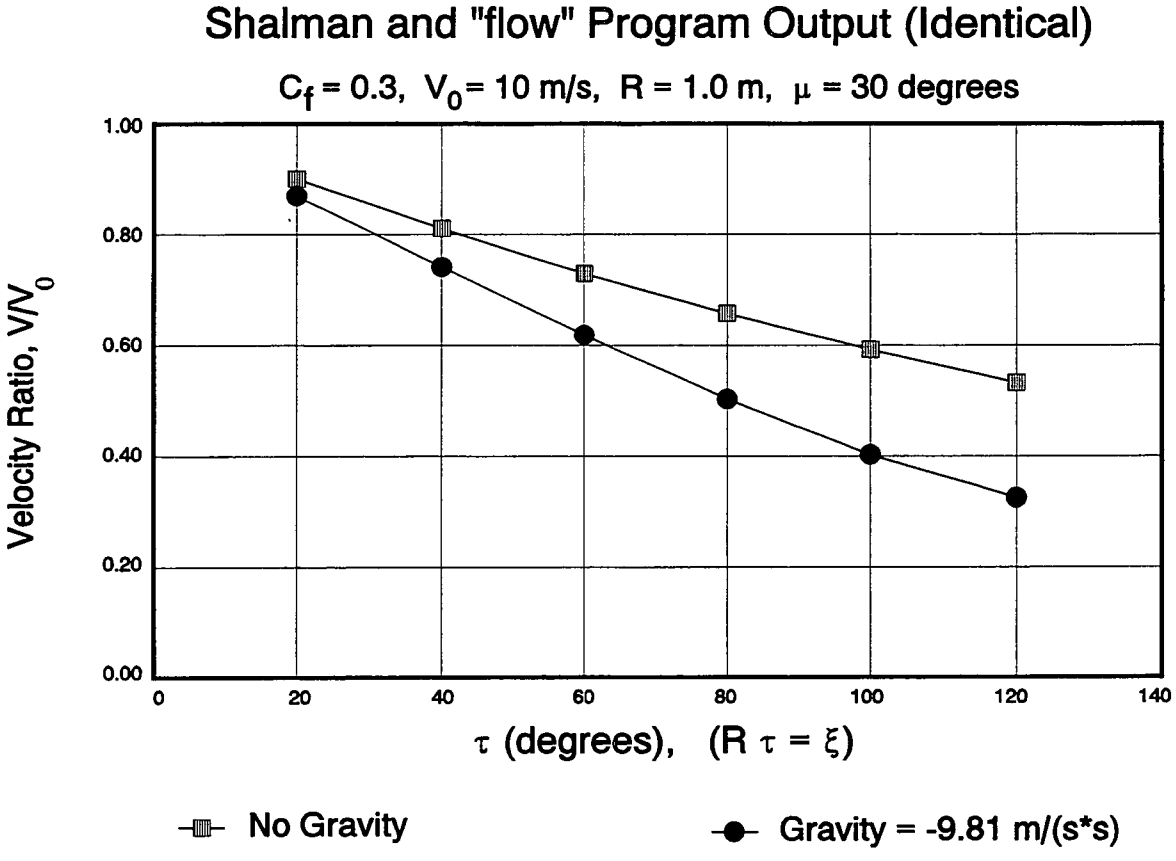

Figure 14. Comparison of the Results from Shalman's Cylindrical Model and the Current Theory ("Flow" Program) Showing the Effects of Gravity and Friction on the Velocity Ratio.

on the flat plate. The final form of these equations is:

$$V = V_0 \left[\frac{\sin\theta_0}{\sin\theta}\right]\left[\frac{\tan(\theta_0/2)}{\tan(\theta/2)}\right]^{C_f \cot\mu}$$

$$y = \frac{V_0^2 \sin^2\theta_0 (\tan(\theta_0/2))^{2C_f \cot\mu}}{g \sin\mu} \int_{\theta_0}^{\theta} \frac{csc^3\theta \cos\theta \, d\theta}{(\tan(\theta/2))^{2C_f \cot\mu}}$$

$$x = \frac{V_0^2 \sin^2\theta_0 (\tan(\theta_0/2))^{2C_f \cot\mu}}{g \sin\mu} \int_{\theta_0}^{\theta} \frac{csc^2\theta \, d\theta}{(\tan(\theta/2))^{2C_f \cot\mu}}$$

Since the curvatures are zero for a flat plate, the "flow" program equations for the accelerations in the ξ and η directions reduce to the following:

$$\ddot{\xi} = G_t + \mu \frac{G_m \dot{\xi}}{\sqrt{(\dot{\xi})^2 + (\dot{\eta})^2}}$$

$$\ddot{\eta} = G_u + \mu \frac{G_m \dot{\eta}}{\sqrt{(\dot{\xi})^2 + (\dot{\eta})^2}} \qquad (22)$$

A simple fortran program was written to integrate the flat plate equations so that the results could be compared with the "flow" program results. The integration is stopped when the particle is within a certain "epsilon" of the edge of the plate (either x or y extent). This program is listed in Appendix B of (10). Two arbitrary cases were compared: the first had V_0 = 15 m/s, plate width = 3 m, plate height = 2 m, C_f = 0.30, $\mu = 50^0$ (clamp angle, Ω, = 140^0), an attack angle (θ_0 or ϕ) = 20^0, and g = 9.8 m/s^2; the second case was identical except the

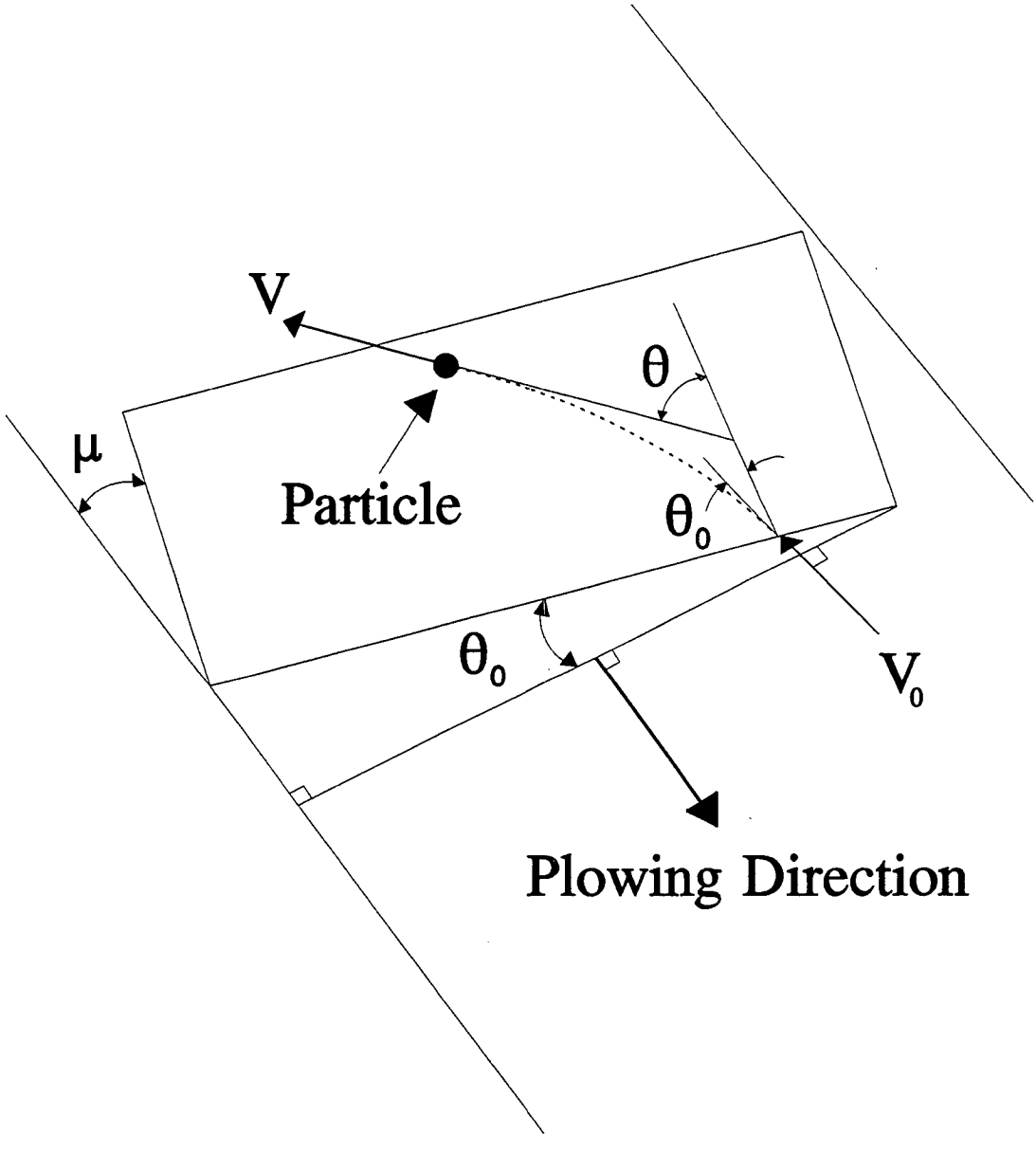

Figure 15. Geometry and Symbols for the Flat Plate Solution.

attack angle was increased to 40^0. The results from both methods are shown in the following table:

Table 1
Comparison of "Flow" Program and "Flat Plate" Solutions

Exit Values	θ_0 = 20 Degrees		θ_0 = 40 Degrees	
	Flow	Flat Plate	Flow	Flat Plate
x (m)	0.758162	0.758160	1.788311	1.788316
y (m)	2.000000	1.999994	2.000000	2.000004
Velocity (m/s)	13.6706	13.6707	13.5952	13.5952

This table shows that the results for both methods are identical up to the precision requested of the program.

Experimental Snowplow

Three experimental snowplows were built by the University of Wyoming for testing purposes as part of the SHRP project (16). The geometry of the second experimental snowplow is shown in Figure 16. This snowplow consists of a flat plate snow scoop connected to a large flat plate moldboard that had a top section (cylindrical or conical shape) that can pivot. The plow is 3.66 m (12 ft) wide with the top section pivot located in the middle. Testing of this plow was done during the winter of 1991 in West Yellowstone, Montana (16). Part of the testing included video taping the snowplow plowing a strip of fresh snow. The snow strip was marked with spray paint stripes running both parallel and perpendicular to the plowing direction. The snowplow truck was equipped with a counter that was monitored by a computer acquisition system from which truck velocities could be obtained from each run. Two test runs (run #85 and run #171) were chosen (with cylindrical top sections) to compare to the current flow theory. The cylindrical head of the moldboard was pivoted at 12° angle to the horizontal in run #85 and was not tilted (pivot angle of zero) so that it had a symmetric shape in run #171.

The "flow" program was adapted to handle the case corresponding to the above snowplow ("plow" program). Three separate SLD runs were required to obtain the information needed

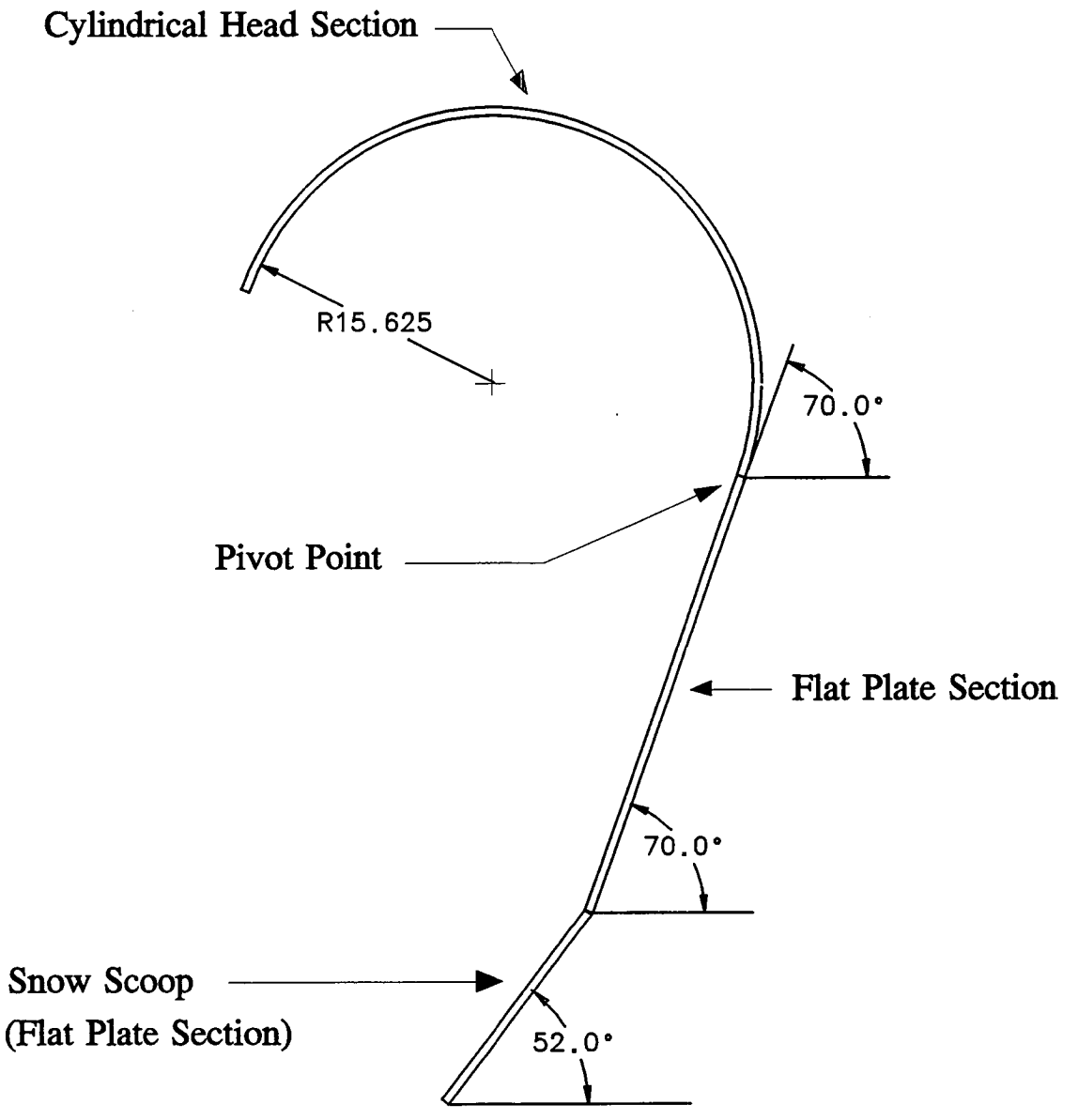

Figure 16. Geometry of the Second Experimental Snowplow.

for each section of the snowplow. The outlet of the first section becomes the inlet to the second section and the same holds for the second and third section. The new input file "plow.dat" contains a clamp angle for each section and the tilt angle of the top section in addition to the information required in the "flow" program input file. The basic workings of the "plow" program are identical to the "flow" program. The only major difference is that the "plow" program must solve the trajectories for three separate surfaces. The program listing and input files for the "plow" program are listed in Appendix C of (10).

Figures 17 and 18 contain one frame from run #85 and run #171, respectively, along with the particle paths predicted by the "plow" program (insets). The input data for the "plow" program used a coefficient of kinetic friction, μ, of 0.04 and a gravitational acceleration of 9.81 m/s^2 (32.17 ft/s^2). This value for μ was chosen since the "snow scoops" were made of a polyethylene material and the other snowplow surfaces were composed of a fairly smooth composite material. The μ value is approximate, since values for snow vary over wide ranges for most materials depending on the type of snow, the ambient temperature, and applied pressures (2,17,18). The truck velocity in run #85 was 13.3 $\pm$ 0.1 m/s (43.6 $\pm$ 0.4 ft/s) and for run #171 was 13.5 $\pm$ 0.1 m/s (44.4 $\pm$ 0.4 ft/s).

The graphical results from the "plow" program were rotated and sized until the geometry outlines matched closely with the video frame. These figures show that there is good agreement with the flow lines in the actual test and the "plow" program output for most of the plow in both cases. It appears that the flow in the cylindrical head is not modelled well by the "plow" program for these cases. A likely reason for this is that the current flow theory does not take into account any wind effects on the snow. These tests were run with fairly low density snow (approximately 100 kg/m^3 (0.194 $slugs/ft^3$)). It seems that the cylindrical head must have a significant air flow through it at plowing speeds which affects the flow of the snow in this region (little effect is seen on the flat plate sections). The effects of the air flow on the snow flow will be reduced for more dense snows, less tightly curved moldboard surfaces, and lower plowing speeds.

General Flow Program

The previous "flow" and "plow" programs rely on the geometrical data obtained from the SLD program. This is fine for finding the flow characteristics of existing snowplows, but is inconvenient for use as a design tool. A more general and efficient method is to obtain the necessary geometric data from a general space curve. This divorces the flow studies from the mechanical aspects of the large deformation of a moldboard which reduces the complexity of the problem. The arc-length can now have its origin at the moldboard origin (nearest the road) rather than at the top edge of the moldboard (as was required when using the SLD program).

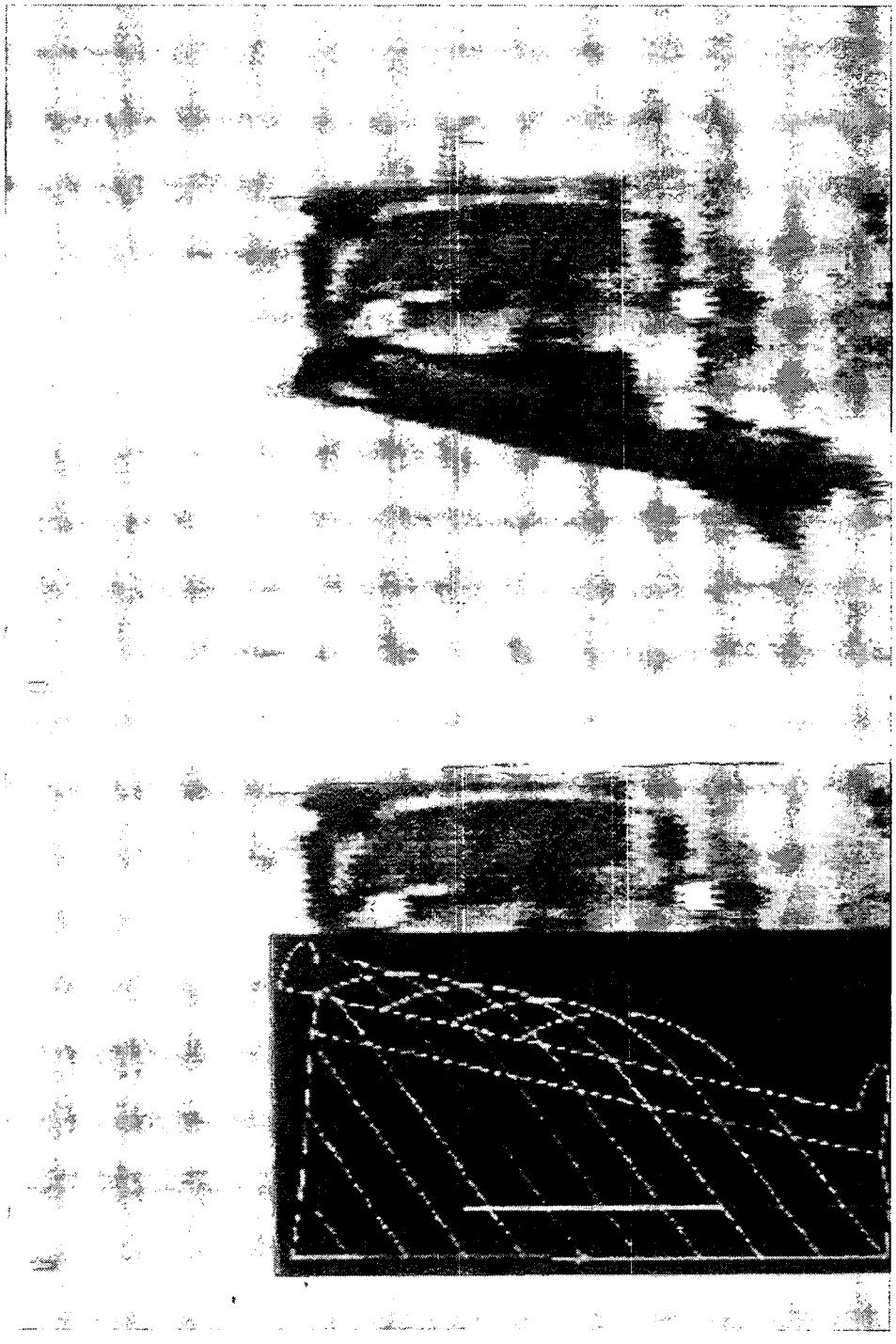

Figure 17. Comparison of Flow Trajectories for the Second Experimental Snowplow with Cylindrical Head Tilted 12 Degrees from the Symmetrical Configuration.

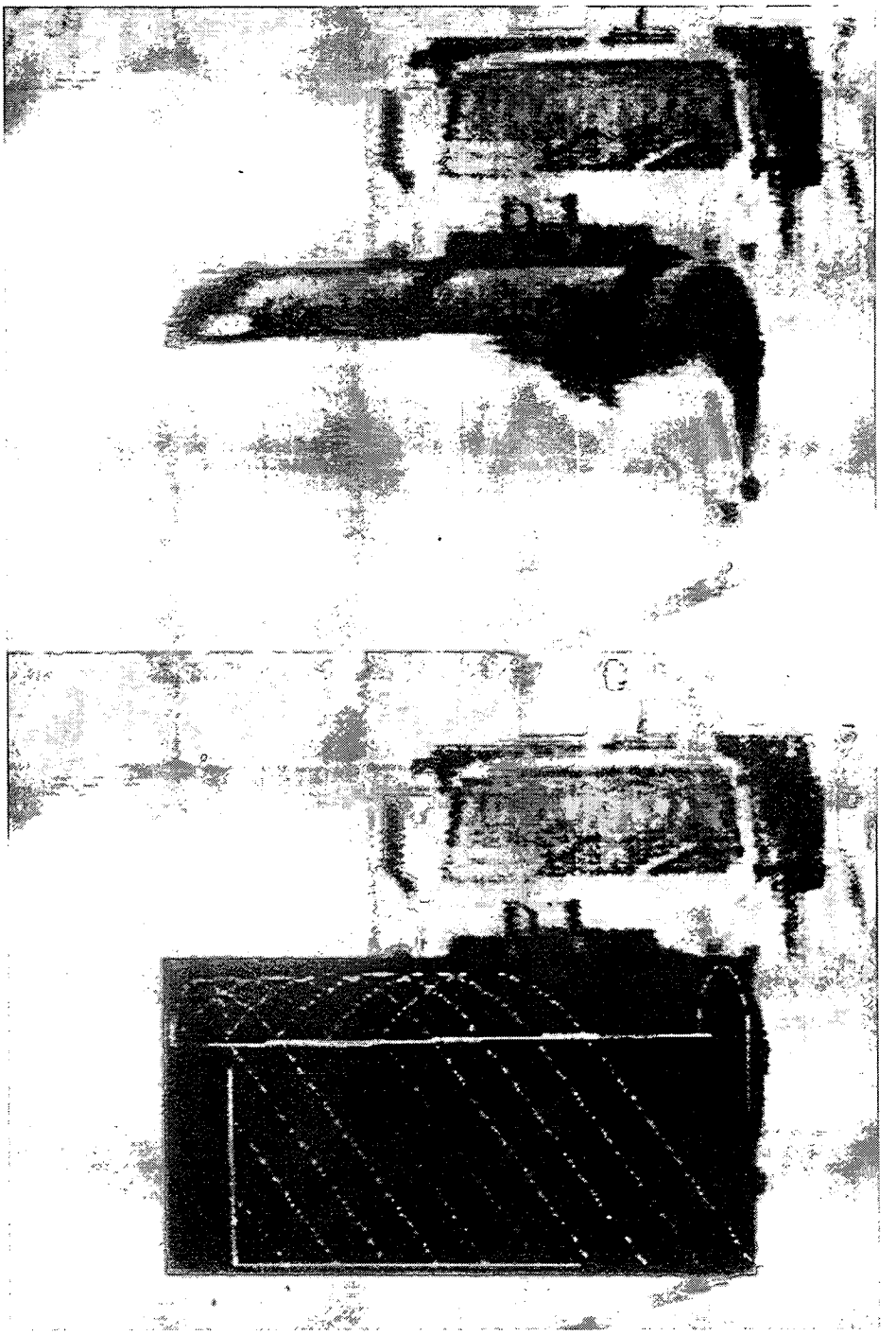

Figure 18. Flow Trajectory Comparison for Second Experimental Snowplow with Cylindrical Head in Symmetrical Configuration.

To distinguish between the former arc-length measure (from the top edge to the bottom) given by the greek letter "ξ", the new length along the space curve will be denoted by the letter "s". The "natural" equations of a space curve are obtained by specifying the curvature, κ(s), and the torsion, τ(s), for the arc-length of the space curve, s, greater than zero. For single-valued continuous functions for κ(s) and τ(s) there exists only one space curve (12).
The integral for the torsion of the space curve ß defining the developable surface for the Simmonds-Libai theory defines the angle ψ as follows:

$$\psi = \int_0^{\xi} \tau(t)\,dt + \psi_0 \,. \tag{23}$$

The normal and geodesic curvatures are then given by:

$$\begin{aligned} k &= \kappa \cos(\psi) \,, \\ g &= \kappa \sin(\psi) \,. \end{aligned} \tag{24}$$

Once the curvature, κ(s), and the angle ψ(s) are specified, the normal and geodesic curvatures are known.

Only ten equations need to be solved to determine the developable surface shape when the above curvatures are given. These are the angle α, the Cartesian coordinates for the plate (u,v), the Euler parameters for the orientation of the curve, and the vector function for $\underline{X}(s)$.

The origin of the space curve for this solution was chosen at the fixed clamp since the solution of these equations is not tied to the load applied at the leading edge. This simplifies the transformation from the developable surface coordinates to global Cartesian coordinates and yields surface coordinates that are easier to comprehend.

Once the plate equations are solved, the solution for the trajectories, velocities, and accelerations of a particle traveling over this surface is very similar to the "flow" implementation. The only changes are simplifications due to the change in defining the origin of the space curve such as redefining the initial conditions for the location and velocities of the particle and the components of gravity.

Cubic spline interpolation was chosen for presenting the functions $\kappa(s)$ and $\psi(s)$ (19). This choice gives continuous first and second derivatives for these functions. The first derivative of these functions is needed to determine the derivative of the geodesic curvature given by the following:

$$g' = \kappa' \sin(\psi) + k\,\psi', \tag{25}$$

where the normal curvature, **k**, is given above.

The organization of the subroutines used, along with the input and output files for the "general flow" program, are shown in Figure 19. Again, the bold lines show the main route of the program and the boxes represent input and output files. The program is separated into two different segments. The path starting with the "genplat" subroutine calculates the shape of the developable surface and the path starting with "rkfehl" calculates the particle trajectories over this surface.

The input for the program is split into two files. The file "flow.dat" contains the width, height, initial alpha, blade angle, attack angle, initial particle velocity (truck velocity), coefficient of sliding friction, acceleration of gravity, initial step size and precision for the plate and trajectory integration subroutines ("pltfehl" and "rkfehl"), the number of values to print out, the estimated total time for a single trajectory across the surface, and whether the plate solution is symmetric or not (the plate solution is simplified when ψ = zero, and there is no initial alpha value).

The file "coef.dat" contains the values for the curvature, κ, and angle ψ at five equidistant locations along the arc length of the space curve. These values are used by "spline" to construct an interpolation table. The interpolated values and first derivatives for κ and ψ are passed to "xkappa" by the subroutine "xsplint" (15). There are several restrictions on the valid range of values of κ and ψ for modeling a snowplow moldboard. If the normal curvature, **k**, changes sign along the surface it means that the surface has gone from a convex to a concave shape in this region. This will most likely cause the particle to loose contact with the surface at this point. Although this particle may reattach itself to the surface at some other point, the current model cannot account for this. Also, values for ψ should be between $\pm \pi/2$. This really is restating the previous condition that the normal curvature not change sign, since at $\psi = \pm \pi/2$ the normal curvature vanishes. This also keeps the space curve "behaving" nicely (keeps it from becoming helical with many loops). In practice, the limits on ψ are more stringent than the above. A tangential developable surface "consists of two sheets which are tangent at the edge of regression along a sharp edge" (12). The intersection of these two sheets is referred

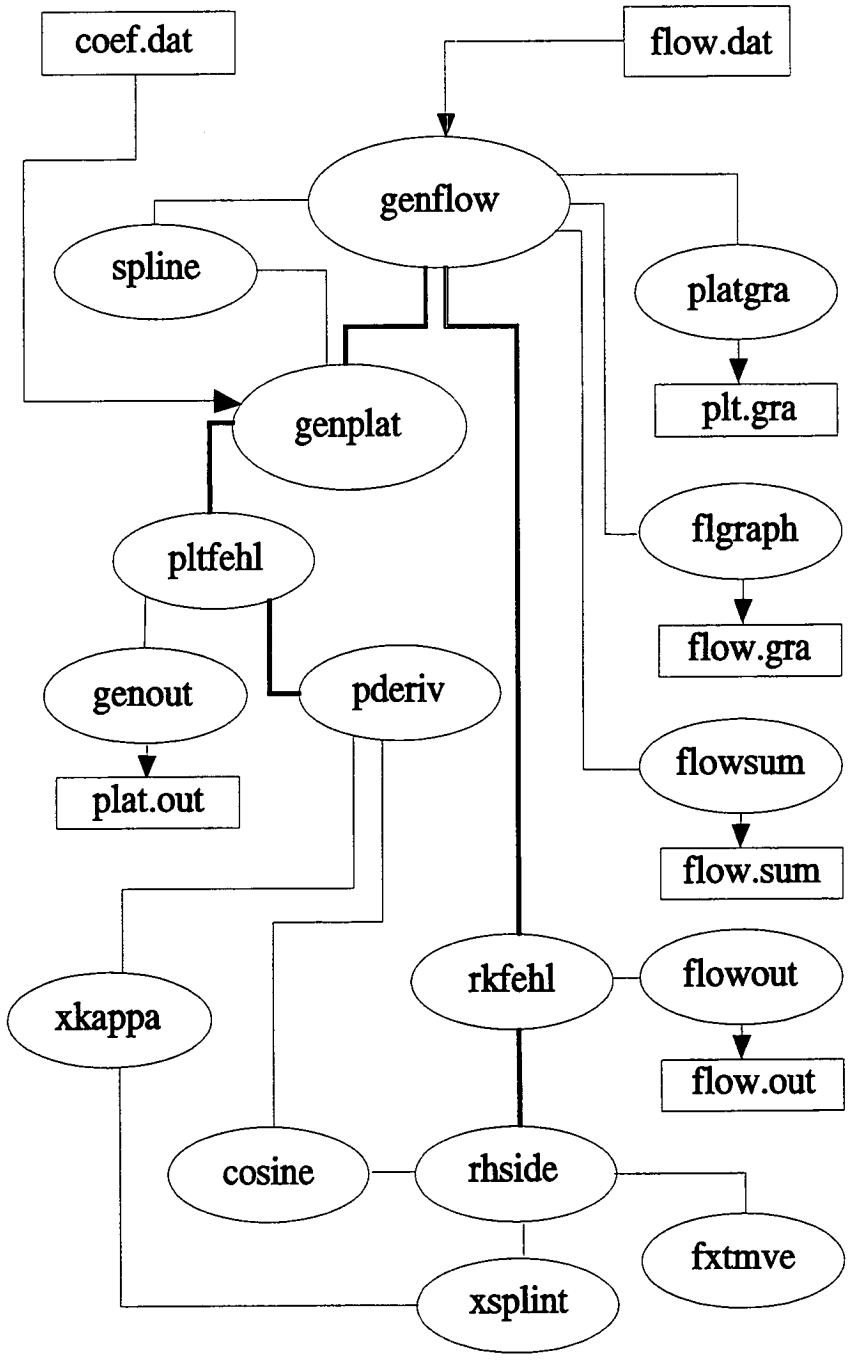

Figure 19. Structure of the "General Flow" Program.

to as the "cuspidal edge". If this edge intersects the physical plate there will be a sharp edge in the plate that will cause a singularity in the integration of the flow trajectories. Simmonds and Libai stated that the edge of regression could be obtained by substituting the inverse of the geodesic curvature into the parametric representation of the deformed plate given by Eq. 1 (11). This implies that the edge of regression will "fall into" the physical plate if the inverse of the geodesic curvature is ever less than the value of η at the edge of the surface. Rather than $\eta_{\pm}$, a value a bit larger than half the width is used as a check for this, since the maximum η-values are unknown prior to using the curvatures to calculate the shape of the developable surface.

The height that is input to the program will be the maximum arc-length, s_{max}, when the geodesic curvature is zero ($\psi(s)$ = zero). When the space curve has a torsion the final value of s_{max} will be less than the height. In the SLD program, the final arc-length was also an unknown (ξ_{max}). The difference here is that the new space curve has the origin at the clamp, while the SLD program had the origin at the loaded edge.

An adaptive step size Runge-Kutta-Fehlberg method (19) was used to solve the ordinary differential equations for both the plate "pltfehl" and the particle trajectories "rkfehl". These two subroutines differ only in the stopping criteria used. The plate solution is stopped when the space curve ß reaches the edge of the plate. The value of the arc-length, s, that this occurs at is generally unknown at the start of integration. The integration of the particle path is stopped either when the particle reaches the edge of the plate, or the particle looses contact with the plate surface. A refinement routine (bisection of the step size) is used by both of these subroutines in order to get precise values of these occurrences.

The output of this program is very similar to the "flow" program output. The only additional file is the file "plt.gra". This file contains the Cartesian coordinates of the edge points for the developable surface. The "flow.gra" and "plt.gra" files can be used to plot the outline of the deformed shape and the particle trajectories along the shape. A small fortran program, "addk.f", was written that reads in these two files and outputs the data in a form that can be input into the I-DEAS™ (20) finite element modeler. The resulting I-DEAS™ program file can be read into the geometric task of the I-DEAS™ finite element program in order to view the particle trajectories over the surface.

Three sample runs are listed in Figures 20, 21, and 22. These three runs have identical geometries. The particles are exposed to the effects of gravity, the surface was given a friction factor of 0.10, and the surface has a "blade" angle of 70 degrees for Figure 20. The surface was tilted back another 20 degrees ("blade" angle of 50 degrees) in Figure 21. There is a marked difference between these two flows. When the surface was tilted back another 20 degrees the particles loose contact with the surface and the trajectories are not leaving from the

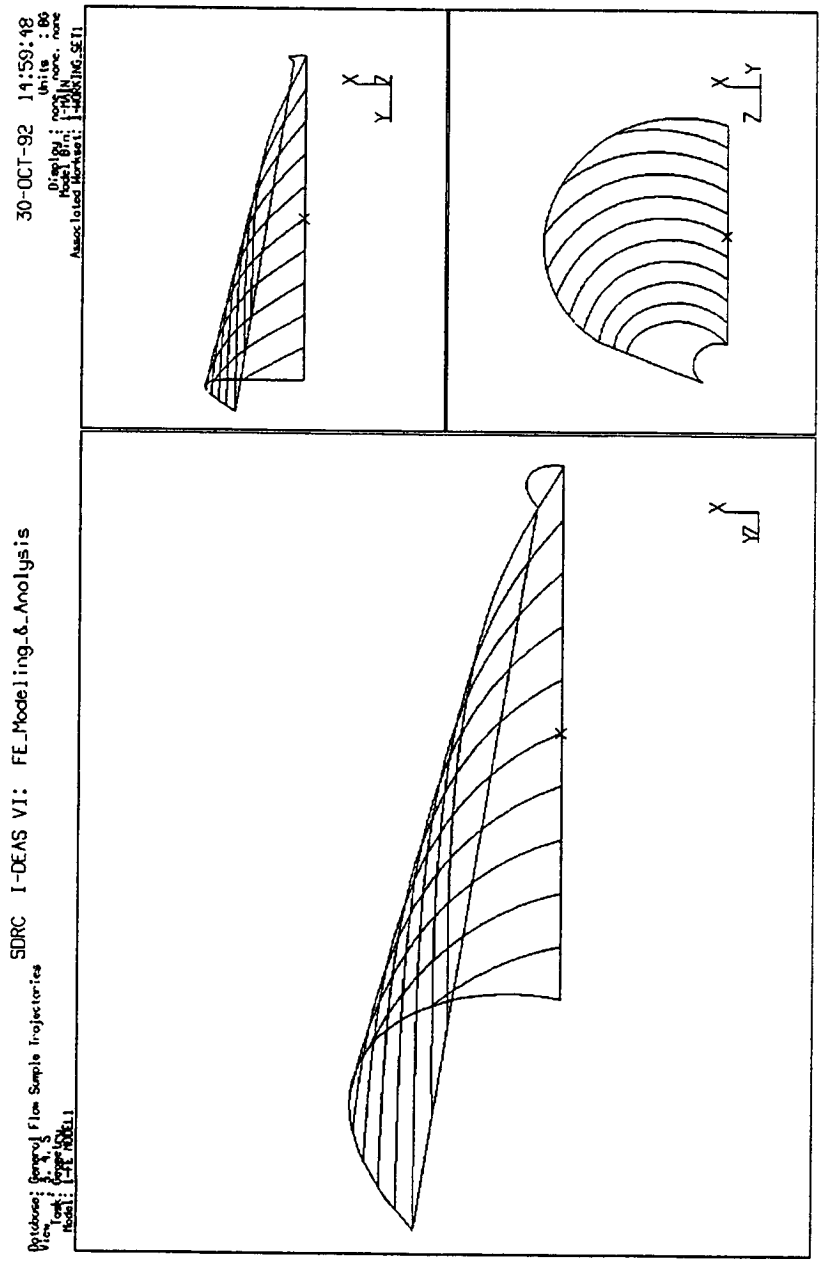

Figure 20. Sample Moldboard Shape and Particle Trajectories Predicted by the "General Flow" Program with a "Blade" Angle of 70 Degrees, and the Inclusion of Frictional and Gravitational Effects.

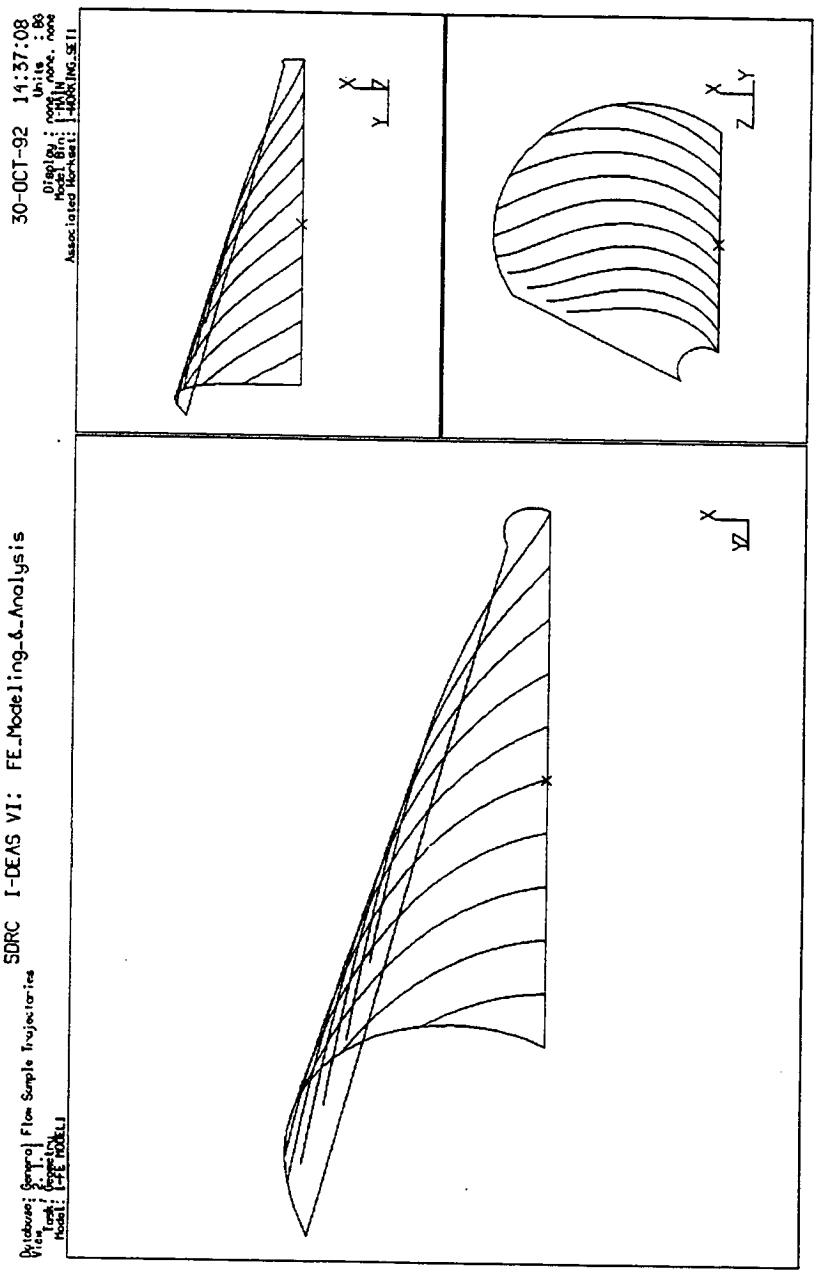

Figure 21. Sample Moldboard Shape and Particle Trajectories with a "Blade" Angle of 50 Degrees and the Effects of Gravity and Friction.

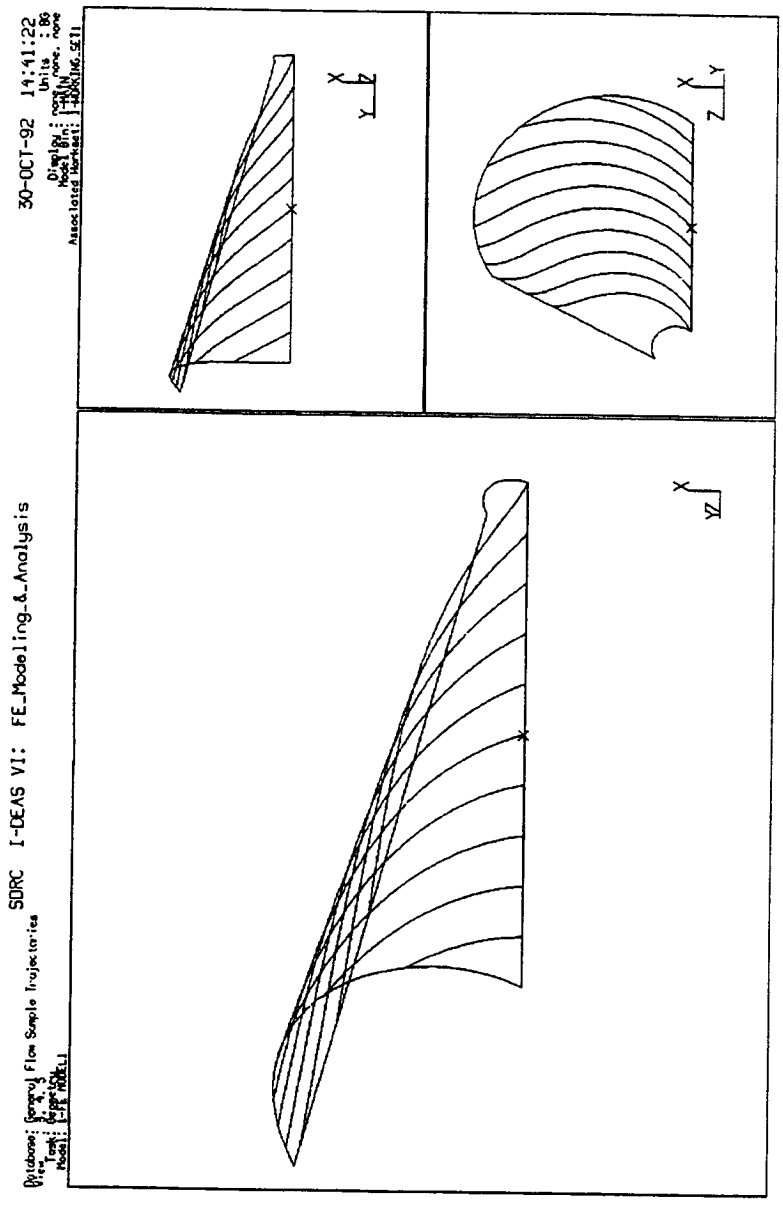

Figure 22. Sample Moldboard Shape Showing Trajectories Predicted with the Absence of Gravitational or Frictional Effects and a "Blade" Angle of 50 Degrees.

front edge of the surface. Figure 22 has the same "blade" angle as Figure 21 but the effects of friction and gravity are absent. These figures show that the inclusion of gravity and friction, as well as different "blade" angles in the problem yield significantly different flow patterns for the same geometry.

The program listing for the "general flow" program, sample input files, sample output files are listed in Appendix D of (10).

Conclusions

The initial purpose of the moldboard analysis was the development of a numerical model that would solve for the particle trajectories using the theory as developed by Nydahl (8). This particle theory was formally developed by Crane (10) using a tensor calculus approach. The numerical approach to calculating the particle acceleration, velocity, and position gave identical results as the less general existing approaches. Comparison with experimental video data showed good correlation but indicated that some other effects may be important in the actual flow of snow over a moldboard.

The "general flow" program was written to add more flexibility to the study of snow flow over a moldboard and to compress the numerical solution into a single program. The "general flow" program for determining velocities and trajectories of particles over a developable surface has much greater applicability and versatility than any previously developed method for determining optimal snowplow moldboard designs. Previously developed methods used to solve specific cases lacked generality, and generally did not include frictional or gravitational effects. The "general flow" program will cover all tangential developable shapes and includes both gravitational and frictional effects (if desired). Thus, this new program should cover all previous methods and allow for analysis of new snowplow shapes. The total time for calculating ten snow particle trajectories (with the effects of gravity and friction included) and plotting the results for viewing on the computer is on the order of two minutes. This allows for a great number of comparisons in relatively little time. The nearly instantaneous feedback one receives when running this program may yield moldboard shapes that move snow more effectively than existing designs.

Materials

Moldboard

The most commonly used material for the moldboard flow surface is steel. In recent years a variety of polymers have been used. Polymers can be shaped into developable surfaces at low cost. They offer manufacturing alternatives which may be lower cost than comparable steel systems. In addition, the sliding friction coefficient of snow along polymer surfaces is generally lower than for steel surfaces as shown in Figure 9. At the same time some polymers exhibit acceptable wear resistance as shown in Figure 10. Ultra high molecular weight polyethylene (UHMWPE) has been used successfully on commercially available plows for nearly a decade. In spite of its good wear resistance UHMWPE has been observed to suffer surface gouging, most likely from sand used to improve traction, which results in small scale surface roughness. This is expected to increase the surface friction. This effect has not been studied to date.

It should be noted that adhesion of UHMWPE to substrates is generally poor so that use of UHMWPE as a liner over a conventional steel moldboard may require mechanical fasteners. UHMWPE has been bonded to rubber which can in turn be bonded to a variety of substrates.

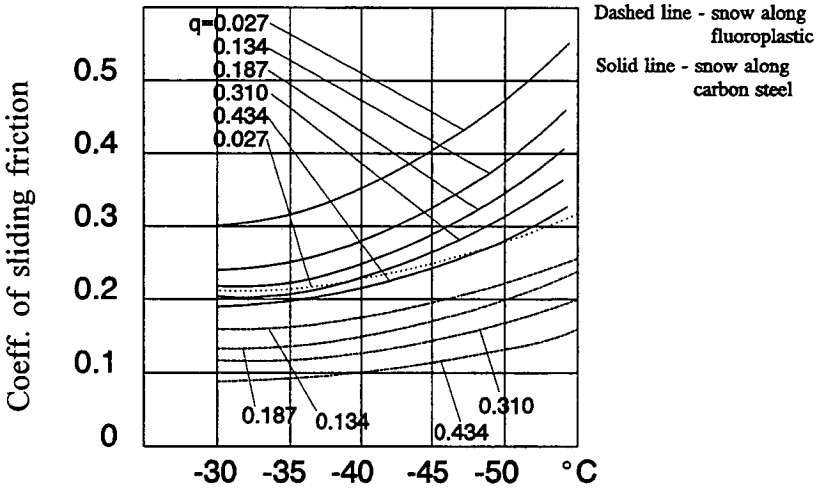

Figure 23. Dependence of the sliding friction coefficient of snow along fluoroplastic and carbon steel on temperature under different specific pressures q (kg/cm^2): (Reproduced from Shalman (2)).

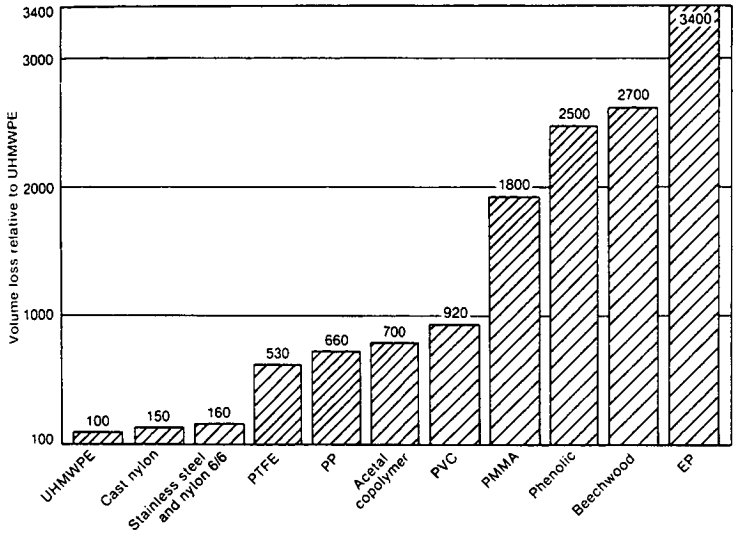

Figure 24. Abrasion resistance of various engineering materials. (Reproduced with permission from "Engineered Materials Handbook," Vol. 2, Engineering Plastics, ASM International. Metals Park, OH. 1988)

Moldboard Support Structure

Typically the ribs and longitudinal stiffeners supporting the moldboard are fabricated from steel plate and standard structural shapes. Steel moldboard surfaces are welded to the ribs using short fillet welds on alternate sides of the rib to minimize failure at the weld root on the moldboard surface. At least one manufacturer clamps the upper and lower edges of a UHMWPE moldboard to steel supports and shapes the moldboard by contact with ribs of the appropriate shape. There is no mechanical attachment of the UHMWPE to the ribs beyond the edge clamping in this case. Several manufacturers are utilizing box steel in a variety of standard cross sections. In addition, at least one manufacurer is putting a steel rear surface skin on the plow so that the entire plow becomes a boxed structure. These techniques improve the strength to weight ratio of the fabricated structures.

Plow Drive Frame

Plow drive frames are also typically fabricated from standard steel structural shapes. A few manufacturers are employing standard boxed steel structural shapes for the drive frame, again with improved strength to weight ratios.

Mechanical Design

The mechanical design of the experimental plows was not intended to serve as a basis for extrapolation for a commercial plow. Each of these plows incorporated design features which facilitated experimentation to investigate snow flow, aerodynamic flow, and particular design features. Therefore detailed design drawings of the entire plows will not be presented. The recommended geometry for the snow flow surface will be described in the summary.

The drive frame developed for the second experimental plow incorporates a large diameter self lubricating center pivot. The goal was to provide a design which would have a long life with minimal wear at the pivot to assure rigid positioning of the plow throughout its life. The use of deep steel sections for the drive frame and wide spacing for the plates taking up the pivot loads eliminates the requirement for multiple pivot pins and load transfering members between the plow and the top of the hitch. It is anticipated that users and manufacturers may want to adopt some of these features therefore details of the drive frame design are presented in Appendix II.

Use of air springs to provide the restoring force for the tripping edge is an innovation which users and manufacturers may also want to consider for adoption. The details of the mechanical design of the system used on the second experimental plow are included as Appendix III.

Summary

Based on all of the research conducted to date it appears that efficient snow removal involves consideration of the entire snow flow surface of the plow. The nature of the flow on the moldboard is dominated by the geometry of the cutting blade. An angle of 50 degrees (plus or minus 10 degrees) with respect to the road reduces the compression of the snow ahead of the blade. This geometry also lifts the snow as a sheet minimizing the acceleration of the snow and therefore the force on the plow and minimizing the disaggregation of the snow which also dissipates energy. The detailed geometry of the moldboard directly above the cutting edge in terms of the initial angle and whether it is curved or planar has a small influence on the plowing forces and the trajectory of the snow up the surface. Experimental plows incorporating initial moldboard angles of approximately 10 degrees and planar lower surfaces worked well. Theoretically, continuously curved moldboards should result in small accelerations of the snow and thus lower plowing forces. In order for the snow to move up and across the moldboard to exit the throat rather than be cast down in front of the plow the plow must have sufficient speed to keep the snow from falling off the moldboard and the plow must have sufficient flow surface that snow from the toe of the plow gets to the exit. This suggests tall moldboards with large-radius upper moldboard sections. Field tests of the experimental plows and observation of plows engaged in routine snow removal operations in many environments indicated that speeds of 10 to 15 m/s (20 to 30 mph) are required to keep snow from falling off the moldboard for a wide range of reversible plows currently in operation. In situations where plowing is conducted at lower speeds there is considerable rehandling of the snow reqardless of the plow geometry. Energy consumed in rehandling the snow dominates all aspects of the plow geometry.

The large radius upper moldboard suggested to provide sufficient flow distance to allow the snow from the toe to reach the exit also influences the aerodynamic flow in the neighborhood of the plow. These large-radius units tend to decrease blowby over the plow thereby improving visibility for the operator and motoring public.

A simplified schematic is presented in Figure 25 which illustrates the geometry recommendations which have been presented.

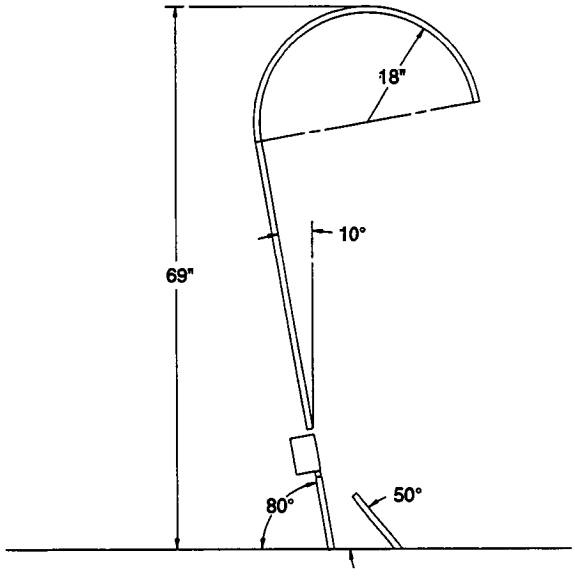

Figure 25. Recommended plow geometry.

The recommendations for tall moldboards and large diameter upper moldboards have implications for increased plow weight which is exactly counter to the suggestions of equipment engineers who sought lighter plows. This led to the development of a plow incorporating the geometry recommendations given above and employing a composite moldboard. The composite moldboard incorporates Azloy™ surface material bonded with Pliobond™ to a pine core. As shown in Figure 26 there are no steel ribs or other support structure. The plow is significantly lighter than a plow of similar size fabricated from steel.

Figure 26. Plow incorporating composite moldboard.

User input during the project indicated that operators, equipment engineers and maintenance engineers believe that the major problems with current snowplows include: visibility for the operator, visibility for the motoring public, weight of the plow/drive frame/hitch causing excessive front axle loads, and durability of the equipment. These problems were not addressed with high priority during the research however the results and recommendations clearly impact each of these areas. The flow algorithm developed has application to the visibility problem and alternative materials offer the potential to decrease weight. Continued research in these areas is required.

Appendix I

Publications and Technology Transfer

Journal Articles

Robert L. Crane and Mike H. Damson. Goal Oriented Design of an Improved Displacement Plow. Transportation Research Record 1304.

William R. Lindberg and Joseph D. Petersen. Negatively Buoyant Jet (or Plume) with Applications to Snowplow Exit Behavior. Transportation Research Record 1304.

Andrew C. Hansen. Analysis of Energy Dissipation Caused by Snow Compaction During Displacement Plowing. Transportation Research Record 1304.

Other Publications

Wade Steiger and Andrew Hansen. Investigation of Forces Incurred During Snow Plowing. Winter Mobility Conference, June 1991.

Theses and Dissertations

Robert Crane. Analysis of the Large Deformation and Flow Characteristics of Developable Surface Snowplow Moldboards. M.S. thesis, University of Wyoming, 1993.

Dennis Horning. Concurrent Scheduling of Multiprocessors for Efficient Eigenproblem Solution. Ph.D. dissertation, University of Wyoming, 1994.

Paul Bruss. Stress Wave Interaction at the Ice/Road Interface. M.S. thesis, University of Wyoming, 1992.

Mike Damson. Numerical Investigation of Flow on a Snowplow. M.S. thesis, University of Wyoming, 1990.

Robert Yraceburu. Dynamic High Density Snow Compaction for Polar Runways. M.S. thesis, University of Wyoming, 1992.

Bo Ruan. Heavy Vehicle Stability. M.S. thesis, University of Wyoming, 1992.

Video and Computer Presentations

"SHRP Snowplow Research," Western State Equipment Managers Conference, Glenwood Springs, CO. September 1991

"SHRP Snowplow Research," Wyoming State Department of Transportation, Laramie, WY. September 1991

"Improved Displacement Snowplow," with Wade Steiger and Robert Crane. Wyoming Engineering Society, Cody, WY. February 1991

"SHRP Snowplow Research," Western States Highway Equipment Managers Conference, Helena, MT. October 1992

"The New Prototype Snowplow," Annual Tri-State Snow Meeting, Cheyenne, WY. October 1992

"Improved Snowplows," 9th TRB Equipment Management Workshop, Research Triangle Park, NC. June 1992

"SHRP Snowplow," 1993 North American Snow Conference, Cleveland, OH. April 1993

Technology Transfer Activities

Videos

"Snowscoop Installation Instruction"	February 1992
"A Presentation for the 9th TRB Equipment Managers Workshop"	June 1992

Exhibits

"Model Composite Snowplow Exhibit," Transportation Research Board Annual Meeting	January 1993
"Composite Snowplow Exhibit," ConExpo, Las Vegas, NV.	April 1993
"Computerized Snowplow Presentation," TransExpo, Transportation Research Board Annual Meeting	June 1991

Appendix II

Mechanical Design of the Drive Frame

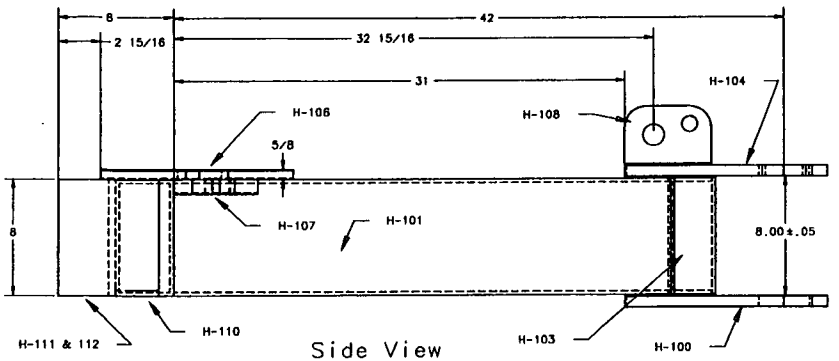

Side View

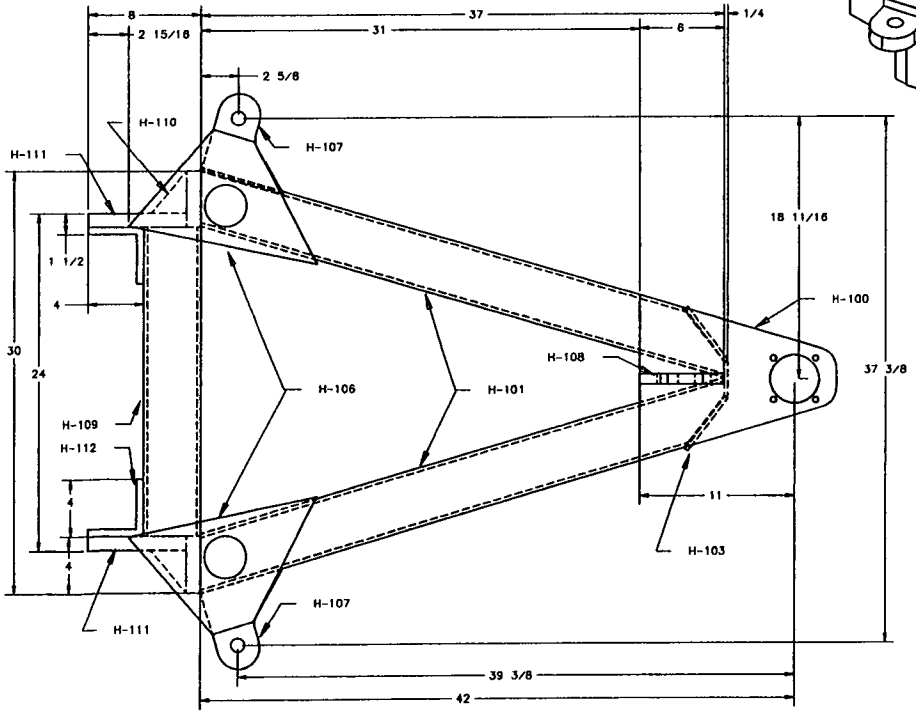

Top View

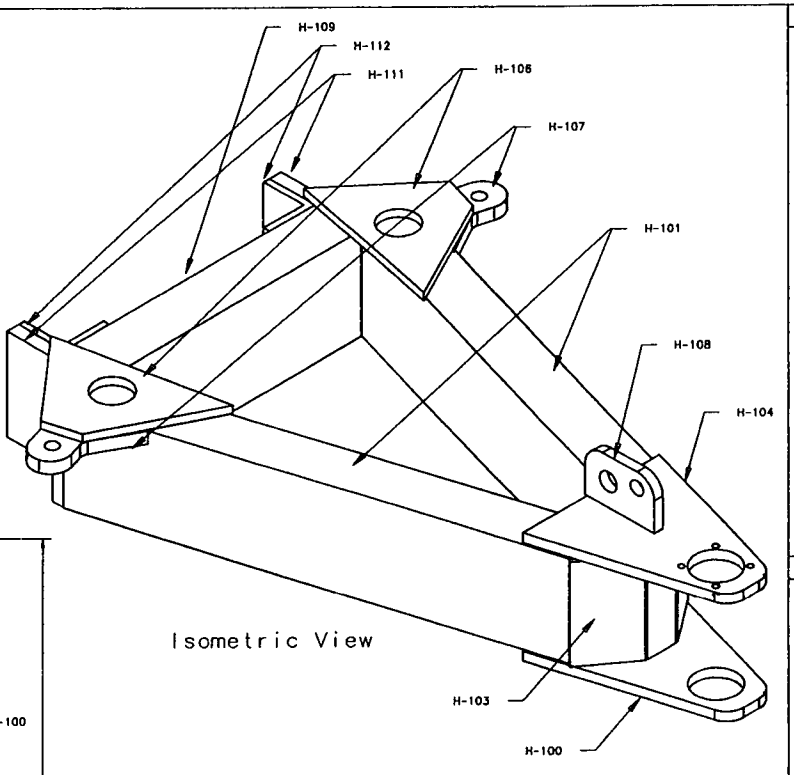

Isometric View

NOTES

1. All Material is ASTM 1018 steel.
2. Warpage of the welded assembly must not exceed 1/8".
3. Round all sharp edges and commercial blast prior to painting assembly yellow.
4. Holes for connection to Husting adaptor should be drilled during finnal assemble.
5. Pin bushings should be instaled before assemble is painted.
6. Bishings are heat fit into plate.

BILL OF MATERIALS

Part#	Description	#REQ.
H-100	3/4 THK. PLT.	1
H-101	RECT. TUBING	2
H-102	BUSHING	2
H-103	FACE PLT.	1
H-104	3/4 THK. PLT.	1
H-105	PIN FLG.	1
H-106	GUSSET	2
H-107	HYD. EAR	2
H-108	LIFT LUG	1
H-109	REC. TUBE 8x4x1/4 22" long.	
H-110	GUSSET	2
H-111	L 8x4x1 8"Sec.	2
H-112	L 4X4X1/2 8"Sec.	2

Center For Information Technology	REV. NO. 2
DRAWN BY NCR	CHECKED BY
DRAWING NO. AH-101	DATE 9/11/91
ALL UNITS IN INCHES	TOLERANCE 1/16 U.N.C.

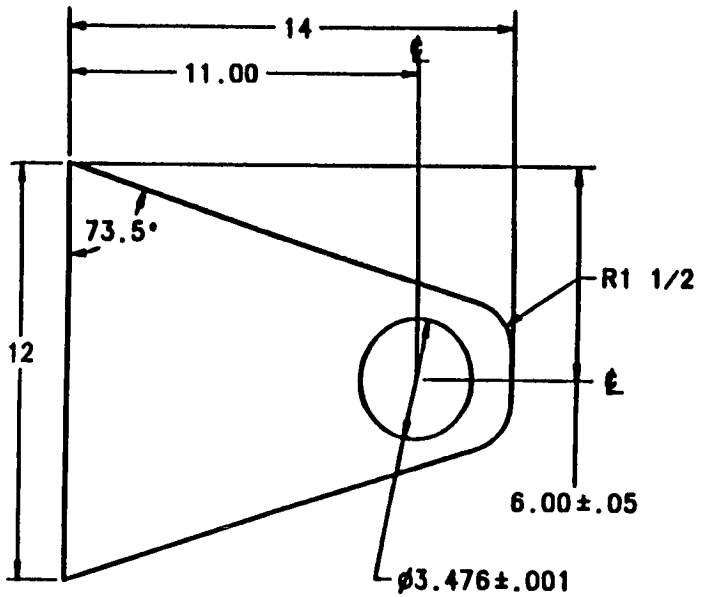

Top View

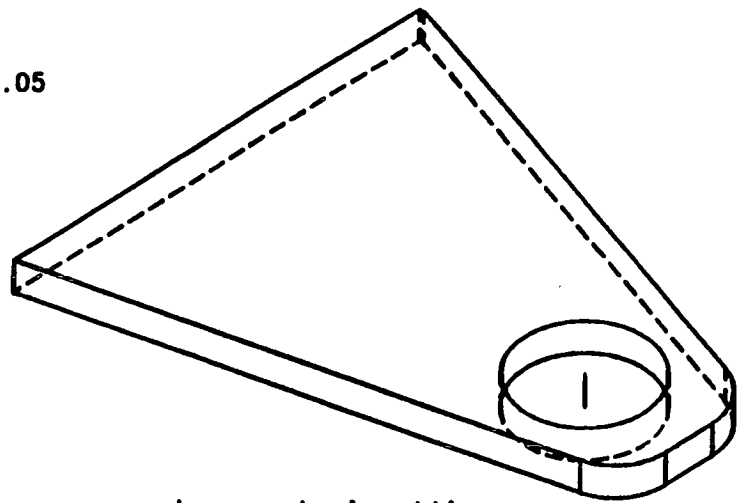

Isometric View

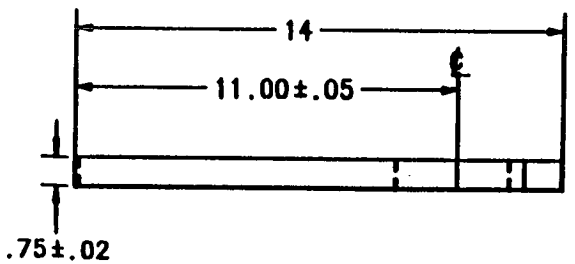

Side View

NOTES

1. Material is ASTM 1018 steel.
2. Drawing # is to be marked upon part.
3. Round sharp edges before assembly.

1 PART REQ.

Center For Information Technology	REV. NO. 2
DRAWN BY NCR	CHECKED BY
DRAWING NO. H-100	DATE 9/13/91
ALL UNITS IN INCHES	TOLERANCE 1/16 U.N.O.

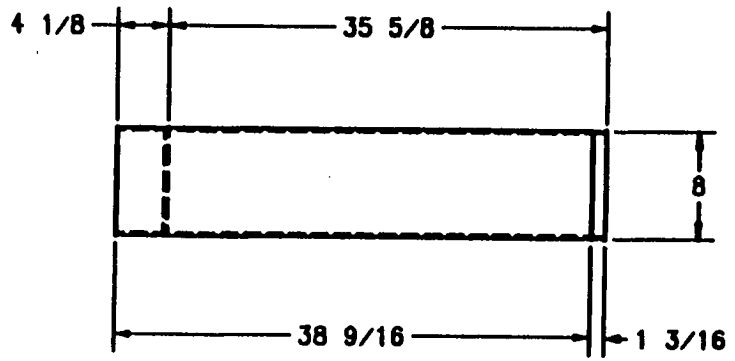

BOTTOM VIEW

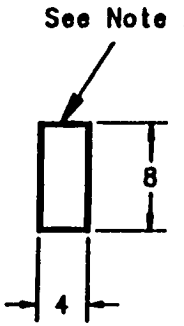

SIDE VIEW

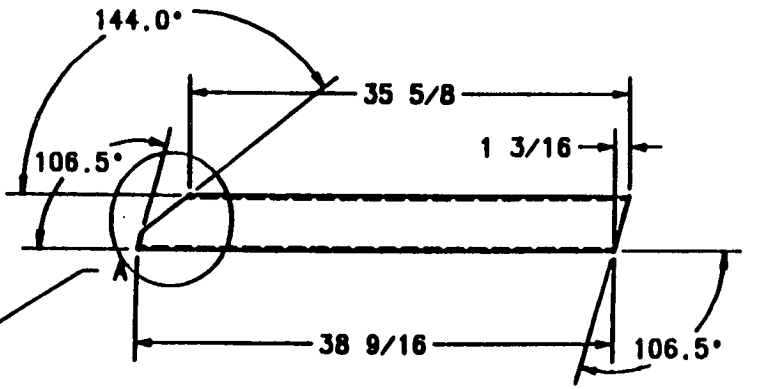

FRONT VIEW

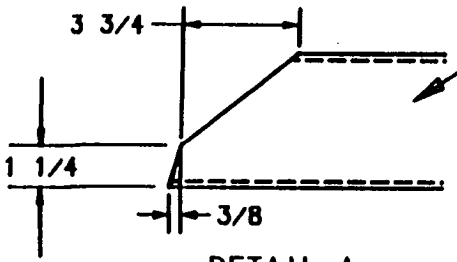

DETAIL A

NOTES

1. Material is ASTM 1018 steel.
2. Rectangular Tubing 8 X 4 X 1/4.
3. Drawing No. is to be marked on parts.
4. Do not round sharp edges until after assembly

2 PARTS REQ.

Center For Information Technology	REV. NO. 2
DRAWN BY RLC	CHECKED BY
DRAWING NO. H-101	DATE 8/22/91
ALL UNITS IN INCHES	TOLERANCE 1/16 U.N.O.

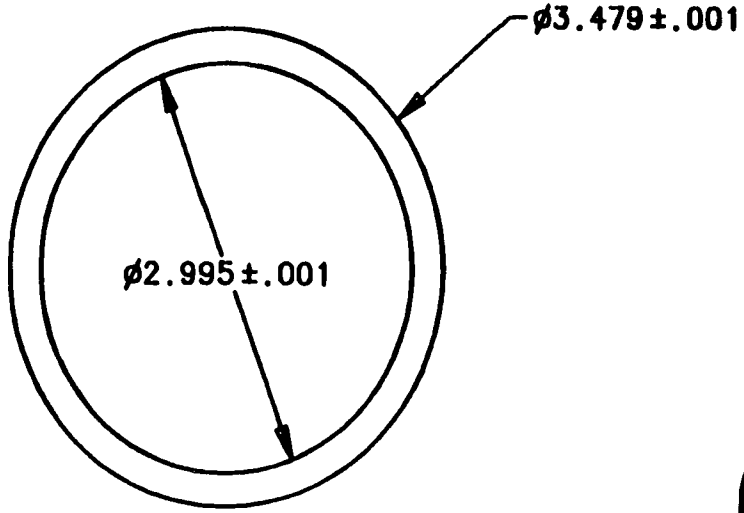

TOP VIEW

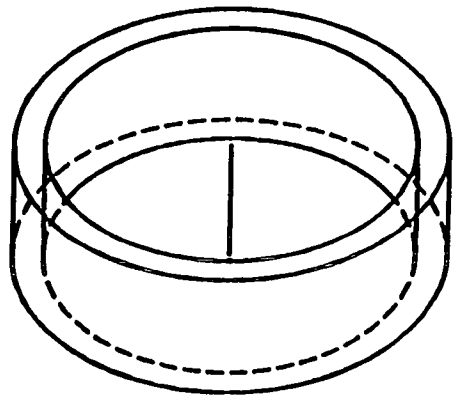

ISOMETRIC VIEW

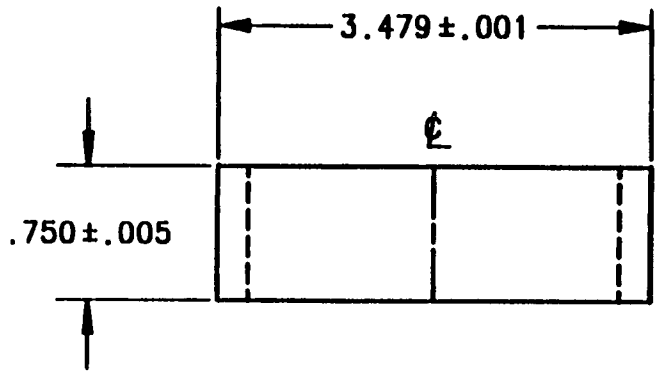

FRONT VIEW

NOTES

1. Material is ASTM 6150 steel.
2. Bored from round stock.
3. See heat treating notes.

2 PARTS REQ.

Center For Information Technology	REV. NO. 1
DRAWN BY RLC	CHECKED BY
DRAWING NO. H-102	DATE 6/6/91
ALL UNITS IN INCHES	TOLERANCE 1/16 U.N.O.

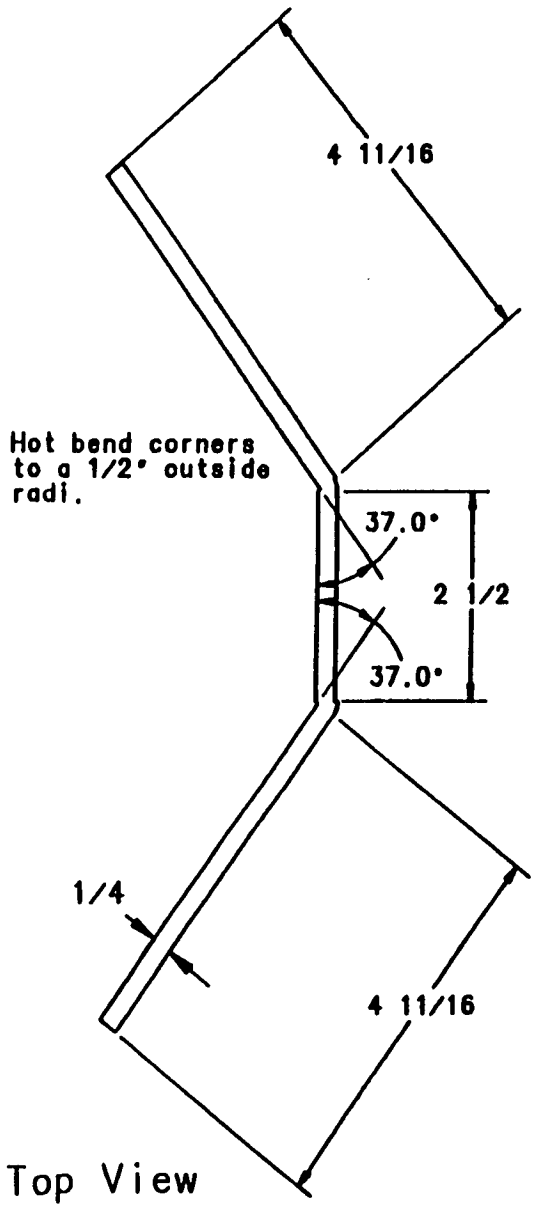

Top View

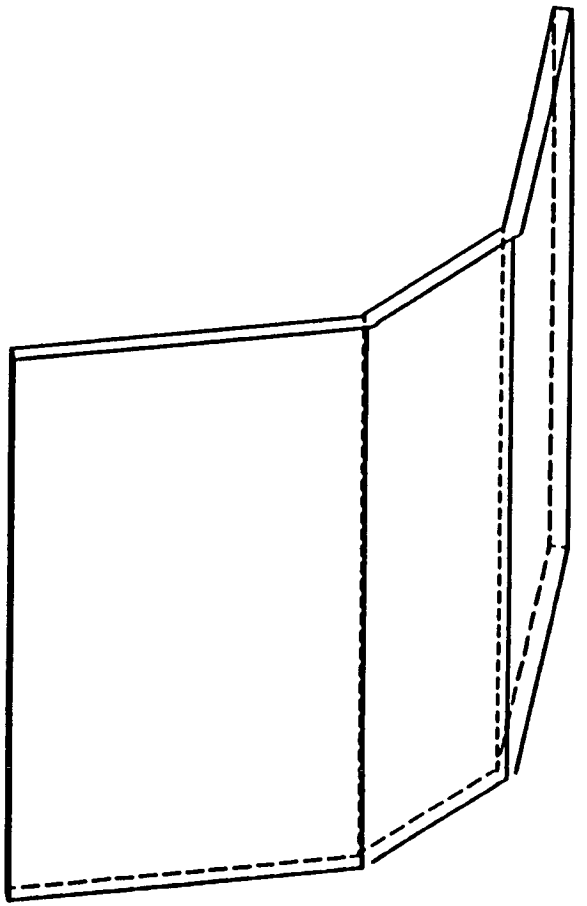

Isometric View

NOTES

1. Material is ASTM 1018 steel.
2. 1/4" plate steel.
3. Drawing No. is to be marked on part.
4. Round all sharp edges before assembly.

1 PART REQ.

Center For Information Technology	REV. NO. 2
DRAWN BY NCR	CHECKED BY
DRAWING NO. H-103	DATE 8/29/91
ALL UNITS IN INCHES	TOLERANCE 1/16 U.N.O.

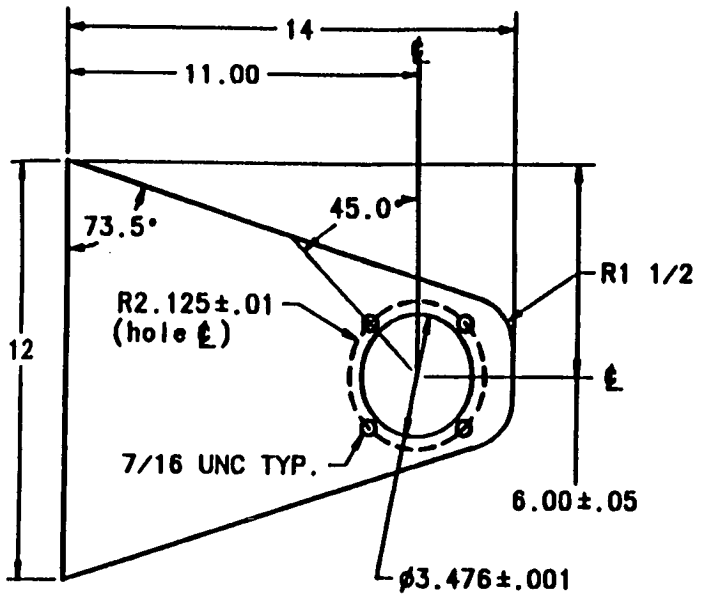

Top View

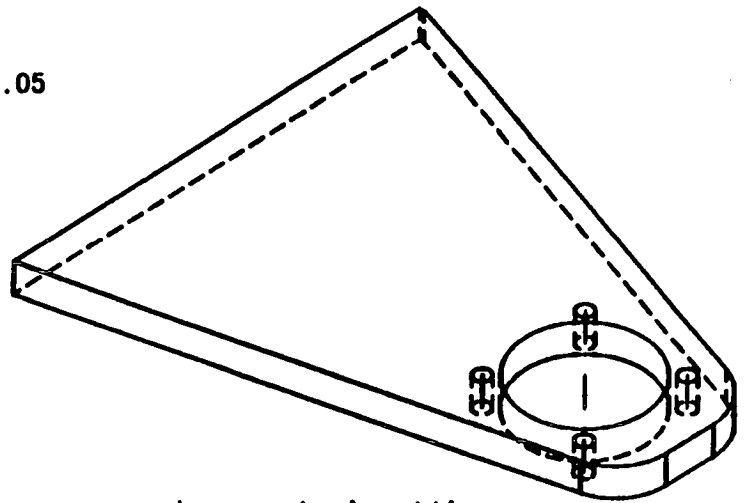

Isometric View

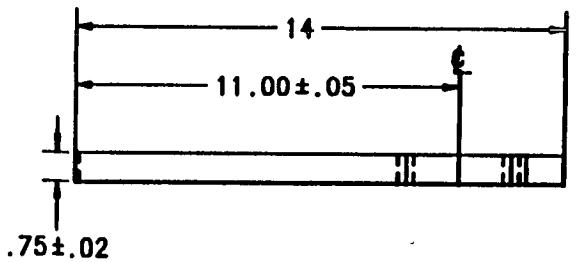

Side View

NOTES

1. Material is ASTM 1018 steel.
2. Drawing # is to be marked upon part.
3. Round sharp edges before assembly.

1 PART REQ.

Center For Information Technology	REV. NO. 2
DRAWN BY NCR	CHECKED BY
DRAWING NO. H-104	DATE 9/13/91
ALL UNITS IN INCHES	TOLERANCE 1/16 U.N.O.

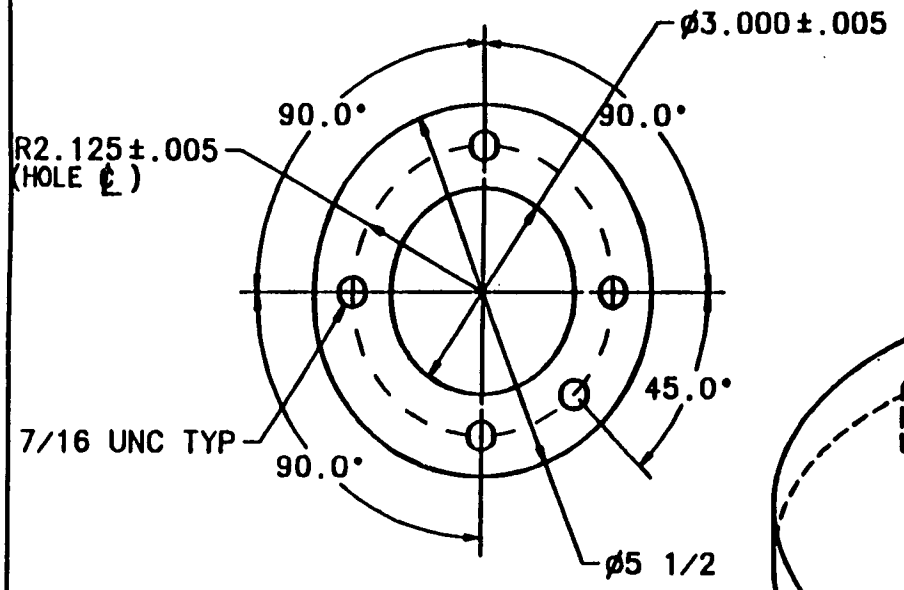

TOP VIEW

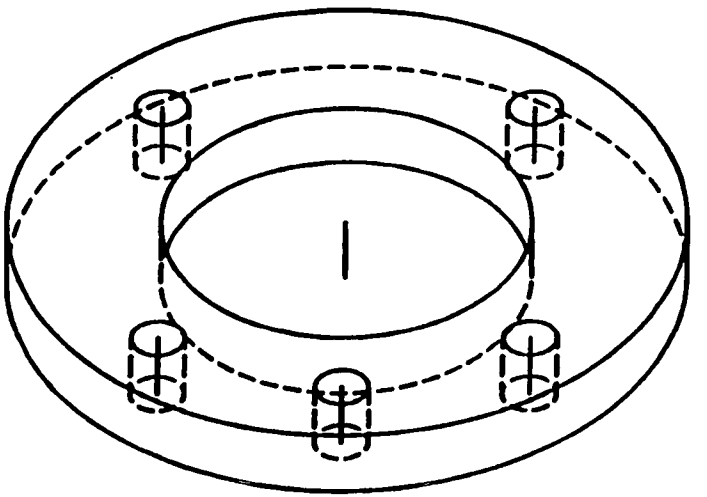

ISOMETRIC VIEW

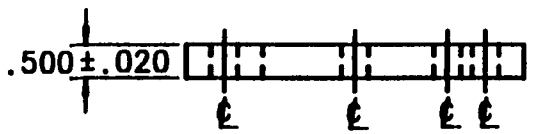

FRONT VIEW

NOTES

1. Material is ASTM 1018 steel.
2. Do not round sharp edges until after assembly.

1 PART REQ.

Center For Information Technology		REV. NO. 1
DRAWN BY RLC	CHECKED BY	
DRAWING NO. H-105	DATE 6/9/91	
ALL UNITS IN INCHES	TOLERANCE 1/16 U.N.O.	

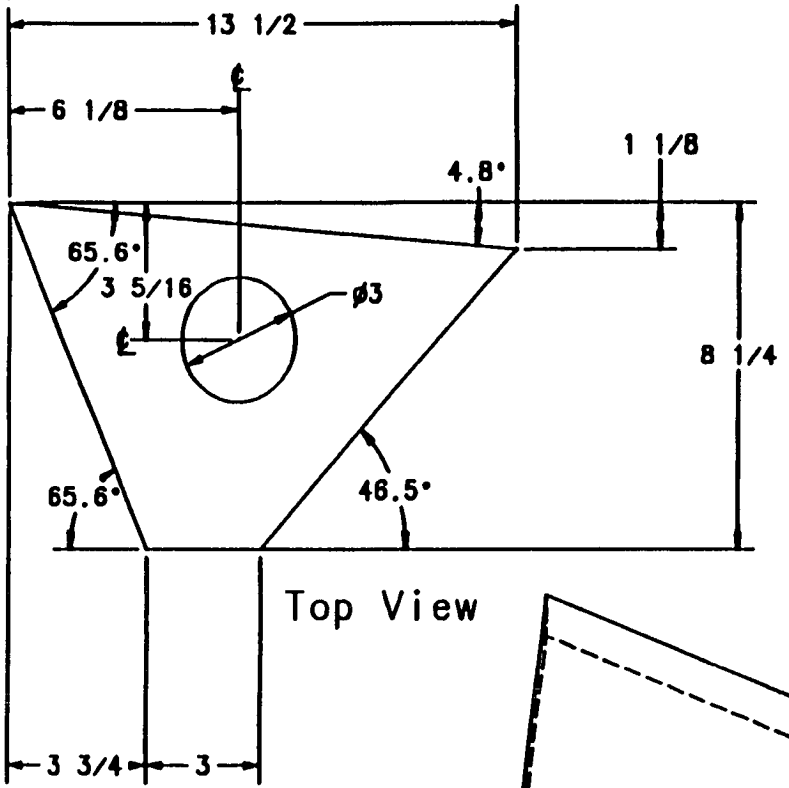

Top View

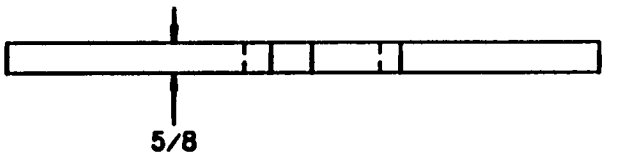

Side View

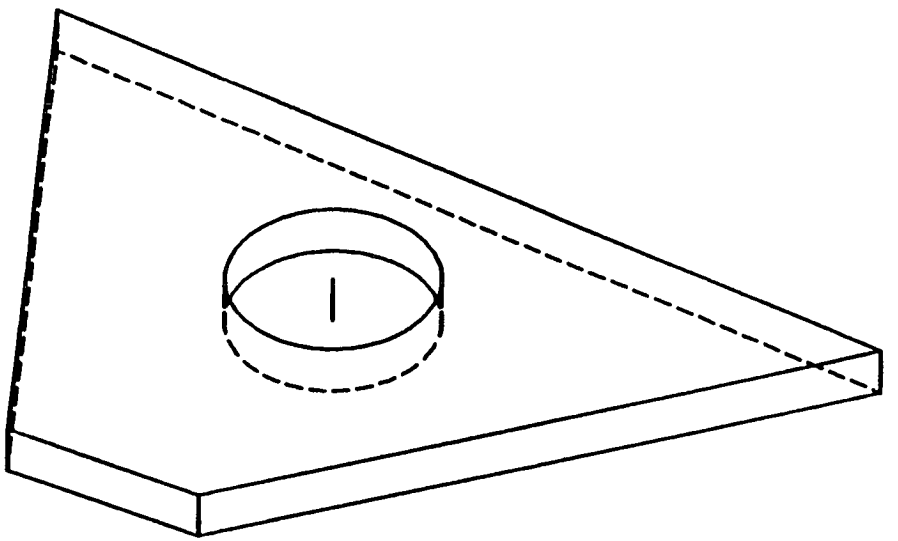

Isometric View

NOTES

1. Material is ASTM 1018 steel.
2. Drawing No. is to be marked on part.
3. Do not round sharp edges untill after assembly.

2 PARTS REQ.

Center For Information Technology	REV. NO. 2
DRAWN BY NCR	CHECKED BY
DRAWING NO. H-106	DATE 8/28/91
ALL UNITS IN INCHES	TOLERANCE 1/16 U.N.O.

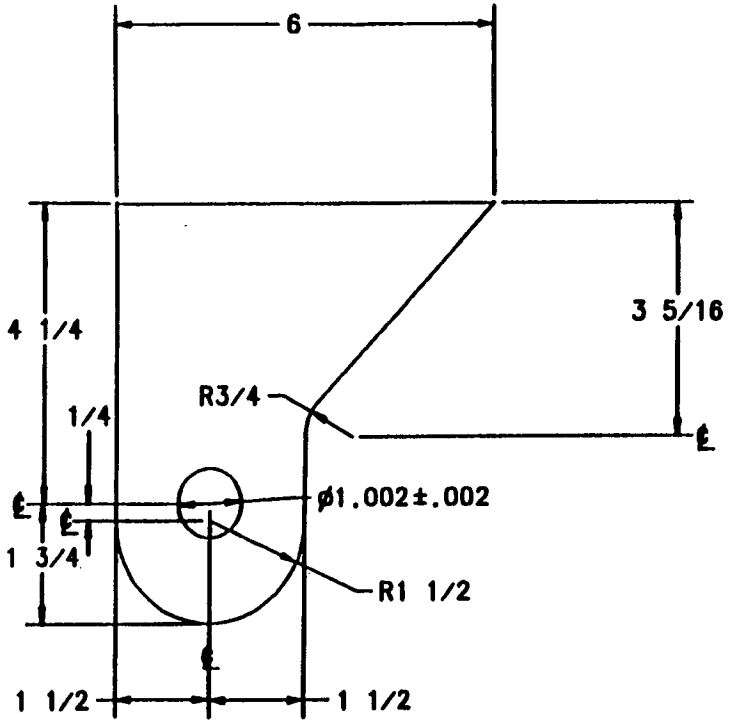

Top View

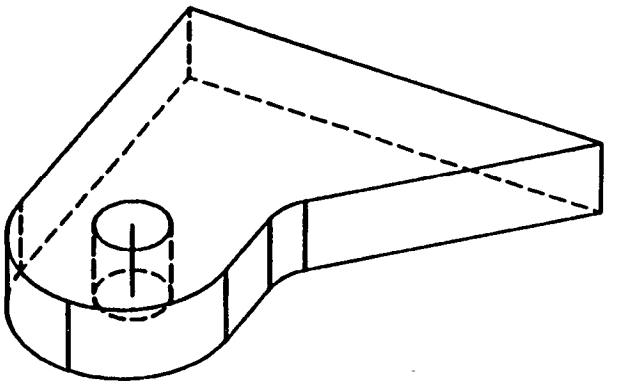

Isometric View

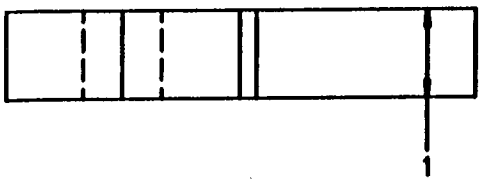

Side View

NOTES

1. Material is ASTM 1018 steel.
2. Drawing No. is to be marked on parts.
3. Do not round sharp edges untill after assembly.

2 PARTS REQ.

Center For Information Technology	REV. NO. 2
DRAWN BY NCR	CHECKED BY
DRAWING NO. H-107	DATE 9/28/91
ALL UNITS IN INCHES	TOLERANCE 1/16 U.N.O.

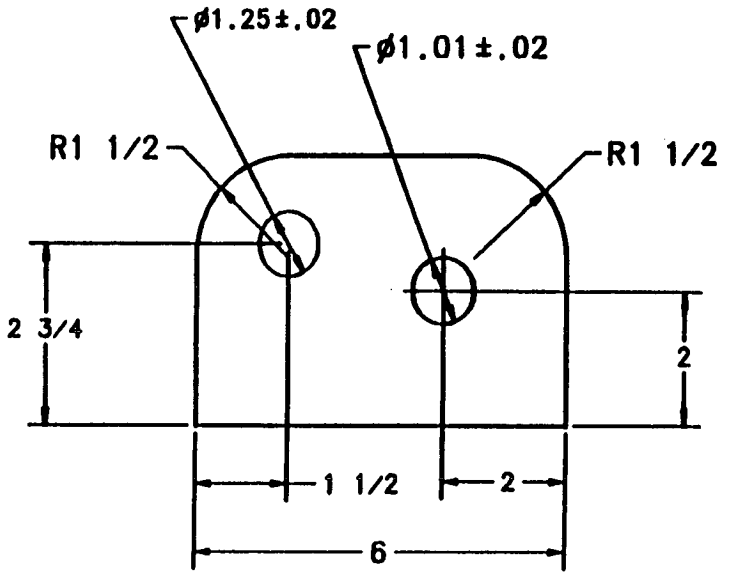

TOP VIEW

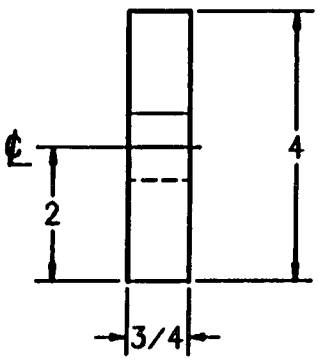

SIDE VIEW

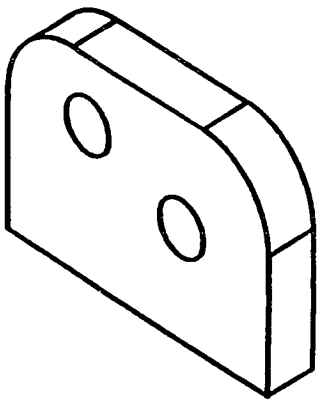

ISOMETRIC VIEW

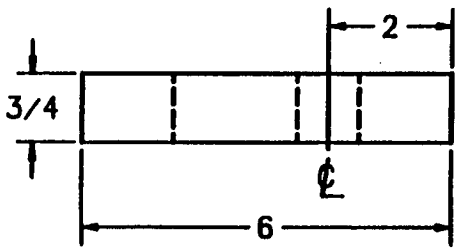

FRONT VIEW

NOTES

1. Material is ASTM 1018 steel.
2. Drawing No. is to be marked on part.
3. Do not round sharp edges until after assembly.

1 PART REQ.

Center For Information Technology	REV. NO. 2
DRAWN BY RLC	CHECKED BY
DRAWING NO. H-108	DATE 8/22/91
ALL UNITS IN INCHES	TOLERANCE 1/16 U.N.O.

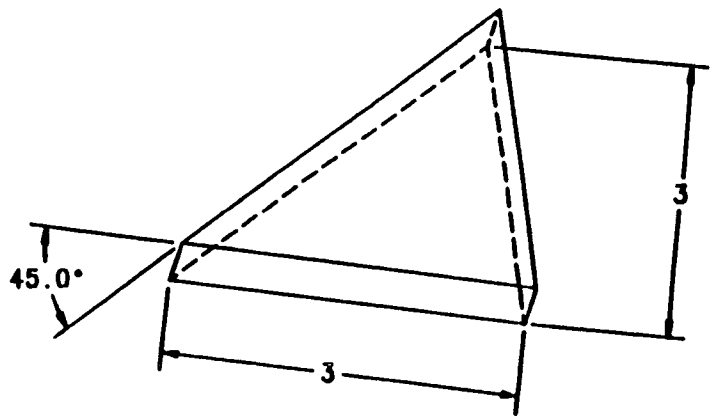

Isometric View

NOTES

1. Material is ASTM 1018 steel.
2. Cut from 3/8" plate material.
3. Round all edges before assembly.

2 PARTS REQ.

Center For Information Technology	REV. NO. 2
DRAWN BY NCR	CHECKED BY
DRAWING NO. H-110	DATE 8/29/91
ALL UNITS IN INCHES	TOLERANCE 1/16 U.N.O.

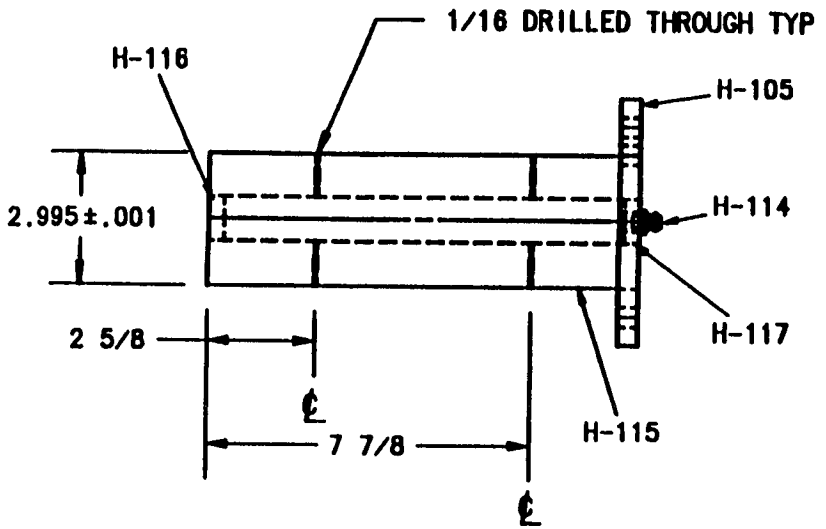

TOP VIEW

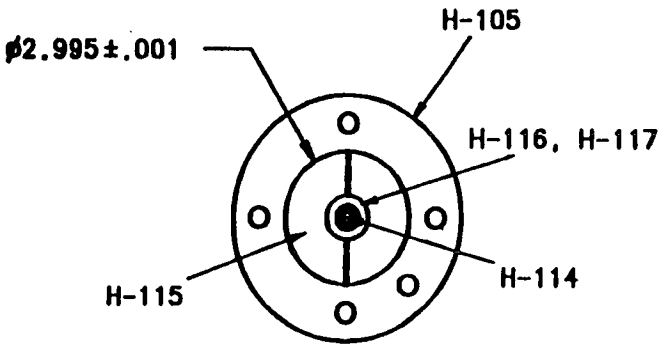

SIDE VIEW

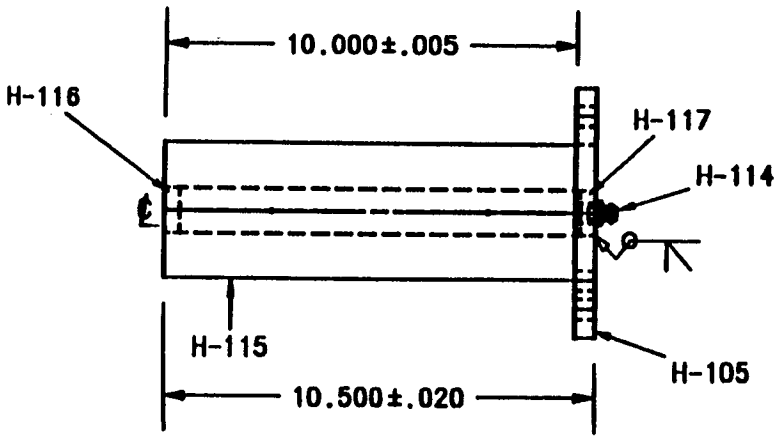

FRONT VIEW

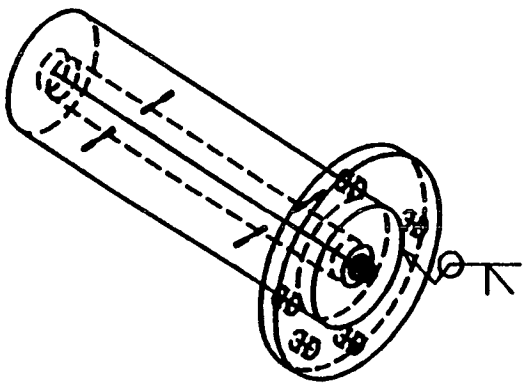

ISOMETRIC VIEW

PAGE 2 OF 2

1 PART REQ.

Center For Information Technology	REV. NO. 1
DRAWN BY RLC	CHECKED BY
DRAWING NO. AH-100-2	DATE 6/11/91
ALL UNITS IN INCHES	TOLERANCE 1/16 U.N.O.

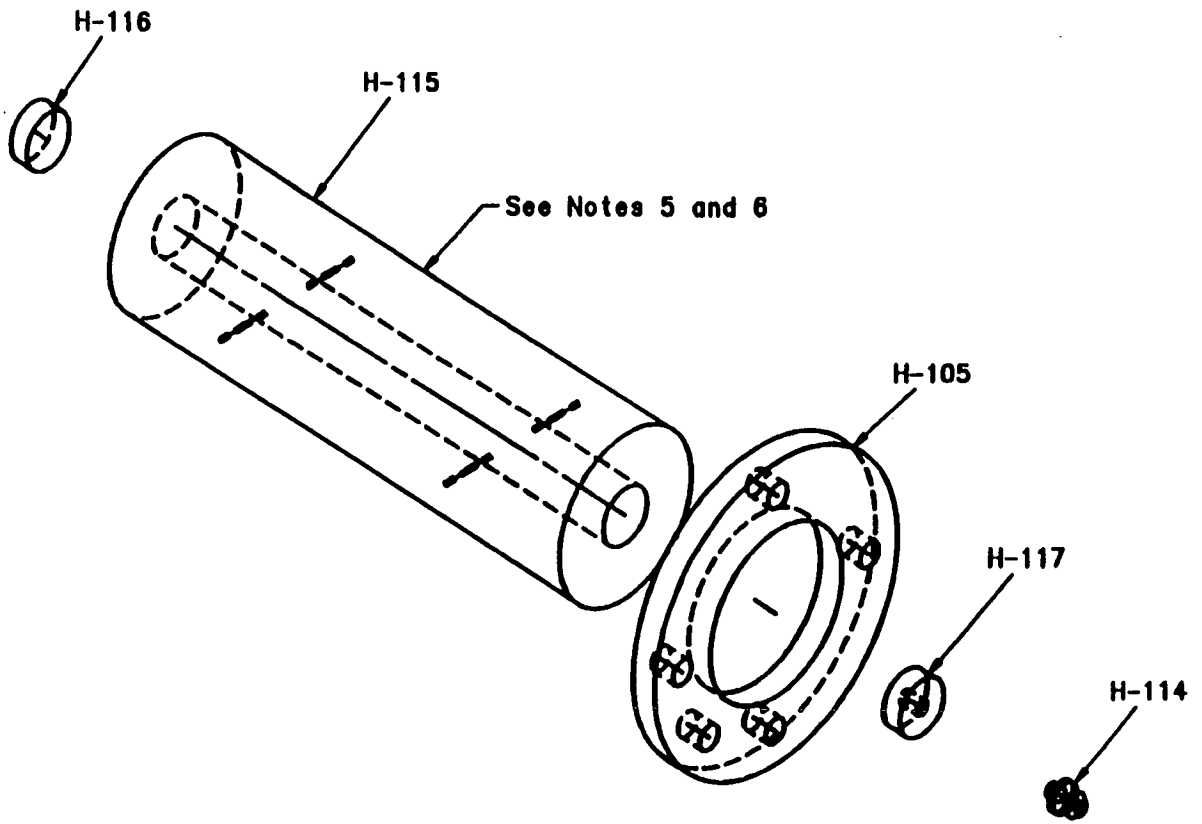

EXPLODED ISOMETRIC VIEW

NOTES

1. Drilled holes must be deburred.
2. All welds and drilled holes are to be made prior to tolerancing this piece.
3. See page 2 for welding instructions.

BILL OF MATERIALS

PART NO.	DESCRIPTION	# REQ.
H-105	1/2 THK. PLT. FLANGE	1
H-114	1/8 NPT GREASE FITTING	1
H-115	ASTM 1018 STEEL COLD-DRAWN SEAMLESS PIPE 3.00 O.D., 1.00 I.D., 1.00 WALL THK.	1
H-116	ASTM 1018 STEEL 3/8 THICK, 1 DIA. PLUG	1
H-117	ASTM 1018 STEEL 3/8 THK., 1 DIA. PLUG WITH 1/4 DIA. THREADED HOLE FOR 1/8 NPT GREASE FITTING	1

Center For Information Technology	REV. NO. 1
DRAWN BY RLC	CHECKED BY
DRAWING NO. AH-100-1	DATE 6/11/91
ALL UNITS IN INCHES	TOLERANCE 1/16 U.N.O.

Appendix III

Mechanical Design of the Air Spring System

Database: proto3
View : No stored View
Task: Assembly
System: 72-TOTAL ROTATED (modified)

SDRC I-DEAS VI: Solid_Modeling

01-APR-92 20: 37: 03
Units : IN
Display : No stored Option
Bin: 1-MAIN
Update Level: Full

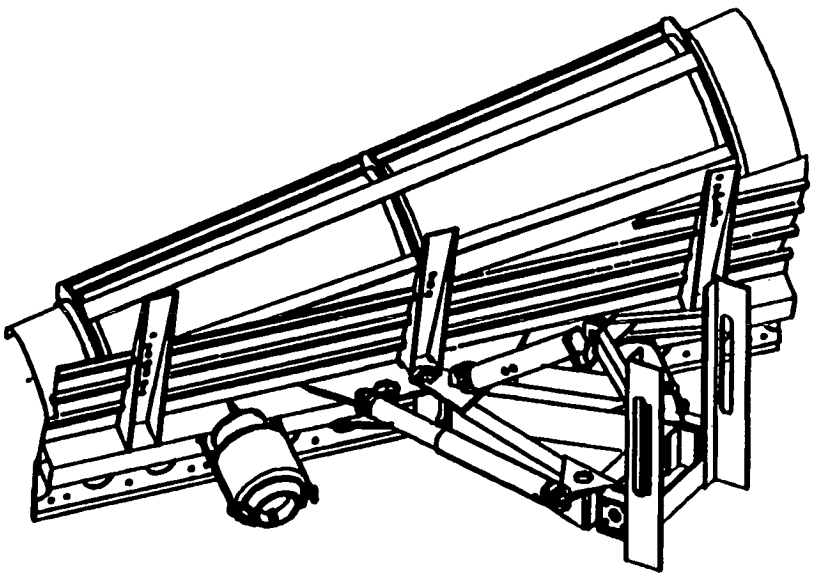

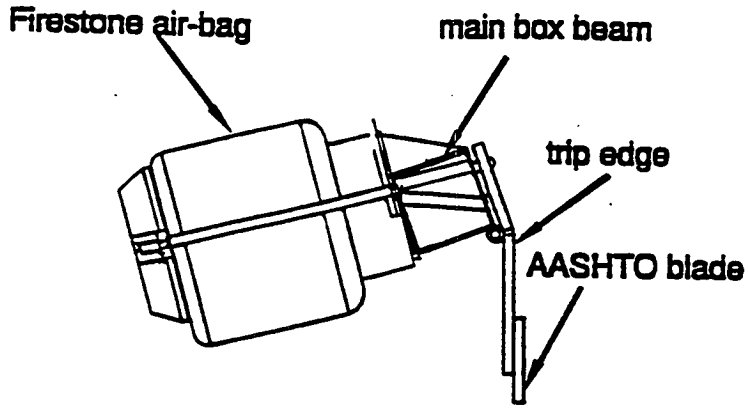
Firestone air-bag
main box beam
trip edge
AASHTO blade

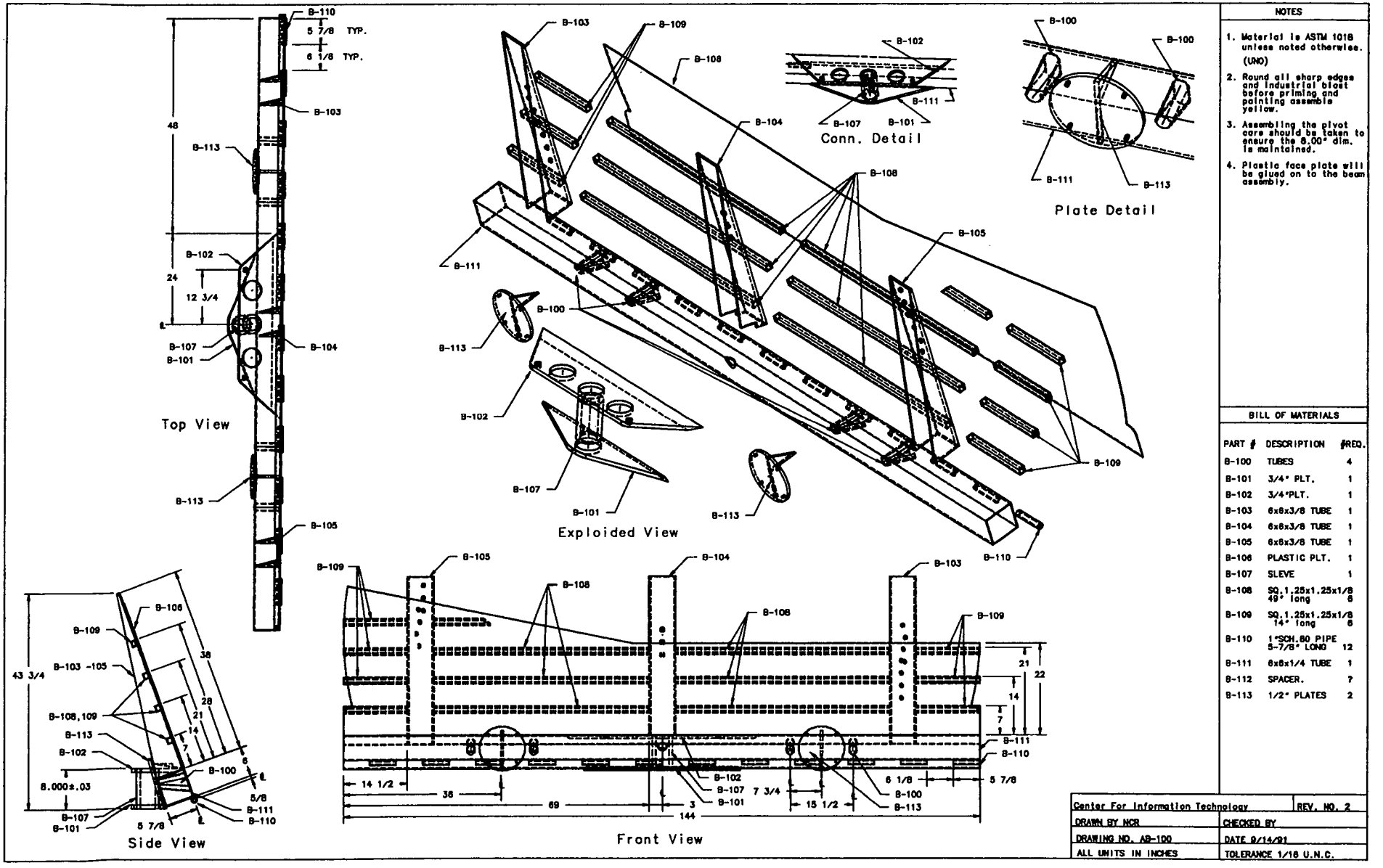

NOTES

1. Material is ASTM 1018 unless noted otherwise. (UNO)
2. Round all sharp edges and industrial blast before priming and painting assemble yellow.
3. Assembling the pivot care should be taken to ensure the 8.00" dim. is maintained.
4. Plastic face plate will be glued on to the beam assembly.

BILL OF MATERIALS

PART #	DESCRIPTION	#REQ.
B-100	TUBES	4
B-101	3/4" PLT.	1
B-102	3/4"PLT.	1
B-103	6x6x3/8 TUBE	1
B-104	6x6x3/8 TUBE	1
B-105	6x6x3/8 TUBE	1
B-106	PLASTIC PLT.	1
B-107	SLEVE	1
B-108	SQ.1.25x1.25x1/8 49" long	6
B-109	SQ.1.25x1.25x1/8 14" long	6
B-110	1"SCH.80 PIPE 5-7/8" LONG	12
B-111	6x6x1/4 TUBE	1
B-112	SPACER.	?
B-113	1/2" PLATES	2

Center For Information Technology	REV. NO. 2
DRAWN BY HCR	CHECKED BY
DRAWING NO. AB-100	DATE 9/14/91
ALL UNITS IN INCHES	TOLERANCE 1/16 U.N.C.

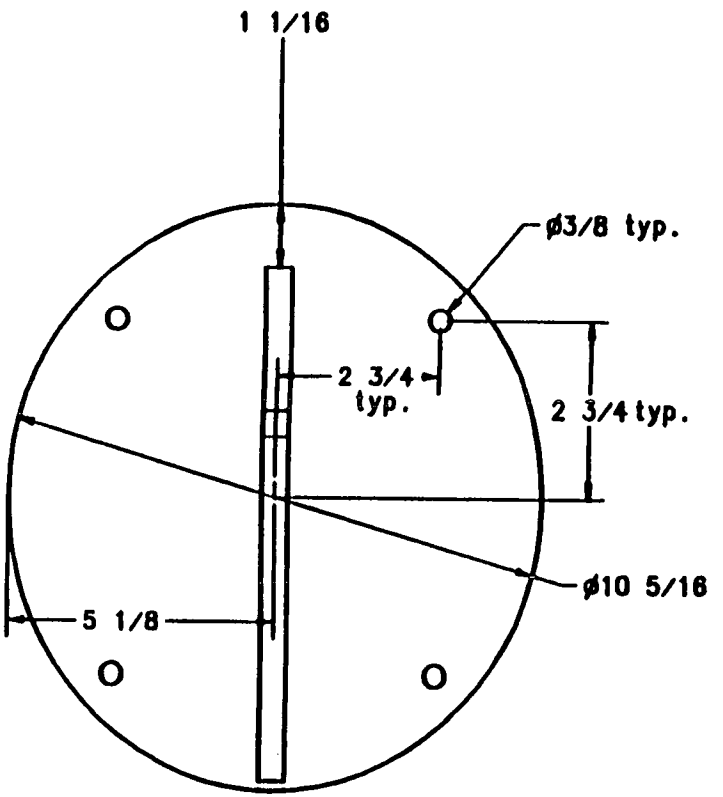

FRONT VIEW

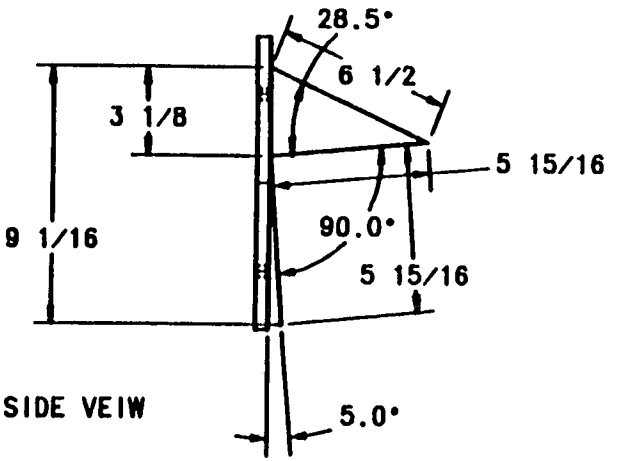

SIDE VEIW

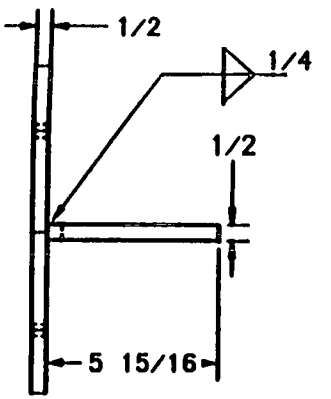

TOP VIEW

1018 steel

2 parts req.

Center For Information Technology		REV. NO. 1
DRAWN BY WS	CHECKED BY	
DRAWING NO. B-113	DATE 6/6/91	
ALL UNITS IN INCHES	TOLERANCE 1/16 U.N.O.	

assesbly of the back plate for the air bags

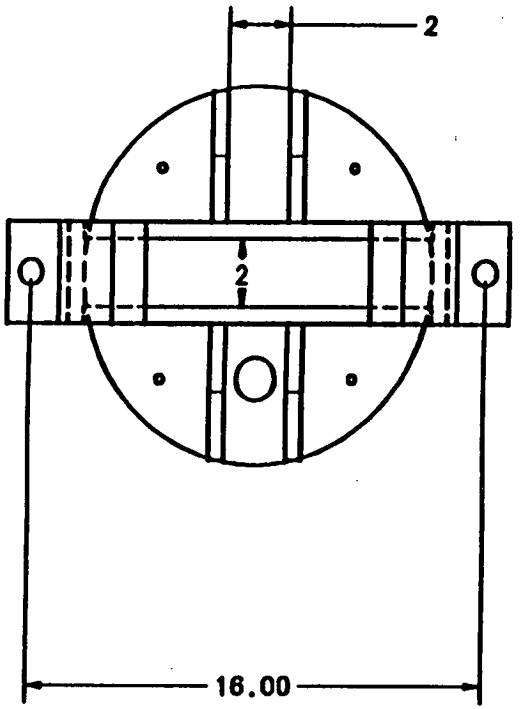

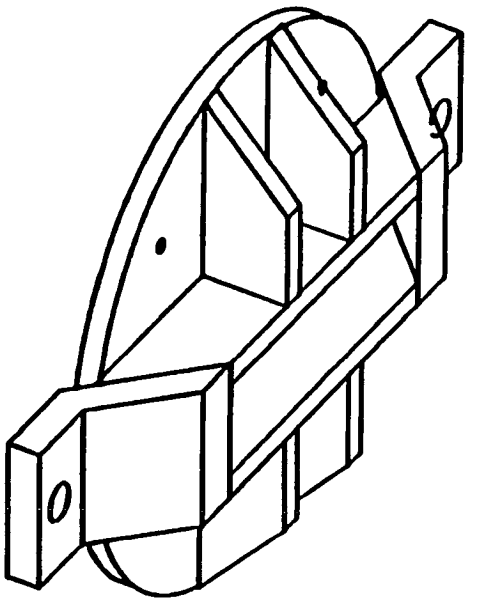

NOTES

Center For Information Technology	REV. NO.
DRAWN BY	CHECKED BY
DRAWING NO.	DATE
ALL UNITS IN INCHES	TOLERANCE 1/16 U.N.O.

4 parts req.
1018 steel

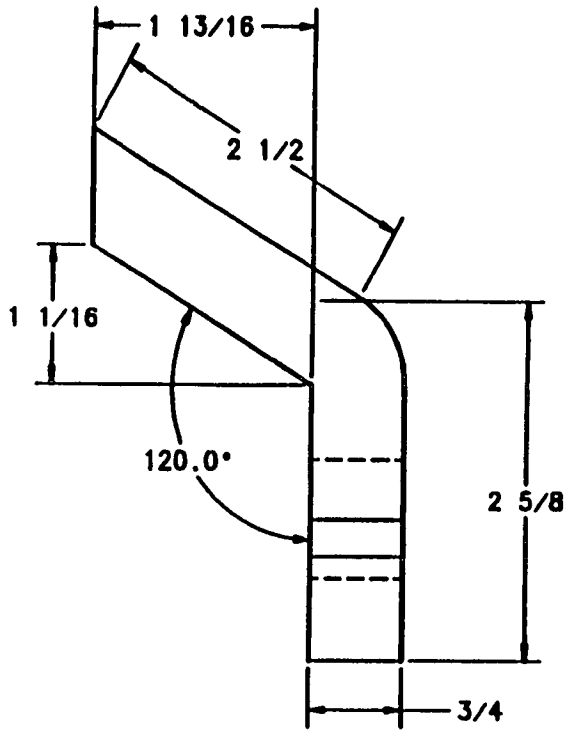

SIDE VIEW

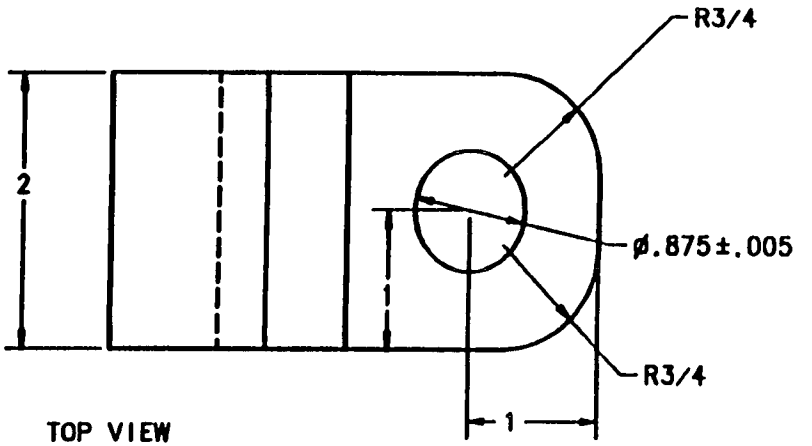

TOP VIEW

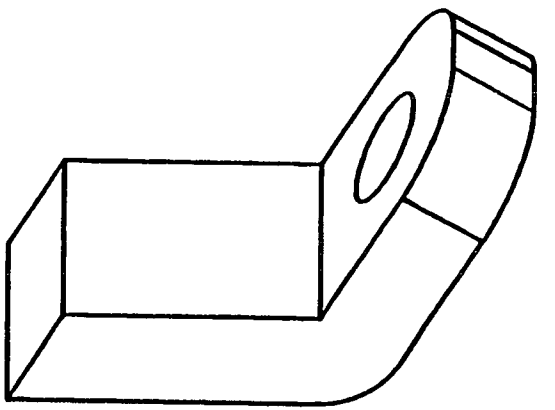

ISO. VIEW

Center For Information Technology	REV. NO. 1
DRAWN BY WS	CHECKED BY
DRAWING NO. P-110	DATE 6/8/91
ALL UNITS IN INCHES	TOLERANCE 1/16 U.N.O.

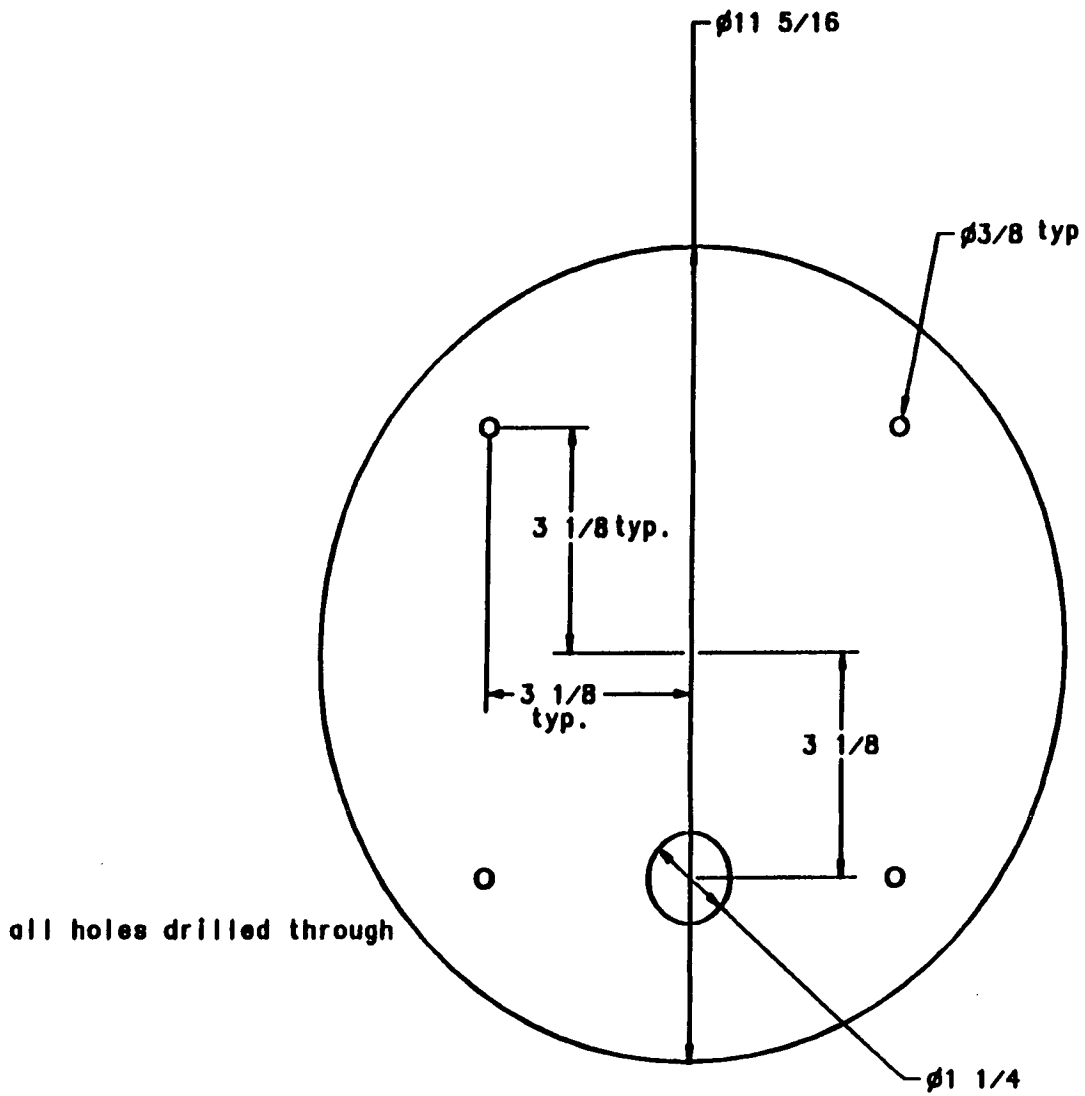

NOTES

cut from 1/2" plate
1018 steel
2 parts req.

Center For Information Technology	REV. NO. 1
DRAWN BY WS	CHECKED BY
DRAWING NO. P-111	DATE 6/5/91
ALL UNIT IN INCHES	TOLERANCE 1/16 U.N.O.

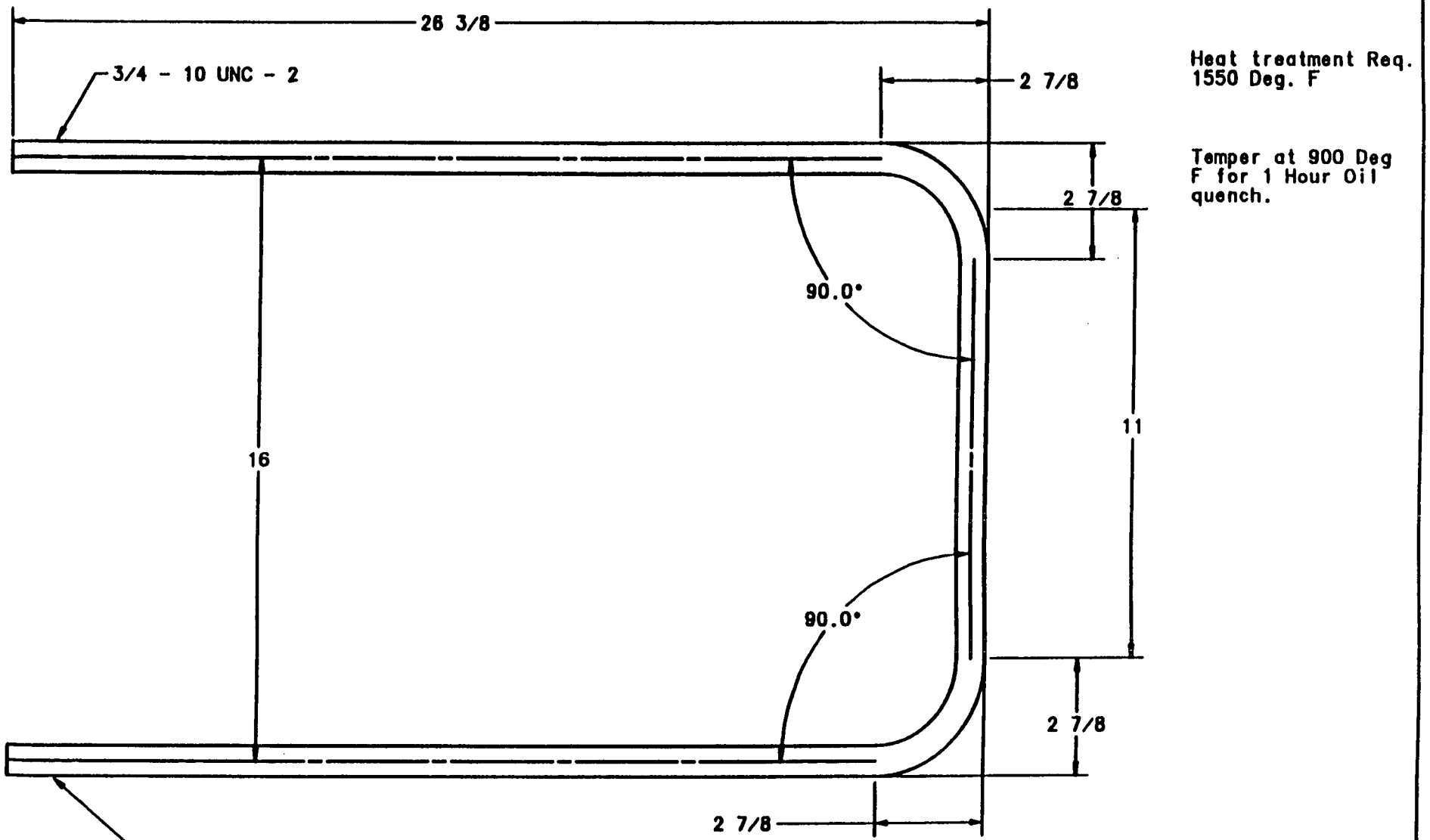

Center For Information Technology		REV. NO. 1
DRAWN BY WS	CHECKED BY	
DRAWING NO. P-118	DATE 6/6/91	
ALL UNITS IN INCHES	TOLERANCE 1/16 U.N.O.	

Appendix IV

Mechanical Design of a Snowscoop

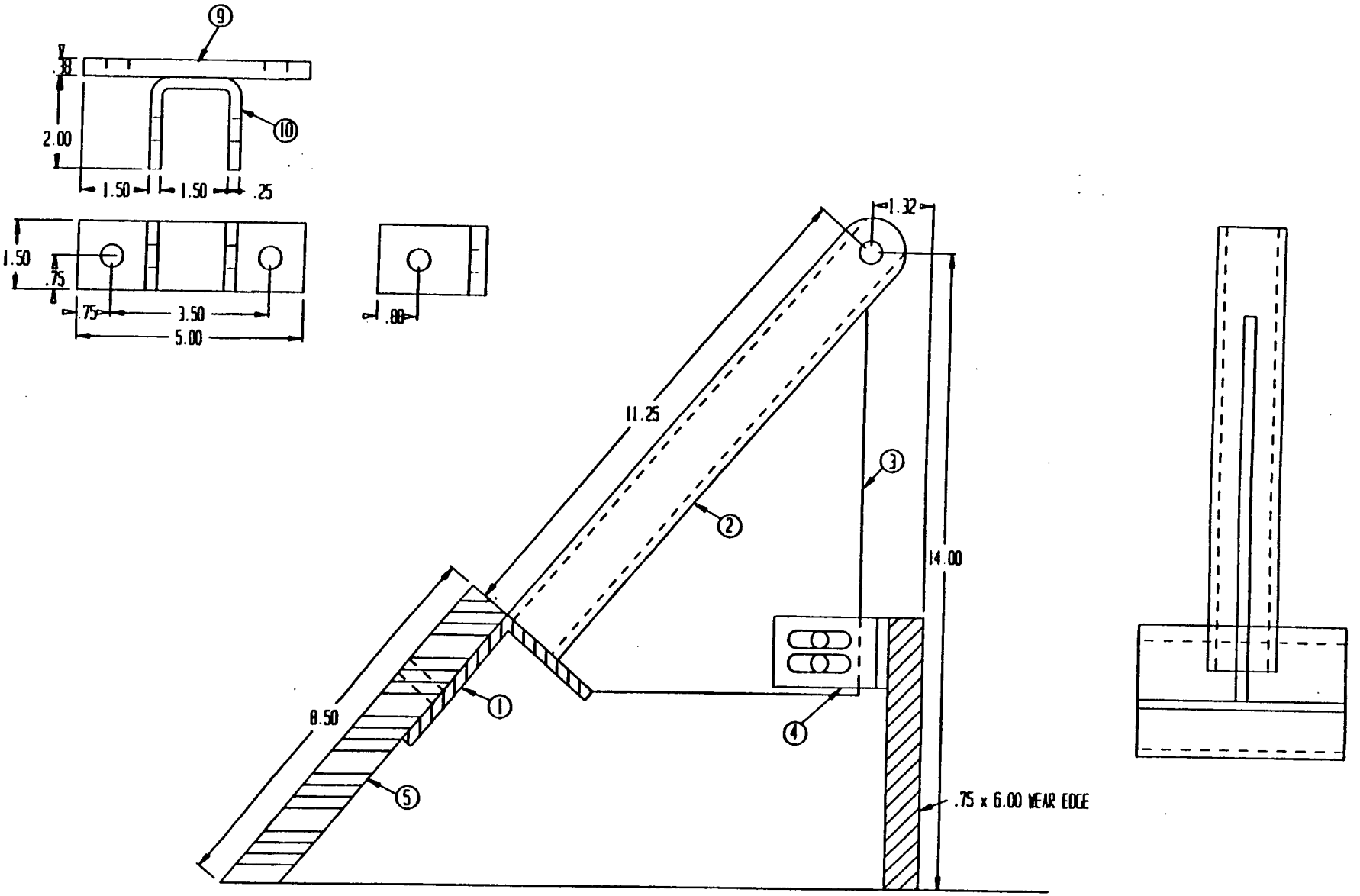
⑨
.38
2.00
⑩
1.50
1.50
.25
1.50
.75
.75
3.50
5.00
.88
1.32
11.25
③
②
14.00
8.50
①
④
⑤
.75 x 6.00 WEAR EDGE

ITEM	QTY	DESCRIPTION
1	1	3.5 X 2.5 X .25 ANGLE X 144.0
2	7	1.5 X 1.5 X 3/16 TUBE 12.0
3	7	.25 PLATE
4	7	2.5 X 2.0 X .25 ANGLE 1.5
5	3	UHMWPE 1.0 X 8.5 X 48
6	13	PLOW BOLT 3/8 X 2.0
7	7	HINGE BOLT 3/8 X 3.0
8	14	STOP BOLT 3/8 X 1.5
9	7	PL .38 X 1.50 X 5.0
10	7	PL .25 X 1.50 X 5.50

Note: Dimensions in inches.

References

1. Minsk, L. D., "Snow Removal Equipment." In Handbook of Snow, edited by D. M. Gray and D. H. Male. Toronto: Pergamon Press Canada Ltd., 1981. 656-661.

2. Shalman, D. A., Snowplows Construction, Theory and Design. 2nd ed. Leningrad: Mashinostroenie, 1973. Translated by the Department of Mechanical Engineering University of Wyoming. Laramie: n.p., 1990.

3. Lindberg, William R. and Petersen, Joseph D., "Negatively Buoyant Jet (or Plume) with Applications to Snowplow Exit Behavior." Transportation Research Record, no. 1304, "Highway Maintenance Operations and Research." National Research Council, Transportation Research Board (1991): 219-229.

4. Ruan, Bo, "Heavy Vehicle Stability." Master's thesis, University of Wyoming, 1992.

5. Damson, Mike H, "Numerical Investigation of Flow on a Snowplow." Master's thesis, University of Wyoming, 1990.

6. Hansen, Andrew C., "Analysis of Energy Dissipation Caused by Snow Compaction During Displacement Plowing." Transportation Research Record, no. 1304, "Highway Maintenance Operations and Research." National Research Council, Transportation Research Board (1991): 177-181.

7. Mellor, Malcolm, "Snow Removal and Ice Control." Cold Regions Science and Engineering, Part III, Sect. A3b, U.S. Army Material Command Cold Regions Research and Engineering Laboratory, Hanover, New Hampshire. Department of the Army Project IV025001A130 (April, 1965).

8. University of Wyoming Department of Mechanical Engineering, "Quarterly Progress and Continuation Report, Strategic Highway Research Program Contract H-206: Improved Displacement Plow and Blowing Snow Research," unpublished data, April 1990.

9. Personal Communication, Jan Verseef, Frink America, Clayton, New York, 1990.

10. Crane, Robert L., "Analysis of the Large Deformation and Flow Characteristics of Developable Surface Snowplow Moldboards." Master's thesis, University of Wyoming, 1992.

11. Simmonds, J. G., and Libai, A., "Exact Equations for the Inextensional Deformation of Cantilevered Plates." ASME Journal of Applied Mechanics 46 (September 1979): 631-636.

12. Struik, Dirk J., Lectures on Classical Differential Geometry. Cambridge: Addison-Wesley Press, Inc., 1950.

13. Malvern, Lawrence E., Introduction to the Mechanics of a Continuous Medium. New Jersey: Prentice-Hall, 1969.

14. Darmon, Pierre, "Large Inextensional Deformation of Thin Orthotropic Cantilevered Plates with Distributed Loads." Ph.D. diss., University of Rochester, 1985.

15. Press, William H., et al., Numerical Recipes, The Art of Scientific Computing. Cambridge: Cambridge University Press, 1989.

16. University of Wyoming Department of Mechanical Engineering, "Second Quarter 1992 Progress Report Strategic Highway Research Program Project H-206." Unpublished data, April 1992.

17. Mellor, Malcolm, "A Review of Basic Snow Mechanics." IAHS-AISH Publication No. 114 (1974): 283-286.

18. Langham, E. J., "Physics and Properties of Snowcover." In Handbook of Snow, edited by D. M. Gray and D. H. Male. Toronto: Pergamon Press Canada Ltd., 1981. 307-310.

19. Kincaid, David R. and Cheney, E. Ward, Numerical Analysis: Mathematics of Scientific Computing. Pacific Grove, California: Brooks/Cole Publishing Co., 1991.

20. I-DEAS™, Structural Dynamics Research Corporation, Milford, Ohio, 1990.

Highway Operations Advisory Committee

Dean M. Testa, *chairman*
Kansas Department of Transportation

Clayton L. Sullivan, *vice-chairman*
Idaho Transportation Department

Ross B. Dindio
The Commonwealth of Massachusetts Highway Department

Richard L. Hanneman
The Salt Institute

Rita Knorr
American Public Works Association

David A. Kuemmel
Marquette University

Magdalena M. Majesky
Ministry of Transportation of Ontario

Michael J. Markow
Cambridge Systematics, Inc.

Gerald M. (Jiggs) Miner
Consultant

Richard J. Nelson
Nevada Department of Transportation

Rodney A. Pletan
Minnesota Department of Transportation

Michel P. Ray
The World Bank

Michael M. Ryan
Pennsylvania Department of Transportation

Bo H. Simonsson
Swedish Road and Traffic Research Institute

Leland Smithson
Iowa Department of Transportation

Arlen T. Swenson
John Deere

Anwar E.Z. Wissa
Ardaman and Associates, Inc.

John P. Zaniewski
Arizona State University

Liaisons

Ted Ferragut
Federal Highway Administration

Joseph J. Lasek
Federal Highway Administration

Frank N. Lisle
Transportation Research Board

Byron N. Lord
Federal Highway Administration

Mohamed Y. Shahin
U.S. Army Corps of Engineers

Harry Siedentopf
Federal Aviation Administration

Jesse Story
Federal Highway Administration

8/16/93

Expert Task Group

George Chulick
California Department of Transportation

Robert A. Hogan
New Hampshire Department of Transportation

Byrt Joseph
The Port Authority of New York and New Jersey

Howard A. Jongedyk
Federal Highway Administration

Charles M. Kahl
North Dakota Department of Transportation

Frank N. Lisle
Transportation Research Board

Robert R. Samuelson
Consultant

Harry Siedentopf
Federal Aviation Administration

Stephen A. Toth
New Jersey Department of Transportation

8/9/93